REPORT DOCUMENTATION PAGE

Public reporting burden for this collection of information is estimated to average 1 hour per response, including the t
gathering and maintaining the data needed, and completing and reviewing the collection of information. Send comm
collection of information, including suggestions for reducing this burden, to Washington Headquarters Services, Direc
Davis Highway, Suite 1204, Arlington, VA 22202-4302, and to the Office of Management and Budget, Paperwork Reduction Project (0704-0108), w.

1. AGENCY USE ONLY (Leave blank)	2. REPORT DATE	3. REPORT TYPE AND DATES COVERED
		FINAL REPORT 30 Sep 92 - 30 Sep 96

4. TITLE AND SUBTITLE	5. FUNDING NUMBERS
Object-Oriented Formulations of Particle-in-Cell (PIC) Plasma Simulations	
6. AUTHOR(S) Professor Birdsall	61102F 2301/ES

7. PERFORMING ORGANIZATION NAME(S) AND ADDRESS(ES)	8. PERFORMING ORGANIZATION REPORT NUMBER
University of California, Berkeley Berkeley, CA 94720-1770	

9. SPONSORING/MONITORING AGENCY NAME(S) AND ADDRESS(ES)	10. SPONSORING/MONITORING AGENCY REPORT NUMBER
AFOSR/NE 110 Duncan Avenue Suite B115 Bolling AFB DC 20332-8050	F49620-92-J-0487

11. SUPPLEMENTARY NOTES

12a. DISTRIBUTION/AVAILABILITY STATEMENT	12b. DISTRIBUTION CODE
APPROVED FOR PUBLIC RELEASE: DISTRIBUTION UNLIMITED	

13. ABSTRACT (Maximum 200 words)

19970218 085

The object-oriented paradigm provides an opportunity for advanced PIC modeling, increased flexibility, and extensibility. Particle-in-cell codes for simulating plasmas are traditionally written in structured FOR-TRAN or C. This has resulted in large legacy codes that are difficult to maintain and extend with new models. In this ongoing research, we apply the object-oriented design technique to address these issues. The resulting code architecture, OOPIC (Object-Oriented Particle-in-Cell), is a two-dimensional (x-y, r-z) relativistic electromagnetic/electrostatic PIC-MCC (particle-in-cell, Monte Carlo collisions) plasma simulation. OOPIC includes a growing number of boundary conditions, and can model complicated configurations, including internal structures, without recompilation. It is applicable to models from DC and RF discharges to high power microwave tubes.

DTIC QUALITY INSPECTED 2

14. SUBJECT TERMS			15. NUMBER OF PAGES
			16. PRICE CODE

17. SECURITY CLASSIFICATION OF REPORT	18. SECURITY CLASSIFICATION OF THIS PAGE	19. SECURITY CLASSIFICATION OF ABSTRACT	20. LIMITATION OF ABSTRACT
UNCLASSIFIED	UNCLASSIFIED	UNCLASSIFIED	

FINAL TECHNICAL REPORT

30 November 96

for

Object-Oriented Formulations of Particle-in-Cell (PIC) Plasma Simulations

Prof. Charles K. Birdsall
University of California
Berkeley, CA 94720-1770

Submitted to
Dr Robert J. Barker
AFOSR/NE

PLASMA THEORY AND SIMULATION GROUP

January 1 to December 31, 1995

Objectives:

Our research group uses both plasma theory and simulation as tools in order to increase the understanding of instabilities, heating, transport, plasma-wall interaction, and large potentials in plasma. We perform plasma device computer experiments to compare with analytic models and laboratory experiments in order to accelerate device design. Development and application of object-oriented PIC code (OOPIC) for fully relativistic, electromagnetic interactions between electron beams and waveguides. Our research for 1995 has been widely reported, as given by the listing following, of Journal Articles, ERL Reports, Talks, and Poster Papers. Abstracts are attached for some of the talks. Sent along with this Report are recent reprints.

—C. K. Birdsall

Principal Investigator			*Post-Doctoral Researcher*		
Prof. C. K. Birdsall	191M Cory Hall	643-6631	Dr. Venkatesh Gopinath	187M Cory Hall	642-3477

Research Engineer

Dr. John Verboncoeur   187M Cory Hall   642-3477

Research Assistants,			*Aids*		
Mr. David Cooperberg	199MD Cory Hall	642-1297	Mr. T. C. Yan	191M Cory Hall	643-6631
Ms. Emi Kawamura	199MD Cory Hall	642-1297	Mr. Don Wong	199M Cory Hall	642-1297
Mr. Keith Cartwright	199ME Cory Hall	642-1297			
Mr. Peter Mardahl	199ME Cory Hall	642-1297			
Mr. J. Morgan Oslake	199ME Cory Hall	642-1297			
Mr. David Locke	199ME Cory Hall	642-1297 (summer 1995)			

Administrative Staff

Mrs. Liz Nagata   195M Cory Hall   643-6633

Visitors

Dr. Jae Joon Oh, from Samsung (SAIT), Korea, December 1994–November 1995

Chang Shih Chan, student from Harvard (National Undergraduate Fellowship in Plasma Physics and Fusion Engineering, run by PPL, Princeton University N.J.). Do case studies with Gopinath and Birdsall, 26 June–end of August 1995

Professor Siegbert Kuhn, Visiting MacKay Lecturer, from University of Innsbruck, Austria (cooperate on "Bounded Plasmas, Theory & Simulation" text), 1 August–10 September 1995

Professor Jae Koo Lee, sabbatical leave from Pohang University, Korea – Long list of projects, August 1995–February 1996

Our Advisers are

Dr. A. Bruce Langdon	L-472 LLNL	422-5444	Dr. Vahid Vahedi	572-8535
Physicist, Lawrence Livermore Natl. Lab			*Lam Research Corp., Fremont*	

Table of Contents

PLASMA DEVICE PARTICLE SIMULATION CODES
PIC-MCC, 1d3v, 2d3v
ELECTROSTATIC AND ELECTROMAGNETIC

from

PLASMA THEORY AND SIMULATION GROUP
EECS Dept. Cory Hall #1770, University of California
Berkeley, California 94720-1770 U.S.A.
e-mail: ptsg@eecs.berkeley.edu
http://ptsg.eecs.berkeley.edu

PTSG offers particle simulation codes, PIC-MCC, with graphics MS-DOS (WinGraphics), Windows 3.1 (WinPlot) and for Unix, X-windows (XGrafix) for use in research and teaching, for PC's, workstations and mainframes. These include the following codes (in C unless noted; X means Unix, X-11):

SPAM, a single particle mover in given **E** and **B** fields, 3d3v;
ES1, ES1 (Fortran), XES1, 1d2v, periodic, electrostatic;
EM1, XEM1, 1d2v, periodic and bounded, electromagnetic;
IBC, XIBC, 1d1v, traveling-wave tube, electrostatic; R,L,C slow-wave circuit;
PDx1, XPDx1, 1d3v, x= p,c,s: planar, cylindrical, spherical; electrostatic, bounded,
   external R,L,C circuit, plus V or I DC or RF sources;
XPD2, 2d3v, in x, y, and in r θ, electrostatic, bounded, external R,L,C circuits, plus V or
   I DC or RF sources;
OOPIC, XOOPIC, 2d3v, flexible boundaries in x,y, and in r, z, electromagnetic, relativis-
   tic, object-oriented, in C^{++} for electron beam devices and bounded plasma systems.
   Also electrostatic versions, as general as XPD2, external circuits, sources.

Internet access to all codes and graphics is updated on WWW as:
http://ptsg.eecs.berkeley.edu
email: codes@langmuir.eecs.berkeley.edu
For instructions on how to download codes, type
finger codes@langmuir.eecs.berkeley.edu

ES1 (Fortran), updated by A.B. Langdon, is available from:
   ftp ftp-icf.llnl.gov
   Name: anonymous
   Password: <your mail address>
   cd pub/es1
   binary
   get es1.tar

Representative publications applying our PTSG plasma device codes, by PTSG and other authors, are as follows (predecessors from 1983 on, such as using our PDW1 and ES2, are not listed):

1991 Vahedi, V., M.A. Lieberman, M.V. Alves, J.P. Verboncoeur, and C.K. Birdsall, ``A One Dimensional Collisional Model for Plasma Immersion Ion Implantation,'' *J. Appl Physics* **69** (4), 15 February 1991, pp. 2008-2014.

Alves, M.V., M.A. Lieberman, V. Vahedi, and C.K. Birdsall, ``Sheath Voltage Ratio for Asymmetric RF Discharges,'' *J. Appl. Physics* **69** (7) 1 April 1991, pp. 3823-3829.

Birdsall, C.K., ``Particle-in-Cell Charged-Particle Simulations, Plus Monte Carlo Collisions with Neutral Atoms, PIC-MCC,'' *IEEE Trans. Plasma Science* **19** (2), April 1991, pp. 65-85 (Invited paper).

1992 Maier, H, ``Self-consistent one-dimensional potential distributions of the singl mitter Q-machine taking into account charge-exchange collisions,'' Diploma thesis, Institute for Theoretical Physics, University of Innsbruck, Austria (Apr. 1992).

Horhager, M., and S. Kuhn, ``New results on weakly nonlinear driven oscillations in the Pierce diode,'' *1992 Intl. Conf. on Plasma Physics* , Innsbruck, Austria, 29 June-3 July 1992, ed. by W. Freysinger, K. Lackner, R.Schrittwieser and W. Lindinger (Institute for Ion Physics, Univ. of Innsbruck, Austria, and European Physical Society, Geneva, Switzerland, 1992), Contrib. Papers III, 1685 8.

Hahn, S.J., and J.K. Lee, ``Kinetic Simulation of the Transient Sheath in Plasma Ion Implantation,'' *Jpn. J. Appl. Phys.* **31** , Part 1, No. 8, 2570 2579, August 1992.

Browning, J., N.E. McGruer, S. Meassick, C. Chan, W.J. Bintz, and M. Gilmore, ``Gated field emitter failures: experiment and theory,'' *IEEE Trans. Plasma Science* **20** (5), 499 506, October 1992.

Bulanov, S.V., S. Kuhn, and A.S. Sakharov, "Particle simulations of boundary condition and hf-field effects on strong double layers in a collisionless bounded plasma," *Phys. Fluids B* **4** (9), 2871 84, Sept. 1992.

Nebel, R.A. et al., ``Inertial-electrostatic confinement studies,'' Presented at APS/DPP, Seattle, Washington, November 1992.

1993 Verboncoeur, J.P., M.V. Alves, V. Vahedi, and C.K. Birdsall, ``Simultaneous Potential and Circuit Solution for 1D Bounded Plasma Particle Simulation Codes,'' *J. Comp. Physics* , **104** , pp. 321-328, February 1993.

McGruer, N.E., J. Browning, S. Meassick, M. Gilmore, W.J. Bintz, and C. Chan, ``Ion- space-charge initiation of gated field emitter failure,'' *J. Vac. Sci. Technol. B* **11** (2), 441-444, March/April 1993.

Greiner, F., T. Klinger, H. Klostermann, and A. Piel, ``Experiments and Particle-in-Cell Simulation on Self-Oscillations and Period Doubling in Thermionic Discharges at Low Pressure,'' *Phys. Rev. Letters* **70** (20), 3071 3074, May 1993.

Vahedi, V., C.K. Birdsall, M.A. Lieberman, G. DiPeso, and T.D. Rognlien, ``Verification of frequency scaling laws for capacitive radio-frequency discharges using two-dimensional simulations,'' *Phys. Fluids B* **5** (7), pp. 2719-2729, July 1993.

Vahedi, V., R.A. Stewart, and M.A. Lieberman, ``Analytic Model of the Ion Angular Distribution in a Collisional Sheath,'' *J. Vac. Sci. Technol. A* **11** , 1275, July/August 1993.

Watanabe, J., and K. Okano, ``Particle simulation of the ion-extraction process from a plasma by a static electric field,'' *Phys. Fluids B* **5** (8), 3092 3096, August 1993.

Qin, S., C. Chan, J. Browning, and S. Meassick, ``Charge transfer cross section of He+ in collisional helium plasma using the plasma immersion ion implantation technique,'' *J. Appl. Phys.* **74** (3), 1548-, 1 August 1993.

Vahedi, V., C.K. Birdsall, M.A. Lieberman, G. DiPeso, and T.D. Rognlien, ``Capacitive RF discharges modeled by Particle-In-Cell Monte-Carlo Simulation. I. Analysis of numerical techniques,'' *Plasma Sources Sci. Technol.* **2** , 261 272, November 1993.

Vahedi, V., C.K. Birdsall, M.A. Lieberman, G. DiPeso, and T.D. Rognlien, ``Capacitive RF discharges modeled by Particle-In-Cell Monte-Carlo simulation. II. Comparisons with laboratory measurements of electron energy distribution functions,'' *Plasma Sources Sci. Technol.* **2** , 273-278, November 1993.

Greiner, F., T. Klinger, H. Klostermann and A. Piel, "Experiments and Particle-in-Cell Simulation on Self-Oscillations and period-doubling in Thermionic Discharges at Low Pressure," *Physical Review Letters*, **70** (20), 3071-3074,1993.

Piel, A., F. Greiner, T. Klinger, H. Klostermann and A. Rohde, "Chaos in Plasmas: A Case Study in Thermionic Discharges," in H. Kikuchi, Herausgeber, *Dust, Noise, and Chaos in Space and Laboratory Plasmas.* Plenum Press, 1993, in press.

Wood, B.P., "Displacement Current and Multiple Pulse Effects in Plasma Source Ion Implantation,", *Journal of Applied Physics*, 4770 (1993).

Verboncoeur, J.P., C.K. Birdsall, "Simulations of Limiting Current in a Crossed-Field Gap: Hull Diode," Electronics Research Lab, Memorandum No. UCB/ERL M93/86, ERL, University of California, Berkeley, 15 December, 1993

1994   Qin, S., and C. Chan, ``Plasma immersion ion implantation doping experiments for microelectronics," to appear in *J. Vac. Sci. Technol. B* , March/April, 1994.

Klostermann, H., F. Greiner, T. Klinger and A. Piel, "Stable and Unstable Modes in a Thermionic Discharge at Low Pressure" *Plasma Sources Sci. Technol.* **3**, 134-141 (1994).

Birdsall, C.K. and S. Kuhn *Bounded Plasma Theory and Simulation* Vols. I,II,III,IV 1979-1993 May 1994.

Rej, D.J., B.P. Wood, R.J. Faehl, and H.H. Fleischmann, "Magnetic Insulation of Secondary Electrons in Plasma Source Ion Implantation," *Journal of Vacuum Science Technology*, **12**, 861 (1994).

Wood, B.P., J.T. Scheuer, M.A. Nastasi, R.H. Olsher, W.A. Reass, I. Henins, and D.J. Rej, "Design of a Large-Scale Plasma Source Ion Implantation Experiment," *Materials Research Society Symposium Series* , Vol. 279, pp. 345-350 (1994).

Greiner, Franko, "Nichtlineare Dynamik von Thermionischen Niederdruckentladungen: Teilchensimulation im Vergleich mit Experimenten," dissertation, SFB-Report 198-A8-5, Kiel, 1994.

Klinger, Thomas, "Experimentelle Untersuchung der Nichtlinearen Dynamik Einer Thermionischen Entladung," SFB-Report 198-A8-4, Dissertation, Kiel, 1994.

Christenson, P.J., Y.Y. Lau, "Transition to Turbulence in a Crossed-Field Gap," *Physics of Plasmas* , pp. 3725-3727 December 1994.

Lichtenberg, A.J., V. Vahedi, M.A. Lieberman, and T.D. Rognlien, "Modeling Electronegative Plasma Discharges," *J. Appl. Phys.* **75**, pp. 2349-2347, March, 1994

M. Fivaz, B. Bumle, A.A. Howling, L. Ruegsegger and W. Schwarzenbach, "Parallel Simulation of Radio-Frequency Plasma Discharges", *6th Joint EPS-APS Intl. Conf. on Physics Computing*, Manno, Switzerland, August 1994.

1995   Greiner, F., T. Klinger and A. Piel, "Nonlinear Dynamical Behavior of Thermionic Filamentary Low Pressure Discharges. Part I: Simulation," *Phys. Plasmas* , 1995.

Klinger, T., A. Rohde, F. Greiner and A. Piel, "Nonlinear Dynamical Behavior of Thermionic Filamentary Low Pressure Discharges. Part II: Experimental." *Phys. Plasmas* , 1995.

Wood, B.P., M.A. Lieberman, and A.J. Lichtenberg, "Stochastic Electron Heating in a Capacitive rf Discharge with Non-Maxwellian and Time-Varying Distributions," *IEEE Trans. Plasma Sci* **23**, 89 Feb. 1995.

T. Klinger, F. Greiner, A. Rohde, A. Piel, and M.E. Koepke, "Van der Pol behavior of relaxation oscillations in a periodically driven thermionic discharge," *Physical Review E,* in press, May 1995.

Quandt, E., H.M. Katsch and P. Mark, "Electron Energy Gain and Loss in a Radiofrequency Discharge in Helium: Comparison of Experiment and Particle-in-Cell Monte-Carlo-Collision Simulation," to be published in *Phys. Rev. Lett.*

M. Fivaz, S. Brunner, W. Schwarzenbach, A.A. Howling and Ch. Hollenstein, "Reconstruction of the Time-Averaged Sheath Potential in an Argon RF Plasma Using the Ion Energy Distribution", *Plasma Sources Sci. Technol.* **4**, 373 (1995).

W. Schwarzenbach, A.A. Howling, M. Fivaz, S. Brunner and Ch. Hollenstein, "Sheath Impedance Effects in Very High Frequency Plasmas", *J. Vac. Sci. Technol.* **A** 1995.

T.H. Chung, H.S. Yoon, and J.K. Lee, "Scaling Laws Verification for Capacitive RF-Discharge Ar Plasma Using Particle-in-Cell Simulations" To appear in *Jour. Appl. Phys.*

Bromley, B.P., G. H. Miley, R.A. Nebel, Kuok-Mee Ling, "PDS1 Simulations of IEC Fusion Devices," *IEEE ICOPS* June 5-8 1995 Madison, Wisconsin.

SHORT COURSES Members of our group (Prof. C.K. Birdsall plus Post-doc Vahid Vahedi) plus Profs. D.B. Graves and M.A. Lieberman have presented 3 day courses on analytic modeling and computer simulation, with emphasis on plasma assisted materials processing (in 1990, San Francisco and Oxford; in 1992, Berkeley and Vienna; in 1993, St. Louis and planned for IEEE ICOPS, Boston, June 1996), using our Plasma Device codes, with hands-on instruction. Prof. Birdsall has taught two week long courses at ICTP, Trieste, on plasma simulation , in 1985, 1991, 1993, and 1995 with Dr. Vahedi, Post-doc John Verboncoeur, and former student Dr. M. Virginia Alves; he also has taught one and two week courses at Uppsala, Tokyo, Torino, and Hitachi City in 1992, 1993, and 1994. Invitations to present similar courses are welcomed.

WORKSHOPS We have given workshops for users of our (and similar) plasma device codes. The first was on collision refinements for PIC-MCC codes, organized by Drs. V. Vahedi (of PTSG) and M. Surendra (of IBM) at the Numerical Simulation of Plasmas Conference, September 1994. The second, was for PDP1, PDC1, PDS1 users who wished to use our new 2d3v PIC-MCC codes (in x,y, and r-θ, and r-z). This workshop was intensive, held in Innsbruck, Austria, 15-18 February 1995. An OOPIC Code (object-oriented PIC) release workshop (electromagnetic, relativistic e beam, collisions with neutrals, x,y r,z r-θ) will be held September 11-13, 1995 in Berkeley, CA. Inquiries are welcome (address to Prof. Birdsall).

CODE CONSULTING AND MAINTENANCE PTSG may answer short inquiries on our various codes, as we are primarily committed to university type plasma device research and development. However, more detailed inquiries for help should be addressed to Computational Physics Software (as: cps@langmuir.eecs.berkeley.edu), a small private firm well skilled in PTSG codes.

Birdsall/Microsoft Docs/PTSG.advertisement.8.8

Developers of the Berkeley Plasma Device Codes, 1983–1994

In 1981, the plasma theory and simulation group (PTSG, UC Berkeley), changed directions to study whole plasma devices, from laboratory plasmas to fusion reactors. With T. Kamimura and S. Ishiguro in Nagoya, we adapted A.B. Langdon's periodic code ES1 to bounded models (see Chapter 4 of our book), observing realistic sheaths at bounding walls. More of the same was done at Cal Tech in the Spring of 1982, as Visiting Chevron Professor of Energy, hosted by Profs. Bridges and Gould, programming by Brian Leahy.

In the spring of 1983, our Plasma Device Workshop collected ideas for new bounded plasma codes from colleagues in Berkeley and from LLNL, Livermore. The senior members were C.K. Birdsall, T.L. Crystal and S. Kuhn, (guest from Innsbruck, who provided much of the motivation, and the initial model (Q-machine)). The result was the code PDW1, 1d3v, with real walls, emitting/absorbing, and an external circuit, written by W.S. Lawson, in Fortran, for Cray use. This code has been used widely, for applications to collisionless bounded plasmas, in the lab, space, and fusion. Perry Gray used PDW1 for a movie of positive-bias instabilities on a Q-machine, shown widely (available on video).

In 1984, K. Theilhaber, using PDW1 as a model, wrote a bounded 2d3v program, ES2, for his work on the magnetized plasma sheath, with Kelvin-Helmholtz modes (available on video). Later, Gray and Lawson wrote PDW2, based on PDW1.

By a happy accident, in 1985, T. Lasinski (NASA Ames Lab) translated ES1 from FORTRAN to C on a PC. The compiler he used did not have a graphics library so he developed his own routines. With this real-time simulation, we saw for the first time the dynamic development of the two-stream instability, and more. PTSG members were enthusiastic about this step away from dependence on main frames and chose to make this beginning go much further. T.L. Crystal did some initial improvements. Then V. Vahedi and J. Verboncoeur developed "WinGraphics" for PC's. They next did the same for PDW1, making it into PDP1, plasma device, planar, 1d3v. In 1989-90, M.V. Alves, visiting from Brazil, helped write PDC1 and PDS1, 1d3v, for concentric cylindrical and spherical electrodes. Later, Vahedi and Verboncoeur developed "XGrafix" for X-11 windows.

The next step, beginning in 1989, was to add collisions between the charged particles and neutral background particles, using Monte-Carlo methods, in order to simulate weakly ionized lab plasmas, from fusion plasmas near limiters and divertors, to glow discharges. Added Berkeley partners (to V.V., J.V., and M.V.A.) were I. Morey, and (from Chemical Engineering) M. Surendra, and D.B. Graves. The result has been PIC-MCC. Recent partners on MCC are T. Rognlien, J. Hiskes, and R. Cohen of LLNL.

In 1991, V. Vahedi and G. DiPeso developed PDP2, a 2d3v (x,y) PIC–MCC bounded plasma computer experiment. The fully bounded version of the x,y PDP2 uses a DADI potential solver based on ideas from D. Hewett (PPRI, LLNL) that allows use of an implicit potential equation. In 1993 P. Mirrashidi, Vahedi and D. Cooperberg developed PDC2 in (r, θ), based on PDP2. Vahedi and DiPeso are nearly finished with PDP2 in r,z.

In 1992, J. Verboncoeur began the physics coding for a C++ object- oriented PIC code (called OOPIC), in r,z, with a relativistic electron beam, fully electromagnetic slow-wave, fast-wave device model, using the Quad EM formulation of A.B. Langdon, based on the integral form of Maxwell's equations. OOPIC now also includes an x,y EM version as well as electrostatic models in r,z and x,y, assisted by P. Mardahl and K. Cartwright. Initial applications are to microwave and millimeter wave amplifiers and oscillators. The GUI is coming from George Mason University; the expert system from N.T. Gladd of BRA provides guidance in choosing parameters.

In 1994 D. Wong upgraded the XGrafix modules for XES1, and for the PD1 and PD2 codes, also adding more diagnostics. V.P. Gopinath is completing the development of XPDC2.

II. Plasma Theory and Simulation Group List of Publications for 1995

Journal Articles

V. Vahedi and M. Surendra "Monte Carlo Collision- Model for Particle-in-Cell Method: Application to Argon and Oxygen Discharges". *Comp. Phys. Comm.*, **87**, May II 1995 pp 179-198 (Also ERL Memo 1994/72 15 September 1994).

J.P. Verboncoeur, A.B. Langdon and N.T. Gladd, "An Object-Oriented Electromagnetic PIC Code." *Comp. Phys. Comm.*, **87**, May II, 1995 pp 199-211 (Also ERL Memo 1994/71 15 September 1994).

ERL Reports

E. Kawamura, V. Vahedi, M.A. Lieberman, and C.K. Birdsall, "Review of Ion Energy Distributions in Capacitively Coupled RF Plasma Reactors" UCB/ERL M95/49, 15 June 1995

J.P. Verboncoeur and C.K. Birdsall, "Rapid Current Transition in a Crossed-Field Diode" UCB/ERL M95/55, 15 June 1995. Accepted for publication, *Physics of Plasmas*

V.P. Gopinath, J.P. Verboncoeur, and C.K. Birdsall, "Similarity of Limited Currents in Planar and Cylindrical Crossed-Field Diodes" UCB/ERL M95/56, 25 June 1995. Submitted to *Physics of Plasmas*

V. Vahedi and G. DiPeso, "Simultaneous Potential and Circuit Solution for Two-Dimensional Bounded Plasma Simulation Codes," UCB/ERL M95/95 29 November 1995 (to be submitted to *Jour. Comp. Physics*)

V.P. Gopinath and M.A. Lieberman, "Simulation and Analysis of a Large Area Plasma Source," UCB/ERL M95/65 25 June 1995

A.B. Langdon, "2D electromagnetics and PIC on a quadrilateral mesh," UCB/ERL M95/96 5 December 1995.

Talks, Posters, Papers

Conference on Numerical Simulations of Plasma Turbulence, Institute for Theoretical Physics, UCSB, April 10-13, 1995

C.K. Birdsall, "Plasmas at the Edge", lead off talk (invited)

22nd IEEE Int'l Conference on Plasma Science, 5-8 June 1995, University of Wisconsin, Madison, WI, (1 invited talk, 6 posters)

K.L. Cartwright and C.K. Birdsall "Two Dimensional Investigation of Ion Acoustic Waves Reflection from the Sheath"

V.P. Gopinath, D. Cooperberg, P. Mirrashidi, Vahedi, J. Verboncoeur, C.K. Birdsall, "XPDC2-RΘ a Two Dimensional Electrostatic PIC Code"

J. Verboncoeur and the OOPIC team, "OOPIC: Object Oriented Particle-in-Cell Code" (Invited)

P. Mardahl, J. Verboncoeur, C.K. Birdsall "A Spectral Comparison of Two Methods of Removing Errors in Gauss' Law in a 2-Dimensional PIC Plasma Simulation"

N.T. Gladd, J.P. Verboncoeur "Issues in Providing Expert Advice for Users of a Particle-in-Cell Simulation Code"

V.P. Gopinath, J.P. Verboncoeur, C.K. Birdsall "Simulation of Transmitted Current in a Cylindrical

Cross Field Diode"

E. Kawamura, V. Vahedi, M.A. Lieberman and C.K. Birdsall "Review of Ion Energy and Angular Distributions in Capacitively Coupled RF Plasma Reactors"

First International Crossed-Field Devices Workshop, University of Michigan, Ann Arbor, August 15,16, 1995

K. Cartwright, J.P. Verboncoeur, V.P. Gopinath, and C.K. Birdsall, "Transverse asymmetry in a crossed-field diode"

J.P. Verboncoeur and C.K. Birdsall, "Rapid current transitions ion a crossed-field diode at the Hull cutoff"

V.P. Gopinath, J.P. Verboncoeur and C.K. Birdsall "Similarity of limiting currents in planar and cylindrical crossed-field diodes"

Gaseous Electronics Conference, October 9-13, 1995, Berkeley, CA

C.K. Birdsall, V.P. Gopinath, J. Verboncoeur, "Plasma Computer Experiments Teaching Laboratory"

D.J. Cooperberg, C.K. Birdsall, "Plasma production by large amplitude plasma surface waves"

E. Kawamura, V. Vahedi, M.A. Lieberman, and C.K. Birdsall, "Ion Energy Distributions in Capacitively Coupled RF Plasma Reactors"

American Physical Society, Div. of Plasma Physics Annual Meeting, Nov. 6-10, 1995, Louisville, Kentucky

K. Cartwright and C.K. Birdsall, "Two Dimensional Investigation of Ion Acoustic Waves Reflection from the Sheath"

D.J. Cooperberg and C.K. Birdsall, "Large Amplitude Plasma Surface Waves"

V.P. Gopinath, J.P. Verboncoeur, C.K. Birdsall, "Similarity of Limiting Currents in Planar and Cylindrical Crossed-Field Diodes"

Workshops (hands on instructions)

PDW2 Workshop 1995, held at Computer Center, University of Innsbruck, Innsbruck, Austria, 15-18 February 1995

Instruction and attendee problem solving, using our new 2d3v PIC-MCC plasma simulation codes. 6 members of PTSG were the instructors. (11 attendees)

Crossed Field Workshop, 31 March 1995, U.C. Berkeley (informal exchanges with University of Michigan, LLNL)

OOPIC Release Workshop, September 11-13, 1995, Berkeley, CA

Release of our OOPIC electromagnetic relativistic e-beam 2d3v codes (r,z r,θ, and x, y), with lectures, demonstrations, hands-on instruction. Instructors on the physics and applications mostly from PTSG. (24 attendees)

Trieste Summer Plasma School, Int'l Center for Theoretical Physics, Trieste, Italy, September 18-October 7, 1995

Three week course/lab on plasma computer experiments, mostly hands-on instruction, by C.K. Birdsall and M. Virginia Alves (Brazil, former PTSG member). Similar to "New Course," below.

New Course

- New U.C. Berkeley course: Plasma Computer Experiments Lab, EECS 298-9, Spring, 1995, 1 unit. This lab accompanied Professor M.A. Lieberman's EECS 239 lecture course, providing PIC-MCC simulations for analytic models in his text. Given by C.K. Birdsall, V.P. Gopinath, J. Verboncoeur. (Copies available; contact Birdsall; fourteen videotapes available; contact Pam Atkinson, atkins@coe.berkeley.edu)

Special Meeting

MURI (Multidisciplinary University Research Initiative) 17 March 1995, U.C. Davis

    J. Verboncoeur "Current State of Object Oriented PIC EM Relativistic Beam Code"

    C.K. Birdsall "UCB Proposed OOPIC Device Modeling"

Visitors to PTSG, 1995

Dr. Jae Joon Oh, from Samsung (SAIT), Korea, December 1994-end 1995

Chang Shih Chan, student from Harvard (National Undergraduate Fellowship in Plasma Physics and Fusion Engineering, run by PPPL, Princeton University N.J.) Do case studies with Gopinath and Birdsall, 26 June-end of August 1995

Professor Siegbert Kuhn, Visiting MacKay Lecturer, from University of Innsbruck, Austria (cooperate on "Bounded Plasmas, Theory & Simulation" text), 1 August-10 September 1995

Professor Jae Koo Lee, sabbatical leave from Pohang University, Korea - Long list of projects, August 1995-February 1996

III. 1995 Plasma and Beam Device Workshops; 2d3v code releases

During 1995 PTSG presented two workshops on our 2d3v codes. We set these up because we felt that simply passing out the codes, with no instruction, would not work.

The first workshop was **PDW2** , held Feb. 15-18, 1995, at the University of Innsbruck, Innsbruck, Austria, with host Professor Siegbert Kuhn (who had been a co-leader on our PDW1 workshop in 1983, Berkeley, which produced our 1d bounded code PDW1). A detailed announcement of the 2d3v electrostatic code capabilities was in our 1994 Annual Report; the first page is repeated here. There were 11 attendees from 8 countries, each of whom achieved at least a first run on their problems (submitted in advance), due in no small part to the skills of PTSG instructors (there were seven).

The second workshop was the **OOPIC Release Workshop** held here in Berkeley in the Hogan and Wang Rooms in Cory Hall, Sept. 11-13, with 24 attendees. The OOPIC Announcement follows. Our group made 13 presentations of typical models (list follows), close to the interests submitted in advance. Two examples are given, following: the Cerenkov maser (or dielectric loaded waveguide), with 0.7c velocity e-beam, and the rzgrating (or disk loaded waveguide) with c/3 velocity positron beam. Both have small currents, weak interactions.

PLASMA DEVICE WORKSHOP 2 (PDW2)

15-18 February, 1995
Computer Center, Technikerstrasse 13
University of Innsbruck, Innsbruck, Austria

This workshop is set up to display and instruct participants in the use of our two-dimensional electrostatic bounded plasma, plasma device, simulation codes. The objective is to help each participant make initial run(s) on their problem(s) during the workshop, and take the codes home. The codes follow on our one dimensional versions (PDx1, x=p,c,s; planar, cylindrical, spherical), developed following our first workshop PDW1 in 1983; participants should be skilled in use of these codes, able to modify the PD2 codes (in C, some in C^{++}) and compile and run and print.

The codes are particle-in-cell, Monte Carlo collisional (PIC-MCC), bounded by electrodes, which are tied to an external circuit, including V or I sources (DC or RF). The 1d3v versions have been widely used for a great variety of problems, from collisionless oscillations and waves to highly collisional DC and RF discharges. The newer 2d3v versions have been developed by our post-docs and students for their own research applications, again seeking oscillation and wave behavior, as well as characterizing DC and RF discharges, plus many other problems. As with the PD1 series, the PD2 codes are adaptable to a large variety of bounded plasma problems, plasma devices, by changes only to the input file (no re-writing, no re-compiling).

It is expected that participants will include plasma physicists, plasma processing engineers, space physicists, non-linear dynamicists, and more.

The order of the workshop will be (most of the time to be on (c)):

(a) Brief presentations of some of our 2d3v research results, with various 2d3v configurations in (x,y), (r, θ) and (r,z) coordinates;

(b) Detailed discussion of the advances from 1d3v to 2d3v, such as setting up electrodes shapes, field solving, smoothing, diagnostics;

(c) Consulting with participants on setting up and running their problems, which are to be submitted in advance (in order to check their feasibility).

The instructors will be Professor C.K. Birdsall and his post-docs and students who are the code developers and appliers. The charges are for the instructors, consulting on participant's problems, and travel costs; $3,000 for universities and $5,000 for industries. Enrollment is limited; early application is encouraged. The workshop/consulting charges may be large relative to lecture courses; the charges are very small compared to development costs or those of commercial codes. And, the workshop provides consulting on initial runs.

OOPIC RELEASE WORKSHOP 1995
September 11,12,13, to be held at EECS Dept.
Cory Hall, University of California, Berkeley CA

This announcement replaces the two prior ones; the Workshop has been moved from Gatlinburg, Tennessee to Berkeley CA.

OOPIC is an object-oriented particle-in-cell (PIC) plasma simulation code, developed for the Air Force Office of Scientific Research (AFOSR) during October 1992-September 1995. It is intended for electron beam device design, but has applicability to plasma physics models. OOPIC is written in C++, runs on Microsoft Windows, to run on fast PC's. XOOPIC runs on Unix workstations. The Workshop will focus on the Unix version, XOOPIC.

OOPIC is fully electromagnetic (using A.B. Langdon's Quad EM algorithms), relativistic, 2d (r,z or x,y and soon in r, theta), is PIC-MCC (collisional) with extensive freedom to vary electron and ion sources, metal and dielectric boundaries, and comes with a large set of graphics. There also is an electrostatic version.

OOPIC codes currently have: orthogonal grids, with boundaries along grid surfaces, which may be conductors or wave launchers/absorbers (in the EM codes) or particle emitters (which can be time-varying), may be stepped or rippled, with internal structures. The ES models may include RF-driven and DC-biased conductors and dielectrics. There may be spatially varying static applied magnetic fields. There may be charged particle-neutral collisions (PIC-MCC). There may be immobile background charge density. The electrons may be Boltzmann (ES models). OOPIC is spatially two-dimensional; however, the fields and velocities all have components along all three coordinates (i.e., 2d3v)

The OOPIC Release Workshop is intended to demonstrate applications of OOPIC. The format will be a lecture-demonstration-interactive workshop, presenting approaches and solutions (run live) to a number (5 to 10) of representative (generic) models, including some submitted by attendees. Prospective attendees are asked to submit their model descriptions as soon as possible in order that they may converse (on email) with code developers who will be the instructors at the Workshop. Attendees will have the opportunity to run OOPIC. Attendees will receive the code, User, Algorithm, and Developer's Manuals, plus a short book on generic device models with input files and outputs, plus OOPIC publications.

The OOPIC Release Workshop is intended to demonstrate that our object-oriented code can be modified easily, that such can be learned quickly, and that special experience in C++ or C is not needed. The Workshop is intended for users, designers, researchers, and is NOT a DX, DT, Maxwell eqn. course per se. Experimentalists are especially welcome.

The first day, Monday, September 11, will be in the Hogan Room, 5th floor, Cory Hall, 9-11am and 2-5pm, for demonstrations of code uses, on a variety of generic models, including showing ease of changing boundaries (no re-write), adding new diagnostics, new boundary conditions (small re-write). All interested parties are welcome to attend this day, as we can accomodate up to 50 or so people, on Monday.

The second and third days, Tuesday and Wednesday, Sept. 12, 13, will be for those who have submitted their own models, who actively run programs, who wish to learn in detail how the code works and how it is modified, especially on the generic models of Monday, and on their own problems. This group will be limited to the number who can work on our computers (8 WS's and 2 fast PC's), with our small group as instructors, in

our research space, Rooms 199MD, ME Cory Hall. (Something on the order of 8 to 16; we will be selective.)

The registration fee will be $300, due August 15, for everyone, for local expenses (check made out to U.C. Regents). Manuals and publications will be mailed sometime after August 15 to attendees. A mechanism will be set up for interaction between attendees and course developers after the workshop, for bug disposal, upgrades, add-ons, new features, et cetera. If supported, help will be free; if not, charges will be necessary.

Our current list of generic device models, which we are working on (to be added to from applicants models), includes: e-beam optics, klystrons, plasma discharges, disk-loaded TWT and variations (e.g., grating boundary), opposing streams, dielectric-loaded guide and e-beam, possibly more. All are PIC, 2d3v, with and without applied B, etc.

The OOPIC Release Workshop Steering Committee members are:

Prof. Charles K. Birdsall, U.C. Berkeley (Chair)birdsall@eecs.berkeley.edu
Dr. Robert Barker, AFOSR, barker@afosr.af.mil
Dr. William Peter, FM Tech., Fairfax, VA,
    peter@langmuir.eecs.berkeley.edu
Dr. John Verboncoeur, U.C. Berkeley, johnv@langmuir.eecs.berkeley.edu
Dr. Thomas Gladd, ntgladd@langmuir.eecs.berkeley.edu
Dr. V.P. Gopinath, U.C. Berkeley, venkates@langmuir.eecs.berkeley.edu

Communications to be to birdsall@eecs.berkeley.edu, with FAX of your models to (510) 642-6330.

OOPIC Input Files

- cmaser.inp
- dcdis.inp
- default.inp
- dring.inp
- ebeam.inp
- gas.inp
- rzgrating.inp
- hollow.inp
- klysimple.inp
- klystron.inp
- plsource.inp
- xybeam.inp
- waveguid.inp

revised: September 10, 1995

cmaser.inp

I. Objective

cmaser.inp is a model of a Cerenkov Maser, or a travelling wave tube. The objective is to model a device examined by Scott A. Von Laven of Dartmouth College in his thesis "Characterization of a Cerenkov Maser", April, 1982.

II. Configuration

This electromagnetic simulation is in the Z-R coordinates (cylindrical geometry). The simulated device is a tube which has a 1.875cm dielectric inner lining coating a metal conductor starting at radius 6.25cm. The relative dielectric constant of the lining is 4.2. A hollow electron beam (inner radius .625cm, outer radius 4.0625cm) of current 7.5A and velocity .7c.

An exit port for EM radiation is on the right hand wall from radius 4.375cm to 6.25cm. This is just behind the dielectric. The beam itself is collected by a metal wall on the right hand side.

III. Discussion

The velocity of the electron beam is larger than the speed of light in the dielectric, which causes the electrons to emit radiation when they pass near it. This interaction produces waves in the millimeter to centimeter range, primarily in the TM01 mode.

The device from Von Laven's thesis is slightly different from the one simulated. In Von Laven's device:

a) the beam goes all the way out to the dielectric (we don't want the surface to charge so we do not allow it)

b) the beam does not strike a metal plate to stop it (we do that because of the difficulty of removing a beam through a port in an electromagnetic simulation)

c) the dielectric thickness is 2.0cm not 1.875cm (1.875 is a convenient thickness because it fits well on the finite mesh)

Waves in the beam are excited by noise. The growth rate for the TM01 mode is such that one can observe the mode spontaneously arising as the beam propagates. By changing the beam velocity one may determine the dispersion relation for the device.

The simulated device's dispersion is slightly different from what Von Laven reported in his thesis (page 7): the points observed are consistent with a slightly higher cutoff frequency than the TM01 mode expected. Perhaps this can be explained by the thinner dielectric: cutoff frequency in a waveguide is inversely proportional to the square root of the dielectric constant. With less dielectric in the guide, perhaps the cutoff would be higher.

Authors: Peter Mardahl, Keith Cartwright, John Verboncoeur, C.K. Birdsall.

References:

Von Laven, Scott A. "Characterization of a Cerenkov Maser", Dartmouth College, Hanover, N.H. 03755

Cerenkov Maser
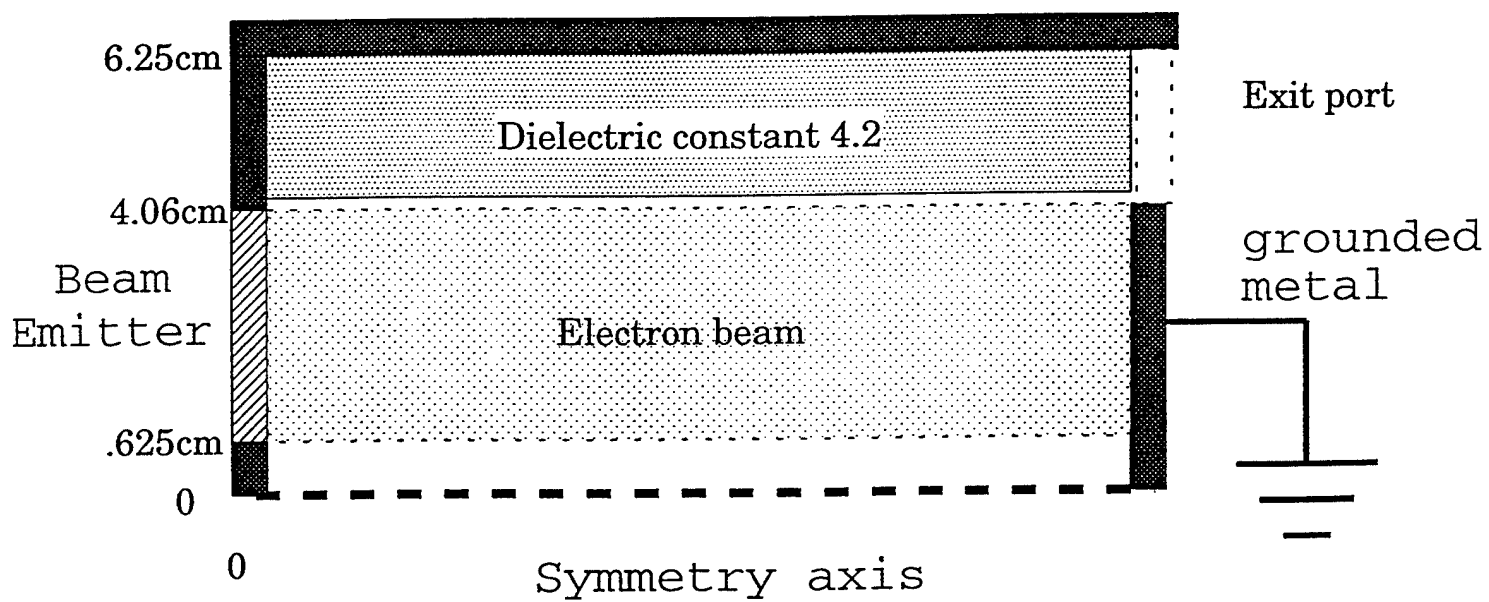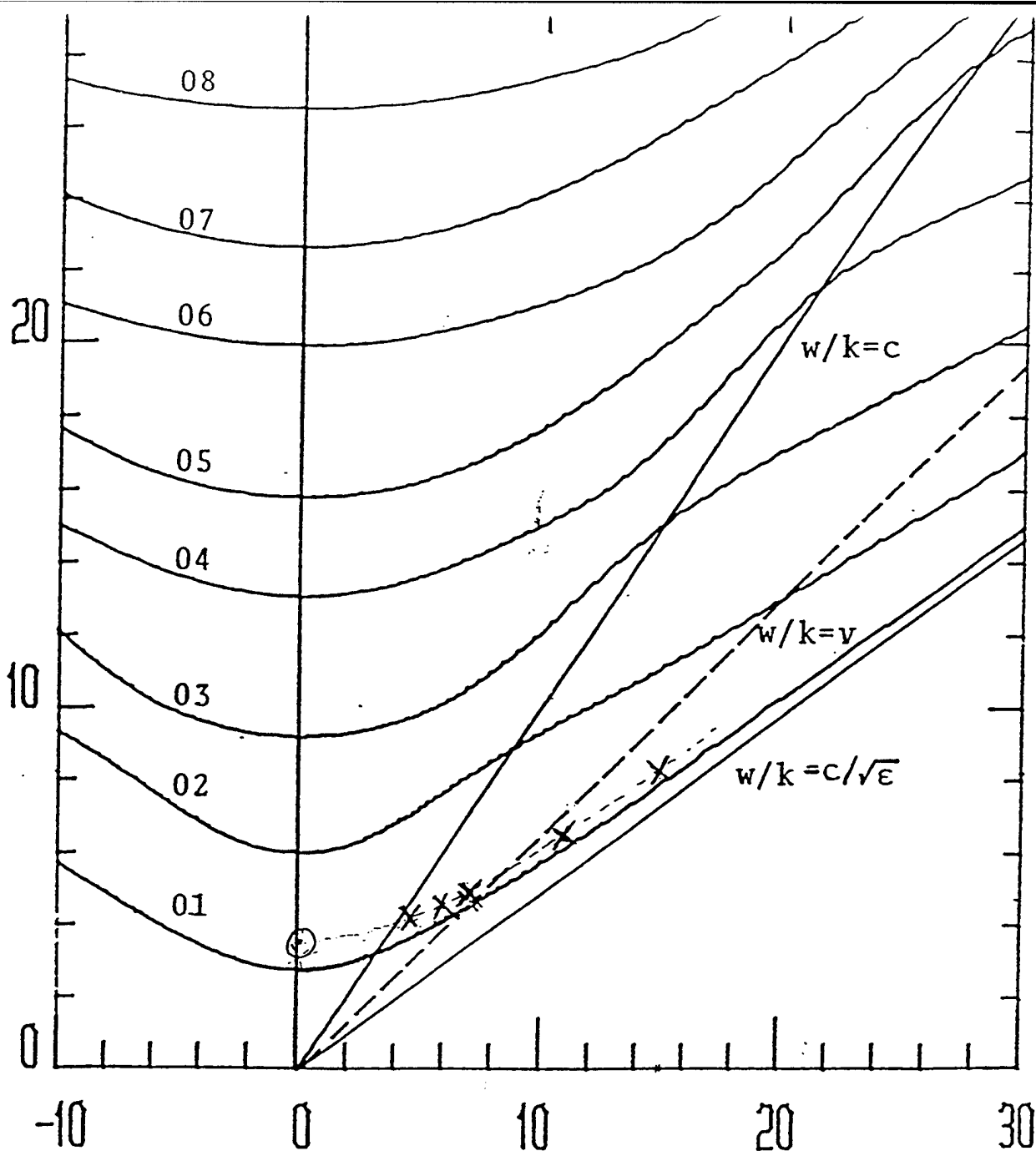
Fig. 2.1. TM$_{0n}$ dispersion curves for a 12.5 millimeter diameter waveguide with a two millimeter thick annular liner of boron nitride (dielectric constant=4.2). The beam line (dotted line) must lie between the vacuum and dielectric light lines (solid lines).

From: → "Chacterization of a Cerenkov Maser" Scott A. Von Laven Dartmouth College Page 7

```
Gap
{
        j1 = 25
        k1 = 20
        j2 = 35
        k2 = 20
        normal = -1
        frequency = 1.46e11
        phase = 0
        A = 0
        C = 0
}
Conductor
{
        j1 = 35
        j2 = 200
        k1 = 20
        k2 = 20
        normal = -1
}
Conductor
{
        j1 = 200
        k1 = 14
        j2 = 200
        k2 = 0
        normal = -1
}
ExitPort
{
        j1 = 200
        j2 = 200
        k1 = 14
        k2 = 20
        normal = -1
        EFFlag = 1
        name = Right Hand side exit port
        C = 0
}
DielectricRegion
{
        er = 4.2
        j1 = 0
        k1 = 14
        j2 = 200
        k2 = 20
}
CylindricalAxis
{
        j1 = 0
        k1 = 0
        j2 = 200
        k2 = 0
        normal = 1
}
```

rzgrating.inp

1. Objective

The input file **rzgrating.inp** models a cylindrical grating slow wave device. It demonstrates a number of interesting phenomena, including the following:

1. Magnetic beam dump.

2. Noise excitation of a waveguide mode.

3. Interaction of a slow wave structure with a beam.

2. Configuration

The configuration is shown in Fig. 2.1. The device consists of an axisymmetric right circular cylinder, 10 cm in length, 1.5 cm in radius. There are 7 conductive disks in the grating structure, each disk measures 5 mm axially and 4.14 mm vertically. The walls are ideal conductors, with a cathode (BeamEmitter) on the left edge, extending from $r = 8.8$ to 10.3 mm at $z = 0$. The BeamEmitter emits a uniform beam of positrons at $V = 48.3\,\text{kV}$ ($v/c = 1/3$), $I = 10$ A. The background magnetic field is 10 T, and there is a beam dump as shown in the Figure. The field solve is electromagnetic.

3. Discussion

The beam passes close to the grating in order to couple with the slow wave circuit. The interaction in this case is weak, and the beam is only slightly perturbed. The modulation of the axial velocity is shown in the phase space plots. The power output is shown in the Poynting plots obtained by integrating the Poynting flux through the right boundary (ExitPort).
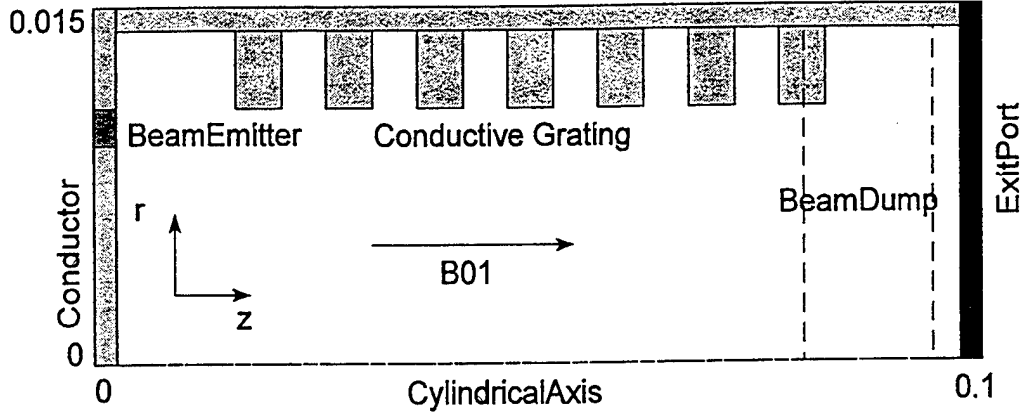
Figure 2.1: Grating traveling wave tube. All measurements are in m.

A beam dump turns the beam from an axial direction to deposit it on the collector (Conductor) on the outside wall. The beam dump field is given by

$$\mathbf{B}(r,z)/B_0 = \hat{\mathbf{z}}\cos\left(\frac{\pi\left(z - z_0\right)}{2l}\right) + \hat{\mathbf{r}}\frac{\pi r}{4l}\sin\left(\frac{\pi\left(z - z_0\right)}{2l}\right),$$

where B_0 is the axial field for $z < z_0$ and l is the axial length of the beam dump. Dumping the beam allows the use of a full wall ExitPort, which cannot operate correctly in the presence of particle current.

Authors: J. P. Verboncoeur (University of California, Berkeley)
Revised: 09-10-95
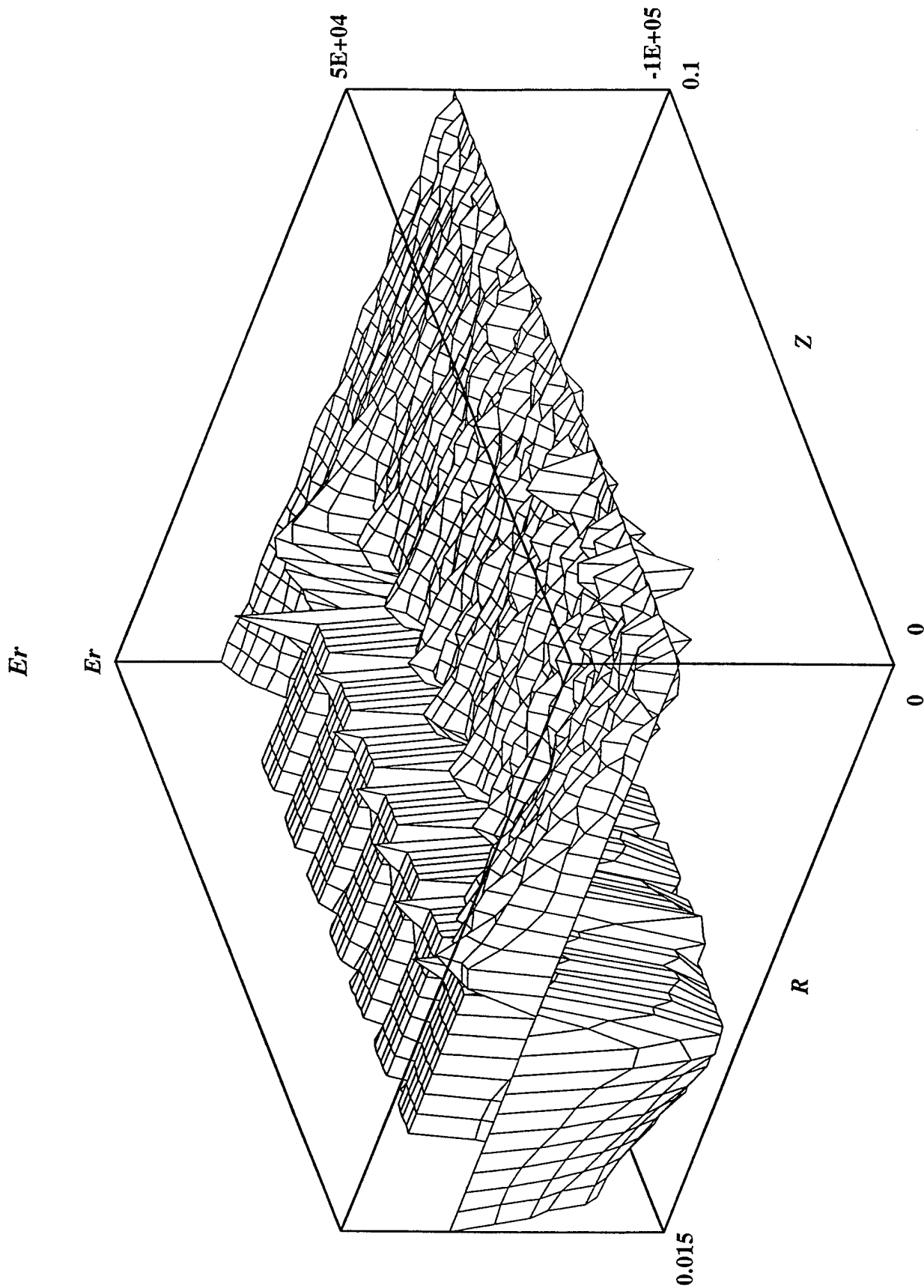
UZ vs Z, all species
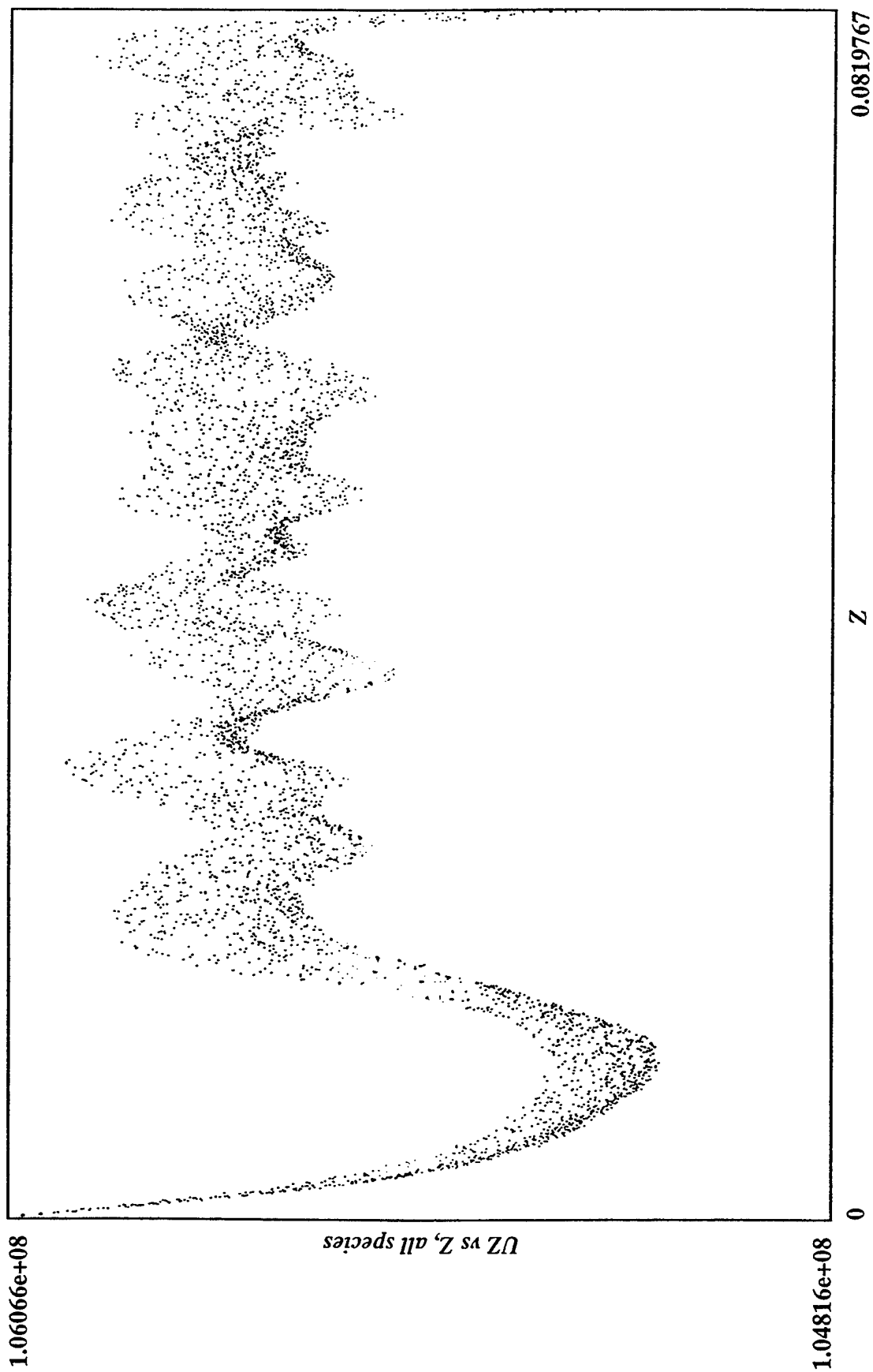
IV. Plasma & Microwave Seminars 1995

Monday 01-30-95
4:00-5:00pm

Hogan Room, Cory Hall

Particle Deposition in a Supersonic Flow at Low Pressure

Dr. J. J. Oh, Samsung

Deposition of particles, suspended in supersonic gas flows, onto the impaction plane in low pressure has been studied numerically. The axisymmetric compressible Navier-Stokes equations were employed to compute supersonic flows and the Lagrangian trajectory model was used for the particle phase. The effect of freestream pressure and particle size on the deposition process onto the impaction surface was investigated. The local characteristics of deposition were also demonstrated in terms of particle size and freestream pressure.

EECS 298-33
PTSG Seminar

Monday 02-06-95
4:00-5:00pm

Hogan Room, Cory Hall

Design of a Large Area Plasma Source for Flat Panel Display Processing

M. A. Lieberman, University of California-Berkeley

The design of a rectangular (30" x 27") uniform high density plasma source will be described. Possible methods of powering this source include inductive rf excitation and microwave excitation using standing or traveling waves.

Deposition of SiOF Films with Low Dielectric Constants

Takashi Fukada
Semiconductor Research Department,
Sumitomo Metal Industries

Monday 27 Feb 1995
299 Cory Hall, 5-5:30 PM

The talk will cover ECR Plasma CVD Process for ULSI Fabrication. In addition, some information about a surface wave coupled plasms source will also be covered.

Pulsed Electron Gun For Time-resolved Absorption Spectroscopy

Xiao Pu

4-5 PM, 557 Cory Hall
6 March 1995

In order to do the time-resolved absorption spectroscopy of transient defects induced by electron excitation, we are motivated to develop a short pulse electron beam gun. For the preliminary test gun we used the 4th harmonic (266nm) of a Nd: YAG Laser to excite an AL photocathode. This delivers electron packets with a duration of 5nsec at energies of 1kev. Our goal is to achieve 1psec electron pulses.

Topics to be presented include:
* Comparisions between our photon-electron system and other cold Cathode emission e-guns
* Electron gun design and set up
* Radiation effects in wide band gap materials
* Pump-probe technique for observing time-resolved effects
* Planar waveguide system for probe beam collection and detection

Further works will be done using the electron gun in the areas of ultra- fast spectroscopy of self-trapped exciton luminescences in Alkali-Halides, and also as pulsed soft X-ray source.

Review of Ion Energy Distributions in RF Plasma Reactors

E. Kawamura, V. Vahedi, M. A. Lieberman,and C. K. Birdsall

Monday, 3 April 1995
Hogan Room, Cory Hall
4-5 PM

We present a historical review and discussion of previous works on ion energy and angular distributions (IED and IAD) arriving at the target in the collisionless regime. This regime is of great interest to experimentalists and modelers studying the new generation of high density sources in which the sheath is much thinner than in the conventional RIE systems. The purpose of the review is to assess what has been done so far, and to determine what further work has to be done to control IEDs. We also wish to clarify some issues about sheaths in high density systems. Having determined the important parameters, we will show some particle-in-cell simulation results of a capacitively coupled rf plasma. The results show that ion modulations in an rf sheath significantly affect the IEDs when $tion/trf < 1$, where $tion$ is the ion transit-time and trf is the rf period.

EECS 298-33
PTSG Seminar

Monday 04-10-95
4:00-5:00pm

Hogan Room, Cory Hall

Micromachined Hot-Filament Vacuum Devices

Kirt R. Williams and Prof. Richard S. Muller

In this project we are studying micro-machined vacuum devices based on thermionic emission (i.e., using a hot cathode) and the technology to fabricate them. These devices have application as sensors and in amplifying and logic circuits (i.e., as vacuum tubes), and are expected to be able to withstand higher temperatures and more intense radiation than conventional semiconductor devices. They can also be used as intense, very localized broadband radiation sources in spectroscopic sensors.

This talk will cover device theory, fabrication, test results, and what we hope to accomplish in simulations.

For more information and some photographs on this research project, see Kirt's World-Wide Web home-page at   http://www-bsac.eecs.berkeley.edu/users/williams/

EECS 298-33
PTSG Seminar

Monday 04-24-95
4:00-5:00pm

Hogan Room, Cory Hall

Traveling Wave Tubes - An old technology?

Yehuda Goren, Teledyne Inc.

Significant progress has been made since the invention of the Traveling Wave Tube (TWT) about 40 years ago. If progress is to continue an understanding of the physics underlying the operation of a TWT is required. Areas of interest include the surface physics of electron sources, the many-body problem of an electron beam in interaction with an electromagnetic field, the physics of permanent magnetic materials as well as a variety of thermo-mechanical and heat conduction problems. All must be dealt with in the design of a modern TWT.

In this seminar we shall try to touch on a few of these subject areas. We shall describe the ways we are approaching these problems from an engineering as well as from a numerical simulation viewpoint, while at the same time identifying some of the limits in our understanding of the physical process involved.

EECS 298-33
PTSG Seminar

Monday 05-01-95
4:00-5:00pm

Hogan Room, Cory Hall

Simulation of Ion Acoustic Waves

K. Cartwright

Preliminary results showing ion acoustic solitons in ES1, PDP1, and OOPIC will be presented. The ES1 results show the growth of ion acoustic waves due to the ion acoustic instability, the results are compared to the linear theory form Krall and Trivelpiece. After nonlinear growth takes place a long term stable wave is formed. This wave is shown to be a soliton of the form $3cSech^2[(c/2)^{1/2}(x - c\tau]$ Where the soliton has the speed c, amplitude 3c, and half-width $(2/c)^{1/2}$. These phenomenon are ion in nature so linear boltzmann electrons are used. In PDP1 ion acoustic solitons are shown to reflect off the sheath. The data analysis developed for the simpler ES1 examples will be extended to the bound case. These waves are launched from one side of the system with a current source with a frequency less than the ion plasma frequency. The coefficients of reflection and transmission as a function of the wavelength is shown. These coefficients are compared to experiments by Schott and theory by Ibrahim and Kuehl. These results are expand in OOPIC to have waves incident at oblique angles. These the oblique angle results can be compared to waves incident at normal angle using the theory in a paper by Watanabe, Matsuoka, and Yajima.

EECS 298-33
PTSG Seminar

Monday 05-08-95
4:00-5:00pm

Hogan Room, Cory Hall

**Phase Locking of High Power Microwave Vircator and Magnetron
Oscillators: Modeling and Experiments**

David Price, Litton Inc.

Very high peak or average microwave power have been realized by phase-locking individual microwave oscillators. In these recent experiments drive powers of the master oscillators are comparable to or even larger than those of the slave oscillators. (This is in contrast to most conventional phase-locking configurations characterized by small master/slave ratios.) Coupled oscillators models based on the Van der Pol eqwuation are compared to experiments on gigawatt level vircator and magnetron microwave generators. Various elements of the coupling phenomenology (frequency pulling and locking, transitions to and from stable phase-locked states, etc.) are both predicted and observed.

Simulation of Transmitted Current in a Cylindrical Cross Field Diode

Venkatesh P. Gopinath, UC Berkeley

The transmitted current in a crossed-field gap has been characterized analytically by a number of authors ˉdimensional PIC simulations of a planar cross-field diode in the region near $\mB = B\_hull$ have been explored by Verboncoeur et. al.ˉIt was shown that for mono-energetic electrons, the transmitted current shows a rapid transition when the injected current exceeds the critical current by just 1. This transition is not observed when the injected electrons are given temperatures as small as 1/10 eV.

In this study cylindrical cross-field diodes have been simulated in one and two dimensions using the simulation programs xpdc1 and xpdc2. The results are compared to analytical theory for accuracy. The behavior of the diodes is studied for two different radii ratios (2,5) around the region of hull cutoff. The results obtained are contrasted with earlier simulations conducted on planar cross field diodes Verboncoeur et. al.ˉLau et. al Hull cut-off field for two different inner/outer (2,5) conductor ratios is studied.

A spectral comparison of methods of removing errors in Gauss's Law

P. Mardahl, University of California - Berkeley

Non-charge conserving current collection algorithms for relativistic PIC plasma simulations can cause errors in Gauss's law. These errors arise from violations of the continuity equation, div(J) = - d(rho)/t The error in the current collection algorithm can be partially corrected by a number of schemes. Here we compare the iterative dynamic ADI scheme of Hewett with the modified Marder scheme of Langdon. The effect of each method on the the spectrum of the error is examined. Computational efficiency and accuracy of the two techniques is compared. Particular cases of interest include corrections in electromagnetic relativistic beam simulations. In addition, the spectral comparison provides insight into the behavior of the schemes applied. This work may provide insight into optimization of dynamic ADI timesteps for supression of selected wavelengths and application of spectral filtering, resulting in improved performance.

Kinetic Modeling of bounded plasmas via "kinetic trajectory simulation"
Basic concepts and applications to 1d2v collisional and 2d3v
collisionless Q-machine models

Dr. Siegbert Kuhn
Plasma Energy Physics Group
Institute for Theoretical Physics
University of Innsbruck
Innsbruck, Austria

August 9 1994, 3-3:45 pm, 181M Cory Hall (Mezzanine Library)

Realistic kinetic modeling of bounded plasmas --- or, more appropriately, {it bounded plasma systems} --- is of interest in both fundamental plasma research and applied disciplines, such as plasma technology and fusion research. By definition, a "bounded plasma system" (BPS) is characterized by the self-consistent interaction of the plasma itself, its material boundaries, and the related external circuit(s). {it Particle simulation} has by now become a routine tool for BPS studies, as is most impressively demonstrated by the widespread and ever increasing usage of the PD ("plasma device") series of bounded-plasma particle codes developed at U.C. Berkeley. Nevertheless, alternative methods are still desirable and needed.

This talk will be concerned with such an alternative, more theory-oriented approach, which has been termed "kinetic trajectory simulation". Along the collisionless single-particle trajectories are calculated, by means of "trajectory integration", velocity distribution functions, rather than moving single particles as in particle simulation. This approach allows quite naturally for realistic electron-to-ion mass ratios, the inclusion of boundary and initial conditions, and high resolution in both configuration and velocity spaces. While kinetic trajectory simulation it is not yet as versatile and universally applicable as particle simulation, the results available so far are sufficient to demonstrate some of these favorable features.

EECS 298-9
PTSG Seminar

Monday 08-28-95
3:00-4:00pm

Wang Room, Cory Hall

Revised Generalized Child-Langmuir Law

Siegbert Kuhn
Plasma & Energy Physics Group
Institute for Theoretical Physics
University of Innsbruck
Innsbruck, Austria

This talk is concerned with recent work by N. Jelic, performed at Innsbruck University. A set of approximate but very reliable algebraic equations defining the potential distribution inside a plane hot-cathode diode is derived. As a result, the current-voltage characteristic of the diode is expressed in the form of a generalized Child-Langmuir law. Unlike the "standard" generalized Child-Langmuir law, the present result provides an explicit functional dependence of the diode current on the external diode parameters.

EECS 298-9
PTSG Seminar

Wednesday 09-06-95
3:00-4:00pm
181M, Cory Hall

Binary States in the High-Temperature Knudsen Thermionic Energy Convertor and Possible Applications

Siegbert Kuhn
Plasma & Energy Physics Group
Institute for Theoretical Physics
University of Innsbruck
Innsbruck, Austria

abstract unavailable

EECS 298-9
PTSG Seminar

Monday 10-02-95
3:00-4:00pm

Wang Room, Cory Hall

Induct95 and Applications to Plasma Processing

P. A. Vitello, Lawrence Livermore National Laboratory

Vitello will describe the code fluid plasma simulation, Induct95. Induct95 solves electron and ion fluid equations, as well as Poisson's equation, on a mesh. It also can include a low frequency electromagnetic solver for modeling inductively coupled plasmas. Applications to rf discharges in argon and chlorine will also be discussed.

EECS 298-9
PTSG Seminar

Monday 10-30-95
3:00-4:00pm
HOGAN Room, Cory Hall

Similarity of Limiting Currents in Planar and Cylindrical Crossed-Field Diodes

V. P. Gopinath, UC Berkeley

Limiting current in a planar crossed-field gap has received attention for over 70 years for B_{Hull} (A. W. Hull, Phys. Rev. 18, 31 (1921), Y. Y. Lau, P. J. Christenson and D. Chernin, Phys. Fl. B 5, 4486 (1993), and recently for $B > B_{Hull}$ (P. J. Christenson and Y. Y. Lau, Phys. Plasmas 1, 12 (1994)). Simulations indicate the ratio of critical to Child-Langmuir current, $I_C(B)/I_{CL}$, scales similarly with magnetic field in planar and

cylindrical geometries, up to $r_{anode}/r_{cathode} = 5$. The comparison is performed above and below Hull cutoff, for small and large radius ratios.

One-dimensional simulations of a planar crossed-field diode in the region near $B = B_{Hull}$ indicate a transition in current with strong sensitivity to the initial velocity distribution of emitted electrons, f(v). Effects of f(v) and secondary emission coefficients at the cathode and anode are explored.

EECS 298-9
PTSG Seminar

Monday 11-20-95
3:00-4:00pm

Wang Room

Accelerated PIC-MCC Workshop

Prof. Jae-koo Lee, Pohang University of Science and Technology

Prof. Lee will discuss techniques applied to plasma problems with a wide spread in timescales, including a fluid Monte-Carlo hybrid scheme and a global model. He will describe ideas for improvement of present schemes.

In addition general discussion on techniques for accelerating PIC-MCC schemes. At this meeting, we will select some initial candidate methods for testing.

EECS 298-9
PTSG Seminar
Monday 11-27-95
3:00-4:00pm

Wang Room

An Adaptive Mesh Refinement Algorithm for Solving Poisson's Equation Using Multigrid

D. Martin, U.C. Berkeley

A method for using Adaptive Mesh Refinement (AMR) to solve Poisson's equation will be presented. AMR allows concentration of computational resources where they are needed by locally refining the finite difference mesh where the error is high. This method is adaptive in the sense that it is able to generate its own refined grids, based on an error estimation criterion, and then solve the problem on the hierarchy of coarse and refined grids. Issues involved include using Richardson extrapolation as an error estimation criterion, efficient grid generation, multigrid solution of Poisson's equation on a composite coarse-fine mesh, and communication between coarse and fine grids. Our implementation of this algorithm will also be discussed, including the use of the BoxLib library of C++ classes, developed by the Applied Math Group at LLNL for the development of block structured finite difference codes.

EECS 298-33
PTSG Seminar
Monday 05-01-95
4:00-5:00pm

Hogan Room, Cory Hall

Simulation of Ion Acoustic Waves

K. Cartwright

Preliminary results showing ion acoustic solitons in ES1, PDP1, and OOPIC will be presented. The ES1 results show the growth of ion acoustic waves due to the ion acoustic instability, the results are compared to the linear theory form Krall and Trivelpiece. After nonlinear growth takes place a long term stable wave is formed. This wave is shown to be a soliton of the form $3c \ \text{Sech}^2[(c/2)^{1/2} \ (x-cau)]$. Where the soliton has the speed c, amplitude 3c, and half-width $(2/c)^{1/2}$. These phenomenon are ion in nature so linear boltzmann electrons are used. In PDP1 ion acoustic solitons are shown to reflect off the sheath. The data analysis developed for the simpler ES1 examples will be extended to the bound case. These waves are launched from one side of the system with a current source with a frequency less than the ion plasma frequency. The coefficients of reflection and transmission as a function of the wavelength is shown. These coefficients are compared to experiments by Schott and theory by Ibrahim and Kuehl. These results are expand in OOPIC to have waves incident at oblique angles. These the oblique angle results can be compared to waves incident at normal angle using the theory in a paper by Watanabe, Matsuoka, and Yajima.

EECS 298-33
PTSG Seminar

Monday 05-08-95
4:00-5:00pm

Hogan Room, Cory Hall

**Phase Locking of High Power Microwave Vircator and Magnetron
Oscillators: Modeling and Experiments**

David Price, Litton Inc.

Very high peak or average microwave power have been realized by phase-locking individual microwave oscillators. In these recent experiments drive powers of the master oscillators are comparable to or even larger than those of the slave oscillators. (This is in contrast to most conventional phase-locking configurations characterized by small master/slave ratios.) Coupled oscillators models based on the Van der Pol eqwuation are compared to experiments on gigawatt level vircator and magnetron microwave generators. Various elements of the coupling phenomenology (frequency pulling and locking, transitions to and from stable phase-locked states, etc.) are both predicted and observed.

Simulation of Transmitted Current in a Cylindrical Cross Field Diode

Venkatesh P. Gopinath, UC Berkeley

The transmitted current in a crossed-field gap has been characterized analytically by a number of authors ¨dimensional PIC simulations of a planar cross-field diode in the region near $B = B_{hull}$ have been explored by Verboncoeur et. al.¨It was shown that for mono-energetic electrons, the transmitted current shows a rapid transition when the injected current exceeds the critical current by just 1%. This transition is not observed when the injected electrons are given temperatures as small as 1/10 eV.

In this study cylindrical cross-field diodes have been simulated in one and two dimensions using the simulation programs xpdc1 and xpdc2. The results are compared to analytical theory for accuracy. The behavior of the diodes is studied for two different radii ratios (2,5) around the region of hull cutoff. The results obtained are contrasted with earlier simulations conducted on planar cross field diodes Verboncoeur et. al.¨Lau et. al Hull cut-off field for two different inner/outer (2,5) conductor ratios is studied.

A spectral comparison of methods of removing errors in Gauss's Law

P. Mardahl, University of California - Berkeley

Non-charge conserving current collection algorithms for relativistic
PIC plasma simulations can cause errors in Gauss's law. These errors
arise from violations of the continuity equation,
$$div(J) = -\partial(\rho)/\partial t$$
The error in the current collection algorithm can be partially
corrected by a number of schemes. Here we compare the iterative
dynamic ADI scheme of Hewett with the modified Marder scheme of
Langdon.
The effect of each method on the the spectrum of the error is
examined. Computational efficiency and accuracy of the two techniques
is compared.
Particular cases of interest include corrections in electromagnetic
relativistic beam simulations. In addition, the spectral comparison
provides insight into the behavior of the schemes applied. This
work may provide insight into optimization of dynamic ADI timesteps
for supression of selected wavelengths and application of spectral

V. Plasma Computer Experiments Lab (new course)
(Abstract same as presented at GEC) Outline follows

Plasma Computer Experiments Teaching Laboratory* C.K. BIRDSALL, V.P. GOPINATH, J. VERBONCOEUR, Univ. of Calif. Berkeley CA 94720 - A plasma simulation laboratory employing 1d3v PIC-MCC codes has been used to enhance a plasma lecture course, both of which emphasize the plasma physics of discharges and materials processing.

Simulations inserted into lecture courses on an occasional basis have long proven to be valuable teaching tools. The present weekly laboratory draws on 20 computer experiments from a workbook, companion to the lecture text.[1] The homework projects range from diffusion to DC and RF discharges in argon, with many questions asked, tracking the lectures.

The codes used are XES1, XPDP1 and XPDC1 (WWW http://ptsg.eecs.berkeley.edu) with numerous input files. The course does not require a background in numerical analysis, or recompilation of the software. All projects are performed by modifying standard sets of (laboratory) parameters, such as lengths, voltages, frequencies, and gas pressure. A computer demonstration will be available, as well as the workbook and examples of student homework. *Work supported in part by ONR Contract FD-N00014-90-J-1198 1."Principles of Plasma Discharges and Materials Processing", M. A. Lieberman and A. J. Lichtenberg, Wiley, 1994.

PLASMA COMPUTER EXPERIMENTS LABORATORY(1995)
PLASMA THEORY AND SIMULATION GROUP (PTSG)
PROF. C.K. BIRDSALL, DR. V.P. GOPINATH, DR. J.P. VERBONCOEUR
EECS DEPARTMENT, CORY HALL,
UNIVERSITY OF CALIFORNIA, BERKELEY, CA 94720-1770
Copyright 1995 by Regents, University of California

FOREWARD
PREFACE
ACKNOWLEDGMENTS
CONTENTS

Videotapes of Spring 1995 may be viewed in 205 McLaughlin. Also available for $279; contact Pam Atkinson, atkins@coe.berkeley.edu (Ask for EECS 298-9 tapes, Spring 1995

Course Notes available: Contact birdsall@eecs.berkeley.edu

Plasma Computer Experiments Laboratory.12.8.95

PLASMAS AT THE EDGE

C.K. Birdsall, Plasma Theory and Simulation Group

EECS Department, U.C. Berkeley, CA 94720-1770

Abstract

We will explore bounded plasmas, with real walls, and external circuits which exhibit a richness of behavior quite different from that of bulk plasmas. We will use a fast desk-top computer to do a number of 1d3v simulations and visualizations, using our Berkeley PIC-MCC codes (XES1 and XPDP1).

For theoretical fun we begin with an unbounded example, **Landau damping,** checking out trapping or not in phase space.

Then we will do a **warm bounded afterglow plasma** in a shorted diode, observing the sheath, electron trapping, plasma and series resonances, plus some interesting structure. We will add a DC **magnetic field** and see the plasma potential become negative.

Next is a **Q machine** with a positively biased collector, with a violent turbulent phase-space instability, with two time scales (ion relaxation and electron plasma frequency).

Last in this 1d3v series is an **RF driven capacitively coupled argon discharge,** collisional, with $V_{RF} \gg kT/e$, that is, driven very hard, with $\omega_{pi} < \omega_{RF} \ll \omega_{pe}$, useful in plasma processing (driving ions into a target).

In 2d3v, we will show a video of K. Theilhaber's **bounded magnetized plasma,** with shear flow in the sheath, leading to a **Kelvin-Helmholtz instability** and vortex formation. The question of particle transport is answered by Parker et al.'s vortex potential modeling, plus a small wave, following test particles: Bohm-like.

This exploration is to whet your appetite for more, for doing such yourselves.

4FP01

Two Dimensional Investigation of Ion Acoustic Waves Refection from the Sheath

K.L. Cartwright and C.K. Birdsall

Department of Electrical and Computer Engineering
University of California, Berkeley CA 94720

Preliminary results show that oblique ion waves propagate from the bulk plasma into and all the way through the sheath in both 1D and 2D simulation. These waves are launched from one side of the system with a AC voltage or a current source with a frequency less than the ion plasma frequency. Our one and initial two dimensional PIC simulations show the details of densities, potentials, fields, particle moments and time–distance plots of the average density minus the instantaneous density. From the time–distance plot the direction and magnitude of the ion acoustic wave is measured. From this the coefficients of reflection and transmission as a function of the incident angle is calculated. Our observations will be compared with laboratory experiments and theory.

4GP02

XPDC2-Rθ A Two Dimensional Electrostatic PIC Code

C. K. Birdsall, D. Cooperberg, V. P. Gopinath, P. Mirrashidi, V. Vahedi and J. Verboncoeur

Electrical Research Laboratory
University of California, Berkeley, CA 94720

A two dimensional particle-in-cell simulation has been written using a cylindrical R-θ Poisson field solver. The simulator is capable of simulating coaxial structures with and without a central conductor. In the presence of a central conductor, an external circuit consisting of V,I sources and R-L-C elements [1], can be self-consistently simulated with the plasma equations. The simulation model includes the PIC-MCC [2] package to model collisions between charged particles and neutral species. The field solve in the θ direction can be done using finite-difference or fourier transforms.

The simulator is currently being used to study the Diocotron and Kelvin-Helmholtz instabilities. The ability to generate movies to study time-varying phenomeneon will be discussed. In addition, comparisons with theory and 1D models will also be presented.

References

[1] J. P. Verboncoeur et. al., "Simultaneous Potential and Circuit Solution for 1D Bounded Plasma Particle Simulation Codes," *J. Comp. Phys.*, Vol 104, No. 2, Feb. 1993.

[2] V. Vahedi and M. Surendra "A Monte Carlo collision model for the particle-in-cell method: applications to argon and oxygen discharges," to appear in *Comp. Phys. Comm.* for publication.

6C05-06 *Invited*

OOPIC: Object Oriented Particle-in-Cell Code

J. P. Verboncoeur and the OOPIC team[†]

Electronics Research Laboratory
University of California, Berkeley 94720

OOPIC is an object oriented particle-in-cell (PIC) code framework designed as a testbed for PIC algorithms. OOPIC consists of three principal components: the graphical user interface (GUI), the expert advisor, and the physics kernel. The GUI includes a geometry editor, an interactive, windowing visualization system, printing and file output capability, and simulation control capability. The expert advisor handles parsing parameter input files, saving modified parameter sets, and applying rules and constraints to ensure the consistency of the simulation.

The physics kernel is a framework for diverse models which can be selected dynamically at run time. OOPIC currently includes electrostatic and electromagnetic field solvers, a Boltzmann electron option ($m_e \rightarrow 0$), cartesian and cylindrical non-uniform grids in two-dimensions. Particle modeling includes relativistic and non-relativistic optimizations, a number of models for collecting charge and current densities, and current corrections including full Poisson and Marder corrections. Boundary condiions in the electrostatic model include dielectrics and equipotential surfaces connected to ground via external RLC circuits. Electromagnetic boundary conditions include TEM, TE and TM wave launchers, a number of wave absorbing models, conductors, and surface impedance models. A number of particle emission models and symmetry boundaries work in both EM and ES, and any boundaries can be configured as complex internal structures.

OOPIC runs under the Windows operating system on 80x86 computers. The advisor and physics kernel also run under XGrafix, a basic visualization system, on Unix workstations.

[†] Also includes Berkeley Research Associates, FM Technologies, and George Mason University

ABSTRACTS OF TALKS AND POSTER PAPERS

PRESENTED AT IEEE ICOPS, MADISON WISC.

5-8 JUNE 1995

A spectral comparison of two methods of removing errors in Gauss' law in a 2-dimensional PIC plasma simulation.

P. Mardahl, J. Verboncoeur, C. K. Birdsall

Department of Electrical Engineering and Computer Science
University of California, Berkeley, CA 94720

Non-charge conserving current collection algorithms for relativistic PIC plasma simulations can cause errors in Gauss' law. These errors arise from violations of the continuity equation, $\nabla \cdot J = -\frac{\partial \rho}{\partial t}$.
Two techniques for removing these errors are examined and compared, the Marder correction, a method which corrects electric fields locally and primarily affects short wavelengths, and a divergence correction, which uses a Poisson solve to correct the electric fields so that Gauss' law is enforced.
The effect of each method on the the spectrum of the error (short wavelengths vs. long) are examined. Computational efficiency and accuracy of the two techniques is compared. Particular cases of interest include corrections in electromagnetic relativistic beam simulations.

References

[1] A.B. Langdon, "On enforcing Gauss' law in electromagnetic particle-in-cell codes." Computer Physics Communications, July 1992, vol.70 (no.3): 447-50.

[2] B. Marder, "A method for incorporating Gauss' law into electromagnetic PIC codes." Journal of Computational Physics, Jan, 1987, vol.68 (no.1): 48-55.

Issues in Providing Expert Advice for Users of a Particle-In-Cell Simulation Code

N. T. Gladd
Berkeley Research Associates
PO Box 241, Berkeley, CA 94710
and
J. P. Verboncoeur
U. C. Berkeley

The fully electromagnetic, 2 ½ D, OOPIC simulation code (Object Oriented Particle In Cell) will be demonstrated at this meeting and made publicly available later in the year for use on problems in vacuum electronic design. OOPIC is the product of a three year research effort to implement a sophisticated PIC simulation model with object-oriented programming techniques. In addition to its physics engine [1], OOPIC possesses a GUI/scientific-visualization system and an expert advisor system to aid users in formulating simulations.

Here we discuss issues involved in providing expert advice to users of a PIC simulation. The primary function of the expert advisor is to aid users in setting up parameters that "correctly" specify a simulation. Parameters here can mean geometrical configurations of conductors, emitters, wavelaunchers, etc., that model a particular physical device. Parameters can be numbers related to physical processes - either simple numbers such as the simulation particle mass or structured sets of numbers such as those required to specify a velocity distribution function. Parameters can also relate to choice or control of underlying algorithms.

Offering advice can be said to consist of politely imposing constraints on the various combinations of parametric values. We will discuss various methods for imposing those constraints including – starting the design process from preexisting correct configuations, permitting the step by step visual construction of simulation models with each geometrical element constrained to be legal, using rule based expert system techniques to impose limits and relations on combinations of parameters, and forcing trial configuations to pass various algorithmic tests before a simulation can be initiated.

Simulation of Transmitted Current in a Cylindrical Cross-Field Diode

V. P. Gopinath, J. Verboncoeur and C. K. Birdsall

Electrical Research Laboratory
University of California, Berkeley, CA 94720

The transmitted current in a crossed-field gap has been characterized analytically by a number of authors [1]- [3]. One dimensional PIC simulations of a planar cross-field diode in the region near $B = B_{hull}$ have been explored by Verboncoeur et. al. [4]. It was shown that for monoenergetic electrons, the transmitted current shows a rapid transition when the injected current exceeds the critical current by just 1%. This transition is not observed when the injected electrons are given temperatures as small as 1/10 eV.

In this study we will extend the simulation to one and two dimensional cylindrical geometries. The limiting current in the neighborhood of the Hull cut-off field for different inner/outer conductor ratios will be studied.

References

[1] C. K. Birdsall and W. B. Bridges, "Electron Dynamics of Diode regions," Academic Press, (1966).
[2] Y. Y. Lau, P. J. Christenson and D. Chernin "Limiting Current in an Crossed-Field Gap," *Phys. Fl. 1.5* 4486 (1993).
[3] A. W. Hull, "The Effect of Uniform Magnetic Fields on the Motion of Electrons Between Coaxial Cylinders," *Phys. Rev* 18, 31 (1921).
[4] J. P. Verboncoeur, M. Weber and C. K. Birdsall , "Transmitted Current in a Crossed-field Diode," Presented at the 36 APS Divison of Plasma Physics, Minneapolis, Nov 1994.

Review of Ion Energy and Angular Distributions in Capacitively Coupled RF Plasma Reactors

E. Kawamura[†], V. Vahedi[*], M. A. Lieberman[†], and C. K. Birdsall[†]

† Department of Electrical Engineering and Computer Science
University of California, Berkeley
Berkeley, CA 94720
* Lawrence Livermore National Laboratory, Livermore, CA 94550

We present a historical review and discussion of previous works on ion energy and angular distributions (IED and IAD) arriving at the target in the collisionless regime. This regime is of great interest to experimentalists and modelers studying the new generation of high density sources in which the sheath is much thinner than in the conventional RIE systems. The purpose of the review is to assess what has been done so far, and to clarify some issues about sheaths in high density systems. Having determined the important parameters, we will show some particle-in-cell simulation results of a dually excited capacitively coupled plasma in which the sheath ions roughly see the scaling as in high density sources. The results show that when $\tau_{ion}/\tau_{rf} < 1$, the oscillating voltage and width of the rf sheath significantly affect the IEDs, where τ_{ion} is the ion transit-time and τ_{rf} is rf period.

IEDs at 10MHz(wider distribution) and 100MHz:
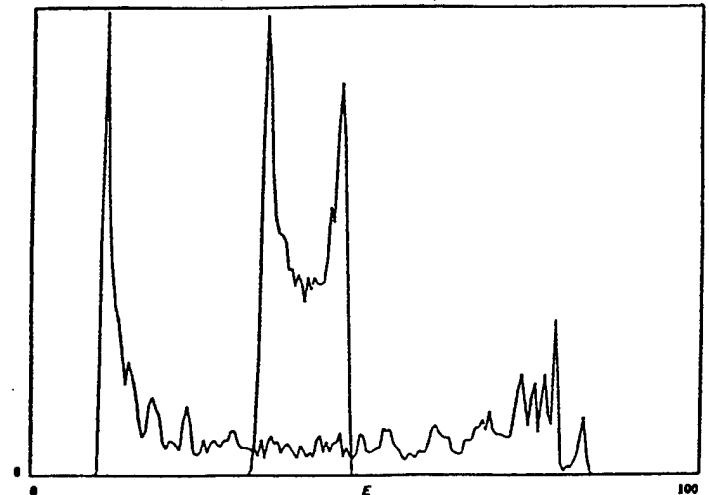
First International Crossed Field Diode Workshop, August 1995,Ann Arbor, Michigan.

Transverse Asymmetry in a Crossed-Field Diode

K. Cartwright, J. P. Verboncoeur, V. P. Gopinath and C. K. Birdsall
Electronics Research Laboratory
University of California, Berkeley, CA 94720

Recent studies of cylindrical crossed-field diodes indicate the transverse dimension may play a role in delaying onset of virtual cathode oscillations for currents above the limiting current [1]. Transverse space charge effects in smooth diodes can result in fields which warm the electrons. Thermal emission of electrons damps virtual cathode oscillations, as shown by Birdsall [2]. The effects of the transverse dimension are explored using two-dimensional planar and cylindrical PIC codes.

References

[1] V. P. Gopinath, J. P. Verboncoeur and C. K. Birdsall, "Simulation of Transmitted Current in a Cylindrical Cross-Field Diode", *Proc. 22nd IEEE Int. Conf. Plasma Sci.*, Madison, WI (1995).

[2] C. K. Birdsall and W. B. Bridges, *Electron Dynamics of Diode Regions*, Academic Press (1966).

Similarity of limiting currents in planar and cylindrical crossed-field diodes

V. P. Gopinath, J. P. Verboncoeur and C. K. Birdsall
Electronics Research Laboratory
University of California, Berkeley CA 94720

Limiting current in a planar crossed-field gap has received attention for over 70 years [1]-[3] for $B < B_{Hull}$, and more recently for $B > B_{Hull}$ [4]. Recent simulations indicate the limiting current curve in cylindrical geometry follows the planar theory closely for $r_{anode}/r_{cathode} \leq 5$ [5]. The comparison between cylindrical geometry and planar theory is extended to the region above Hull cutoff, and large radius ratios are investigated for both regions.

One-dimensional simulations of a planar crossed-field diode in the region near $B = B_{Hull}$ have shown current transition and strong sensitivity to initial conditions of emitted electrons [6]. Similar transition in cylindrical geometry is explored, for both cold drifting emission and thermal emission.

References

[1] A. W. Hull, "The Effect of Uniform Magnetic Fields on the Motion of Electrons Between Coaxial Cylinders", *Phys. Rev.* 18, 31 (1921).

[2] C. K. Birdsall and W. B. Bridges, *Electron Dynamics of Diode Regions*, Academic Press (1966).

[3] Y. Y. Lau, P. J. Christenson and D. Chernin, "Limiting Current in a Crossed-Field Gap", *Phys. Fl. B* 5, 4486 (1993).

[4] P. J. Christenson and Y. Y. Lau, "Transition to Turbulence in a Crossed-Field Gap", *Phys. Plasmas* 1, 12 (1994).

[5] V. P. Gopinath, J. P. Verboncoeur and C. K. Birdsall, "Simulation of Transmitted Current in a Cylindrical Cross-Field Diode", *22nd IEEE Int. Conf. on Plasma Sci.*, Madison, WI (1995).

[6] J. P. Verboncoeur, M. Weber and C. K. Birdsall, "Transmitted Current in a Crossed-Field Diode", *36th APS Div. Plasma Phys. meeting*, Minneapolis, MN (1994).

Rapid current transitions in a crossed-field diode at the Hull cutoff

J. P. Verboncoeur and C. K. Birdsall
Electronics Research Laboratory
University of California, Berkeley, CA 94720

The transmitted current in a vacuum crossed-field gap has been characterized analytically by a number of authors [1], [2], [3] and [4]. The transmitted current at the Hull cutoff, $B = B_{Hull}$, is explored using a one dimensional PIC simulation. For mono-energetic (cold) emission, a rapid transition in transmitted current is observed when the injected current exceeds the critical current by just 1%. The transition is found to be very sensitive to the electron temperature at the cathode, even for $T_e/V = 10^{-5}$, where T_e is the emitted electron temperature and V is the anode voltage.

References

[1] A. W. Hull, "The Effect of a Uniform Magnetic Field on the Motion of Electrons Between Coaxial Cylinders", *Phys. Rev.* 18, 31 (1921).

[2] C. K. Birdsall and W. B. Bridges, *Electron Dynamics of Diode Regions*, Academic Press (1966).

[3] Y. Y. Lau, P. J. Christenson and D. Chernin, "Limiting Current in a Crossed-Field Gap", *Phys. Fl.* 5, 4486 (1993).

[4] P. J. Christenson and Y. Y. Lau, "Transition to Turbulence in a Crossed-Field Gap", *Phys. Plasmas* 1, 12 (1994).

POSTER SESSION DD: HELICAL RESONATORS AND MICROWAVE PLASMAS
Tuesday afternoon, 10 October 1995 .
Berkeley Marina Marriott
Angel/Quarterdeck Rooms, 15:45–17:30

DD 1 Plasma production by large amplitude plasma surface waves, $\omega < \omega_{pe}$. D. J. COOPERBERG AND C. K. BIRDSALL, *University of California at Berkeley*[*]—Surface waves in a warm, unmagnetized, bounded plasma have been investigated via electrostatic $2\frac{1}{2}$d particle simulation. Our study focuses on a slab configuration in which the y direction is periodic and the x direction is bounded by grounded, absorbing conducting walls. Our prior simulation has produced dispersion relations and eigenfunctions for surface waves analogous to the Gould-Trivelpiece[1] waves in cylindrical systems for which the $k_y = 0$ cutoff of the asymmetric mode defines the series resonance and secondary branches whose cutoffs represent Tonks-Dattner resonances.[2] The current work demonstrates progress made in studying 2 species, low voltage, collisional systems sustained both by uniform ionization for which the randomly excited surface wave modes remain in a linear regime and also by resonant interaction with surface waves which are excited beyond the linear regime. Surface wave sustained plasmas have been studied extensively by Moisan et al. in cylindrical devices and this work hopes to extend such studies to planar configurations more suitable for large area plasma processing.

[1]A. W. Trivelpiece and R. W. Gould, J. Appl. Phys. 30, 1784 (1959)
[2]D. J. Cooperberg and C. K. Birdsall, Bull. APS II, 39, 7, 1552 (1994)
[*]This work supported by Office of Naval Research contract N00014-90-J-1198.

POSTER SESSION ID: GLOW MODELING
Wednesday afternoon, 11 October 1995
Berkeley Marina Marriott
Angel Rooms, 16:15–18:00

ID 1 Plasma Computer Experiments Teaching Laboratory[*] C.K. BIRDSALL, V.P. GOPINATH, J. VERBONCOEUR, Univ. of Calif. Berkeley CA 94720 - A plasma simulation laboratory employing 1d3v PIC-MCC codes has been used to enhance a plasma lecture course, both of which emphasize the plasma physics of discharges and materials processing.

Simulations inserted into lecture courses on an occasional basis have long proven to be valuable teaching tools. The present weekly laboratory draws on 20 computer experiments from a workbook, companion to the lecture text.[1] The homework projects range from diffusion to DC and RF discharges in argon, with many questions asked, tracking the lectures.

The codes used are XES1, XPDP1 and XPDC1 (WWW http://ptsg.eecs.berkeley.edu) with numerous input files. The course does not require a background in numerical analysis, or recompilation of the software. All projects are performed by modifying standard sets of (laboratory) parameters, such as lengths, voltages, frequencies, and gas pressure. A computer demonstration will be available, as well as the workbook and examples of student homework. [*]Work supported in part by ONR Contract FD-N00014-90-J-1198 1."Principles of Plasma Discharges and Materials Processing", M. A. Lieberman and A. J. Lichtenberg. Wiley. 1994.

EB 4 Ion Energy Distributions in Capacitively Coupled RF Plasma Reactors,[*] E. KAWAMURA, V. VAHEDI[†], M.A. LIEBERMAN, and C.K. BIRDSALL, U. C. Berkeley and [†]LLNL - Drawing on a review of previous works on ion energy distributions (IED) arriving at the target in the collisionless regime, we determine what factors influence the shape of the IEDs. This regime is of great interest to experimentalists and modelers studying the new generation of high density sources in which the sheath is much thinner than in the conventional RIE systems. Having determined the important parameters, we will show some particle-in-cell simulation results of a current driven rf plasma sheath. The results show that for $\tau_{ion}/\tau_{rf} \ll 1$, the sheath is resistive and the IEDs are broad and bimodal with a dominant low energy peak. Here, τ_{ion} is the ion transit-time across the sheath, and τ_{rf} is rf period. As τ_{ion}/τ_{rf} increases, the sheath becomes capacitive, the IED narrows, and the two peaks become more equal in height.

[*] Work supported by LLNL under U.S. D.O.E. Contract W-7405-ENG-48, U.S. D.O.E Contract DE-FG03-90ER54079, and in Berkeley, O.N.R. Contract FD-N00014-90-J-1198.

3S 12　Large amplitude plasma surface waves, $\omega < \omega_{pe}$. D. J. COOPERBERG, C. K. BIRDSALL, *University of California at Berkeley*[1] — Surface waves in a warm, unmagnetized, bounded plasma have been investigated via electrostatic $2\frac{1}{2}$d particle simulation. Our study focuses on a slab configuration in which the y direction is periodic and the x direction is bounded by grounded, absorbing conducting walls. Our prior simulation has produced dispersion relations and eigenfunctions for surface waves analogous to the Gould-Trivelpiece[2] waves in cylindrical systems for which the $k_y = 0$ cut-off of the asymmetric mode defines the series resonance and secondary branches whose cutoffs represent Tonks-Dattner resonances[3]. The current work demonstrates progress made in studying 2 species, low voltage, collisional systems sustained both by uniform ionization for which the randomly excited surface wave modes remain in a linear regime and also by resonant interaction with surface waves which are excited beyond the linear regime. The stability of discharges sustained by plasma surface waves will be discussed.

[1]This work supported by Office of Naval Research contract N00014-90-J-1198.
[2]A. W. Trivelpiece and R. W. Gould, J. Appl. Phys. 30, 1784 (1959)
[3]D. J. Cooperberg and C. K. Birdsall, Bull. APS II, 39, 7, 1552 (1994)

3S 13　**Two Dimensional Investigation of Ion Acoustic Waves Reflection from the Sheath** KEITH L CARTWRIGHT, C.K. BIRDSALL, *UC Berkeley* — Preliminary results show that obliquely propagating ion acoustic solitons propagate from the bulk plasma into and all the way through the sheath in 2d PIC simulation. These solitons come in to the simulation region from a boundary that approximates the bulk of the plasma. For normal incident solitons the 2d results are compared to 1d results. Our initial two dimensional PIC simulations show the details of densities, potentials, fields, velocity moments and time-distance plots of the average density minus the instantaneous density. From the last time distance plot the direction and magnitude of the ion acoustic wave is measured. This gives the relationship of the trajectories of the solitons transmitted and reflected from the sheath. Our observations will be compared with laboratory experiments,[1] and theory.[2][3] Acknowledgments: This work was supported in part by ONR grant number N00014-90-J-1198.

4R 31　· Similarity of Limiting Currents in Planar and Cylindrical Crossed-Field Diodes [1]V. P. GOPINATH, J. P. VERBON-COEUR, C. K. BIRDSALL, *Electronics Research Laboratory, University of California, Berkeley, CA 94720* — Limiting current in a planar crossed-field gap has received attention for over 70 years for $B < B_{Hull}$ [2], and recently for $B > B_{Hull}$ [3]. Simulations indicate the ratio of critical to Child-Langmuir current, $I_C(B)/I_{CL}$, scales similarly with magnetic field in planar and cylindrical geometries, up to $r_{anode}/r_{cathode} \leq 5$. The comparison is performed above and below Hull cutoff, for small and large radius ratios. One-dimensional simulations of a planar crossed-field diode in the region near $B = B_{Hull}$ indicate a transition in current with strong sensitivity to the initial velocity distribution of emitted electrons, $f(v)$. Effects of $f(v)$ and secondary emission coefficients at the cathode and anode are explored.

[1]This work supported in part by AFOSR grant F49620-92-J0487 and ONR grant FD-N00014-90-J-1198.
[2]A. W. Hull, *Phys. Rev.* 18, 31 (1921), Y. Y. Lau, P. J. Christenson and D. Chernin, *Phys. Fl. B* 5, 4486 (1993).
[3]P. J. Christenson and Y. Y. Lau, *Phys. Plasmas* 1, 12 (1994).

VII. SOME POSTER PAPERS

A spectral comparison of two methods of removing errors in Gauss's law from 2d electromagnetic PIC plasma simulations.

Peter Mardahl, Dr. J. P. Verboncoeur

Transverse Asymmetry in a Crossed–Field Diode

K. L. Cartwright, J. P. Verboncoeur, V. P. Gopinath and C. K. Birdsall

Electronics Research Laboratory
University of California, Berkeley, CA 94720
e-mail kc@bohm.eecs.berkeley.edu

Abstract

Recent 1d studies of cylindrical crossed-field diodes indicate that the dimension(s) transverse to the gap may play a role in delaying onset of virtual cathode oscillations for currents above the limiting current. Transverse space charge effects in smooth electrodes diodes may produce fields which warm the electrons in both the transverse and longitudinal components of velocity. Thermal emission of electrons damps virtual cathode oscillations. The effects of the transverse dimension are explored using two-dimensional planar PIC codes. The simulations confirm that adding the transverse direction does delay the onset of virtual cathode oscillations.

One and Two Dimensional Investigation of IAW Reflection from the Sheath

K.L. Cartwright and C.K. Birdsall
Electronics Research Laboratory
University of California, Berkeley, CA 94720

Preliminary results show that ion waves propagate from the bulk plasma into and all the way through the sheath in 1D PIC simulation. These waves are launched from one side of the system with a current source with a frequency less than the ion plasma frequency. Our one and initial 2d PIC simulations show the details of densities, potentials, particle moments and time–distance plots of the time average density minus the instantaneous density. From the time–distance plot the direction and magnitude of the ion acoustic wave is measured. From this the coefficients of reflection and transmission as a function of pulse width is calculated. Our observations are compared with laboratory experiments and theory.

A spectral comparison of two methods of removing errors in Gauss's law from 2d electromagnetic PIC plasma simulations.

Peter Mardahl, Dr. J. P. Verboncoeur

(Prof. C.K. Birdsall)

Department of Electrical Engineering and Computer Science

University of California, Berkeley

Berkeley, CA 94720

Abstract

Non-charge conserving current collection algorithms for electromagnetic PIC plasma simulations can cause errors in Gauss's law. These errors arise from violations of the charge continuity equation, $\nabla \cdot J = -\partial\rho/\partial t$, which in turn causes violations in Gauss's law, $\nabla \cdot D = \rho$.

Two techniques for removing these errors are examined and compared: the Marder correction as modified by A.B. Langdon [1], a method which corrects electric fields locally and primarily affects short wavelengths, and a divergence correction [4], which uses an iterative Poisson solve to correct the electric fields so that Gauss's law is enforced. The Poisson solve used is the Dynamic ADI method of Hewett[3]. The effect of each method on the the spectrum of the error (short wavelengths vs. long) is examined. Computational efficiency and accuracy of the two techniques are compared.

Particular cases of interest include corrections in electromagnetic relativistic beam simulations. In addition, the spectral comparison provides insight into the behavior of the schemes applied. This work may provide insight into optimization of Dynamic ADI timesteps for suppression of selected wavelengths and application of spectral filtering, resulting in improved performance.

1 Model

1.1 The Problem

Non-charge conserving current weightings, such as a linear current weighting used in combination with a linear charge weighting, violate continuity, $\nabla \cdot J = -\partial \rho / \partial t$, in turn causing errors in Gauss's law: $\nabla \cdot D = \rho$. However, these current weightings do reduce noise. Simulators therefore tend to use such weightings and then correct the electric fields so that $\nabla \cdot D = \rho$ is satisfied.

To fit the discrete mathematical mesh, we recast $\nabla \cdot D = \rho$ as $\oint_S D \cdot dS = \int_V \rho dV$ around each grid node as shown in Figure 1:
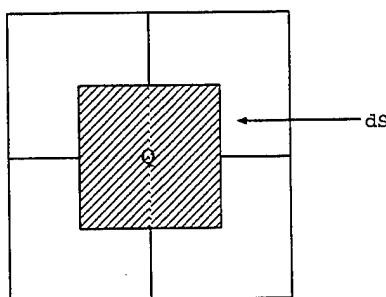
Figure 1: Typical Cell

Consider this 1-D example of how linear weighting of current and charge could lead to a violation of Gauss's law by violating continuity. In this example, a particle of charge Q moves from position p_1 to p_2, in a single timestep of length Δt.
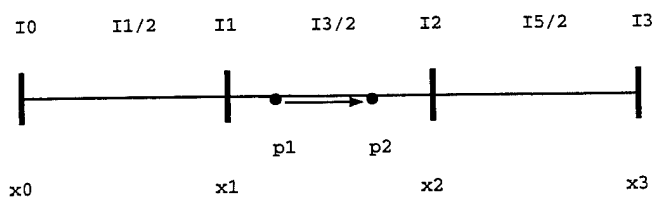
Figure 2: 1D example mesh

Assuming this is the only particle in motion, this would lead to the accumulation of the following charges at mesh points, using a linear weighting of the charge to adjacent mesh points:

$$q_1^t = \frac{x_2 - p_1}{x_2 - x_1} Q \tag{1}$$

$$q_2^t = \frac{p_1 - x_1}{x_2 - x_1} Q \tag{2}$$

$$q_1^{t+\Delta t} = \frac{x_2 - p_2}{x_2 - x_1} Q \tag{3}$$

$$q_2^{t+\Delta t} = \frac{p_2 - x_1}{x_2 - x_1} Q \tag{4}$$

$$\Delta q_1 = q_1^{t+\Delta t} - q_1^t = \frac{p_1 - p_2}{x_2 - x_1} Q \tag{5}$$

$$\Delta q_2 = q_2^{t+\Delta t} - q_2^t = \frac{p_2 - p_1}{x_2 - x_1} Q \tag{6}$$

Weighting the current is done by first finding the midpoint of the displacement of the particle, and then using that midpoint to weight the current to the nodes. Then, the current at the nodes is averaged to obtain the current at the half-nodes.

$$I_{midpoint} = \frac{Q(p_2 - p_1)}{\Delta t (x_2 - x_1)} \tag{7}$$

$$I_1 = \left(x_2 - \frac{p_2 + p_1}{2} \right) \frac{I_{midpoint}}{x_2 - x_1} \tag{8}$$

$$I_2 = \left(\frac{p_2 + p_1}{2} - x_1 \right) \frac{I_{midpoint}}{x_2 - x_1} \tag{9}$$

$$I_{\frac{1}{2}} = \frac{0 + I_1}{2} = \left(x_2 - \frac{p_2 + p_1}{2} \right) \frac{I_{midpoint}}{2(x_2 - x_1)} \tag{10}$$

$$I_{\frac{3}{2}} = \frac{I_2 + I_1}{2} = \frac{I_{midpoint}}{2} \tag{11}$$

$$I_{\frac{5}{2}} = \frac{I_2 + 0}{2} = \left(\frac{p_2 + p_1}{2} - x_1 \right) \frac{I_{midpoint}}{2(x_2 - x_1)} \tag{12}$$

We sum the currents into and out of each node to calculate the change in charge:

$$\Delta q_0 = -I_{\frac{1}{2}} \Delta t \tag{13}$$

$$\Delta q_1 = (I_{\frac{1}{2}} - I_{\frac{3}{2}}) \Delta t \tag{14}$$

$$\Delta q_2 = (I_{\frac{3}{2}} - I_{\frac{5}{2}}) \Delta t \tag{15}$$

$$\Delta q_3 = I_{\frac{5}{2}} \Delta t \tag{16}$$

After performing some algebra, we have:

$$\Delta q_0 = \left(\frac{p_2 + p_1}{2} - x_2 \right) \frac{Q(p_2 - p_1)}{2(x_2 - x_1)^2} \tag{17}$$

$$\Delta q_1 = \left(x_1 - \frac{(p_1 + p_2)}{2} \right) \frac{Q(p_2 - p_1)}{2(x_2 - x_1)^2} \tag{18}$$

$$\Delta q_2 = \left(x_2 - \frac{(p_1 + p_2)}{2} \right) \frac{Q(p_2 - p_1)}{2(x_2 - x_1)^2} \tag{19}$$

$$\Delta q_3 = \left(\frac{p_2 + p_1}{2} - x_1 \right) \frac{Q(p_2 - p_1)}{2(x_2 - x_1)^2} \tag{20}$$

Equations 18 and 19 disagree with 5 and 6. Since the currents $I_{\frac{1}{2}}, I_{\frac{3}{2}}, I_{\frac{5}{2}}$ are the source currents used to advance Maxwell's curl equations: $\nabla \times H = J + \partial D / \partial t$ and $\nabla \times E = -\partial B / \partial t$, the resultant electric fields reflect a different change in charge at the nodes, i.e., a violation of continuity leading to a violation of Gauss's law.

Similar difficulties arise with weighting currents directly to the half-cells as in Figure 3.
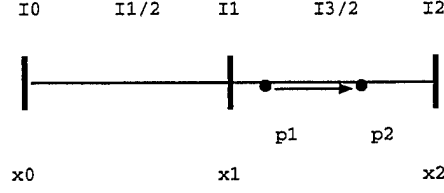
Figure 3: Current weighting to half-cells

This weighting results in the following expressions:

$$I_{1/2} = \frac{I_{midpoint}}{x_1 - x_0} \left(\frac{x_1 + x_2}{2} - \frac{p_1 p_2}{2} \right) \tag{21}$$

$$I_{3/2} = \frac{I_{midpoint}}{x_1 - x_0} \left(\frac{p_1 p_2}{2} - \frac{x_1 + x_2}{2} \right) \tag{22}$$

$$\Delta q_0 = \frac{Q(p_2 - p_1)}{2(x_1 - x_0)^2} \left((x1 + x2) - (p1 + p2) \right) \tag{23}$$

$$\Delta q_1 = \frac{Q(p_2 - p_1)}{2(x_1 - x_0)^2} \left(\frac{x_0 + 2x1 + x2}{2} - (p1 + p2) \right) \tag{24}$$

$$\Delta q_2 = \frac{Q(p_2 - p_1)}{2(x_1 - x_0)^2} \left((p1 + p2) - (x1 + x2) \right) \tag{25}$$

which again differ from Equations 5 and 6.

However, not all current weightings will disagree with the linear weighting of charge to the grid. If one weights all the current to the nearest half grid point, then the current will agree with Equations 5 and 6. The following equations show this: (refer to Figure 3 for definitions.)

$$I_{1/2} = 0 \tag{26}$$

$$I_{3/2} = \frac{Q(p_2 - p_1)}{\Delta t(x_2 - x_1)} \tag{27}$$

$$\Delta q_1 = -I_{3/2}\Delta t = \frac{p_1 - p_2}{x_2 - x_1}Q \tag{28}$$

$$\Delta q_2 = I_{3/2}\Delta t = \frac{p_2 - p_1}{x_2 - x_1}Q \tag{29}$$

1.2   Corrections Used

1.2.1   Boris Correction

The Boris-type correction (modified slightly from [4]) is given by:

$$E_{corrected} = E - \nabla\delta\phi \tag{30}$$

such that

$$\nabla \cdot \epsilon E_{corrected} = \rho \tag{31}$$

52

Where $E_{corrected}$ is an electric field which obeys Gauss's law, and $\nabla\delta\phi$ is the correction to E, the uncorrected field.

$$\nabla \cdot (\epsilon E - \epsilon\nabla\delta\phi) = \rho \tag{32}$$

so we require a solution to the elliptic equation:

$$\nabla \cdot \epsilon\nabla\delta\phi = \nabla \cdot \epsilon E - \rho. \tag{33}$$

This elliptic equation can be solved using a number of direct and iterative schemes with varying degrees of efficiency.

1.2.2 Langdon-Marder Correction

The Marder scheme used is the one proposed by A.B. Langdon [1]. He proposes essentially the following scheme, which has been slightly modified to allow for nonuniform ϵ:

$$\epsilon E^{n+1}_{corrected} = \epsilon E^{n+1} + \Delta t \nabla d(\nabla \cdot \epsilon E^{n+1} - \rho^{n+1}) \tag{34}$$

This is a modification of the Marder scheme, which is less implicit:

$$\epsilon E^{n+1}_{corrected} = \epsilon E^{n+1} + \Delta t \nabla d(\nabla \cdot \epsilon E^{n} - \rho^{n}) \tag{35}$$

where d is the diffusion parameter, which should satisfy (in 2d):

$$d \leq \frac{1}{2\Delta t}\left(\frac{\Delta x^2 \Delta y^2}{\Delta x^2 + \Delta y^2}\right) \tag{36}$$

to ensure stability of the method. The superscripts n, $n+1$ indicate simulation timestep: Langdon's proposed modification is simply to use the E and ρ at the current time rather than from the previous timestep.

1.2.3 Irrotationality of the correction

Both the Marder-Langdon and the Boris correction arise from the gradient of a scalar field $\nabla\phi$, which can be seen from Equations 33 and 35. This combined with the vector identity $\nabla \times \nabla\phi = 0$ demonstrates that both corrections have no effect on the solenoidal parts of the fields.

This property is important, since only the rotational part of the electric field is used in advancing the magnetic field in time $\nabla \times E = -\partial B/\partial t$.

1.3 Geometry and Implementation

The methods were implemented and tested within the framework of the OOPIC 2-d electromagnetic PIC code. [6]

In the interes of clarity and convenience of Fourier Analysis, this investigation is performed in Cartesian coordinates. The testing space was discretized into either a 16x16, 32x32, or 64x64 square mesh.

Figure 4 illustrates where the field components are located on the mesh. Electric field E and current I are defined at the midpoints of lines connecting the nodes of the mesh, while ρ and ϕ are defined on the nodes.

The Boris correction was implemented by using the Dynamic Alternating Direction Implicit (DADI) [3] method to solve Equation 33. The DADI method is an iterative scheme which makes use of a "fictitious timestep" to attempt to speed up convergence to a correct solution. Successive iterations of DADI will choose successive "fictitious timesteps" using a heuristically-chosen rule. If a poor choice of initial "fictitious timestep" is made, the problem will take longer to converge to the solution.

The Marder correction was implemented by putting equation 35 into finite difference form and applying it to the charge densities and the fields in the simulation.

The wavelength components of the error are analyzed using a 1d Fast Fourier Transform along each mesh-line, producing Kx vs. y, and Ky vs. x. Only a certain finite set of wavelengths are observable: those which can exist on the mesh.
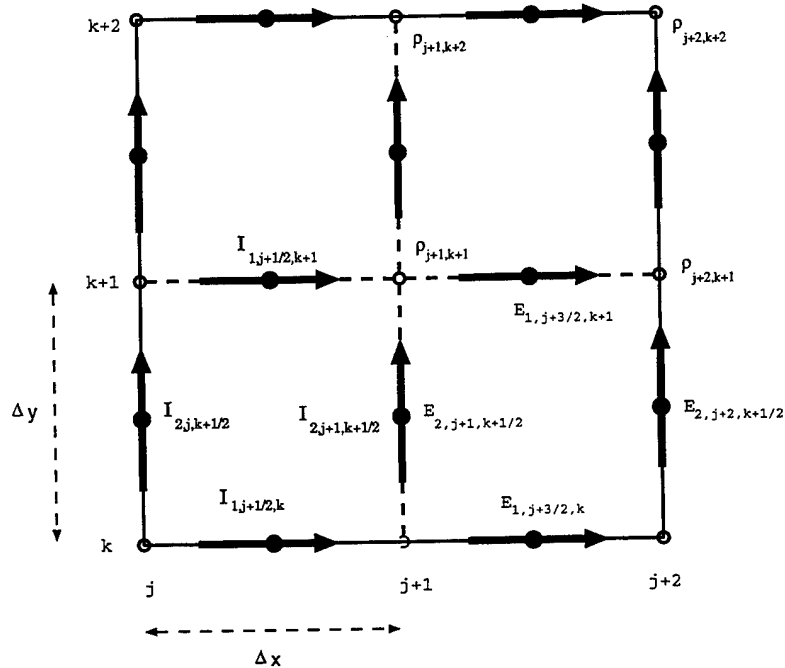
Figure 4: Mesh used with OOPIC

2 Results

2.1 Delta Function Test Case

The methods were tested first on a delta function divergence error, by having zero electric fields and setting $\rho = \delta(x - x_0)\delta(y - y_0)$. A delta function has the property of having components at every wavelength. This allows examination of the behavior of each correction on all wavelengths simultaneously.

For this case, the system is loaded in the center with the closest approximation to a delta function possible on a discrete mesh using a computer: a nonzero charge density at only one mesh point. The walls are metal and potentials should satisfy a Dirichlet condition. All corrections should relax the solution to the Poisson solution in the system for a point charge, or equivalently, reduce the error in Gauss's law to zero. Initially, the fields are set to zero.
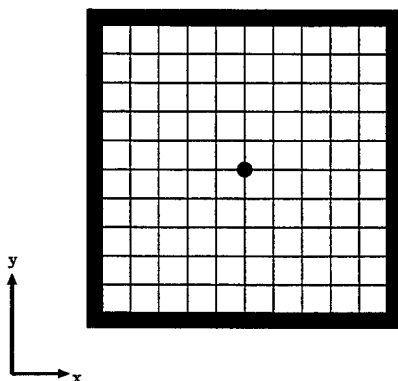
Figure 5: Delta function charge distribution in a square system with uniform mesh.

2.1.1 Boris Correction on the Delta Function

40 Iterations of DADI on a delta function

Kxlavex2(t)

10

2

1E-08

Iteration

KX1

40   0.5
0
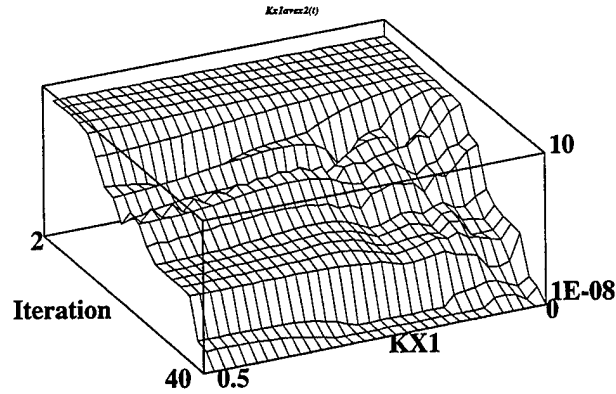
40 Iterations of DADI on a delta function after reset

Kxlavex2(t)

10

79

1E-08

Iteration

KX1

120   0.5
0
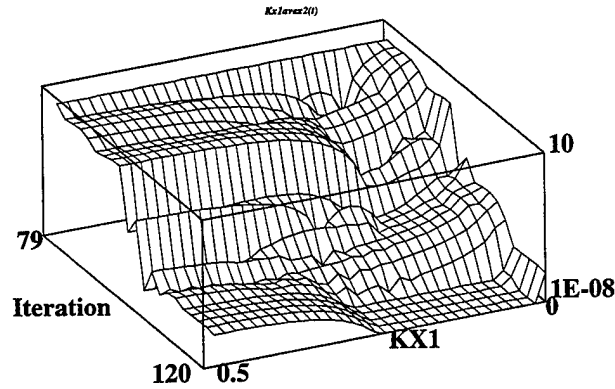
Figure 6: Shown here is the effect of 40 iterations of DADI on the different error wavelengths. The top graph shows a slow start followed by a rapid removal of short wavelengths (high K_{x1}), and then a more even removal. In the bottom graph, iteration of DADI was started using the "fictitious timestep" from the 79'th iteration of the previous problem. This led to a much different initial rate of convergence. Note that the vertical scale is logarithmic: errors of around 10^{-7} are near machine precision.

2.1.2 Marder Correction on the Delta Function

60 Iterations of Marder (d = 0.1dmax)

60 Iterations of Marder (d = 0.8 dmax)
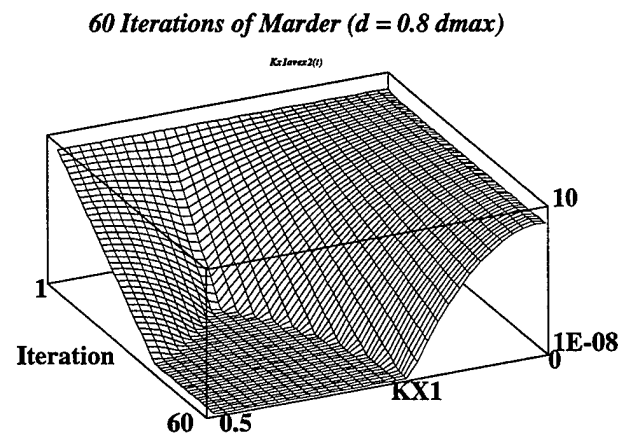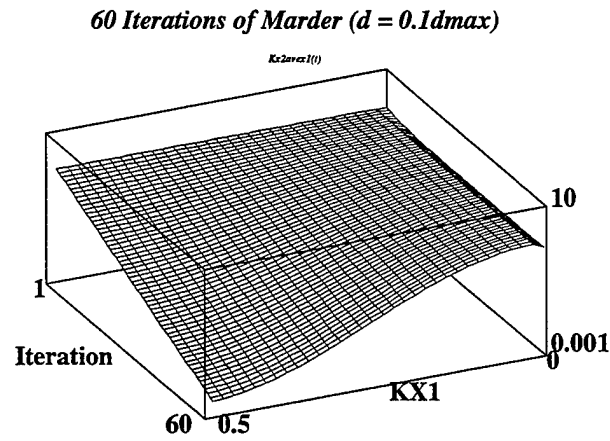
Figure 7: From these two graphs, it is evident that short error wavelengths (high KX1) are damped much more quickly by the Marder-Langdon type correction than long errorwavelengths. Also noteworthy is that the convergence of this correction is monotonic, unlike the Boris correction implemented with DADI. Note that the choice of diffusion parameter affected not only the rate of convergence but also the wavelength of fastest convergence. Again, the vertical scale is logarithmic.

2.2 Single Wavelength Test Cases

In addition to the delta function test case described above, some error test cases of the form

$$\nabla \cdot D - \rho = sin(\frac{n\pi x}{L})sin(\frac{n\pi y}{L}) \tag{37}$$

were tried, where n is an integer and L is the length of a side of the system. This type of error would show up as discrete spikes in Fourier transforms, since only a single wavelength is introduced.

For both the Marder-Langdon and Boris corrections, the spikes in k-space remained discrete and did not spread out at all: the error remained in one wavelength until the error was of the order of machine precision. Even errors with multiple wavelengths introduced at the outset had this property, though each wavelength of error was removed at a different rate.

2.3 Relativistic Beam Test Case

The previous two test cases were somewhat contrived, in that a divergence error was simply introduced into the system arbitrarily. This case is a little more reminiscent of a more practical simulation, but is still somewhat ideal.

In this case, a simulated beam with a very high velocity was fired through the system along the x direction. Figure 8 shows the geometry for this example. The beam had a low enough current and a high enough energy that the particles drift unperturbed through the system; i.e, $qE\Delta t/m << \sqrt{2\varepsilon/m}$ where ε is the initial beam energy.

The simulated beam is generated by injecting enough computer particles at random locations on the left hand wall to maintain an approximately constant current across the system.

This example is interesting because it should generate large errors every timestep for a current weighting which is non-charge conserving. The error is shown in Figure 9.
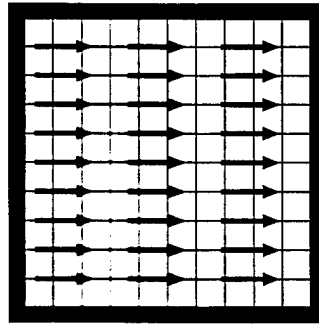
Figure 8: A simulated relativistic beam travels from left to right.
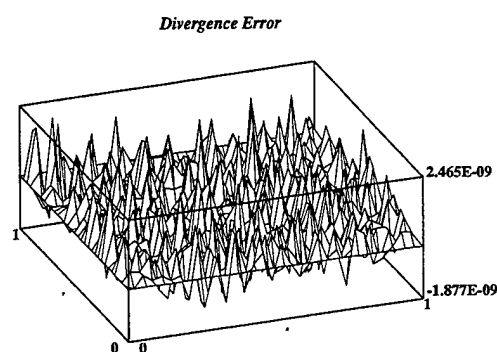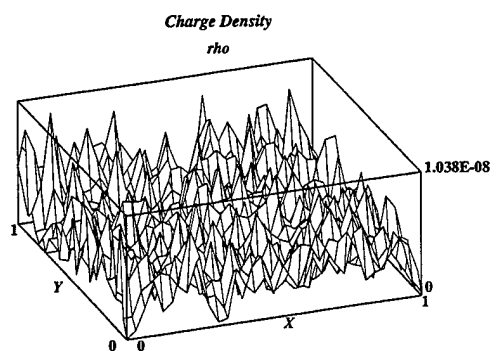
Figure 9: Charge density and divergence error in a relativistic beam simulation, with no corrections applied. Note that the magnitude of the error is about 1/4 of the magnitude of the charge density, i.e., $\delta\rho/\rho \simeq 1/4$. Both graphs are noisy because of the low number of particles used.
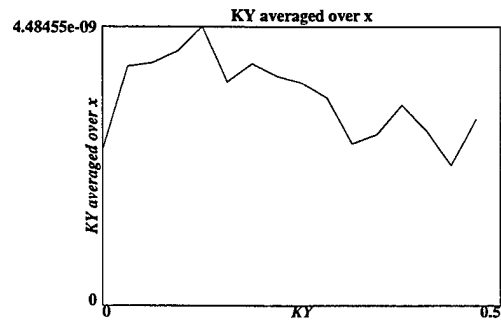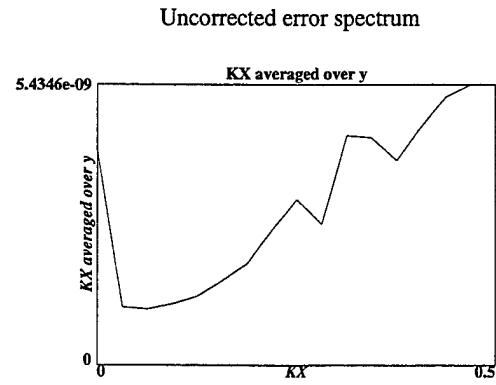
Uncorrected error spectrum

Figure 10: Error spectrum in a simulation with no corrections applied. Note that not all the error is in short wavelength (high k).

2.3.1 Boris Correction Applied to the Relativistic Beam

2 Iterations of DADI

KX averaged over y

KY averaged over x
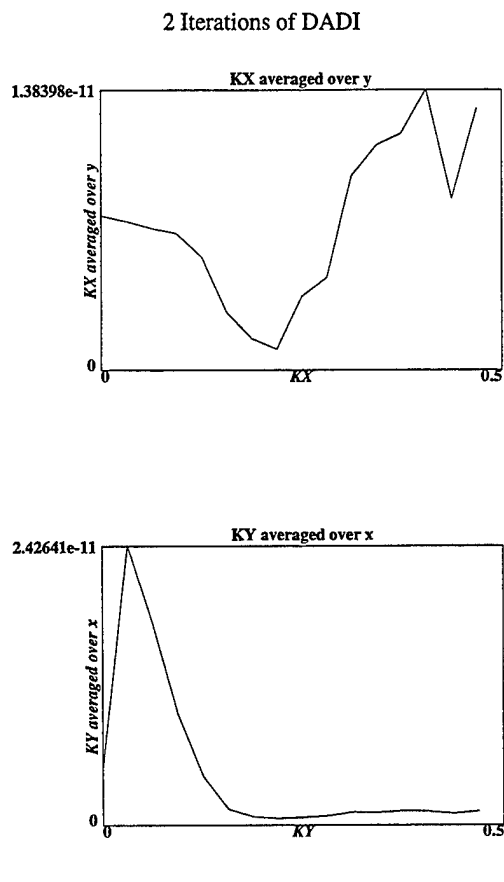
Figure 11: Error spectrum in a simulation which has had two iterations of the Dynamic ADI Boris correction applied in each simulation timestep. The magnitude of the error is greatly reduced from the uncorrected simulation of Figure 10.

2.3.2 Marder Correction Applied to the Relativistic Beam

10 Iterations of Marder, d = 0.8 dmax
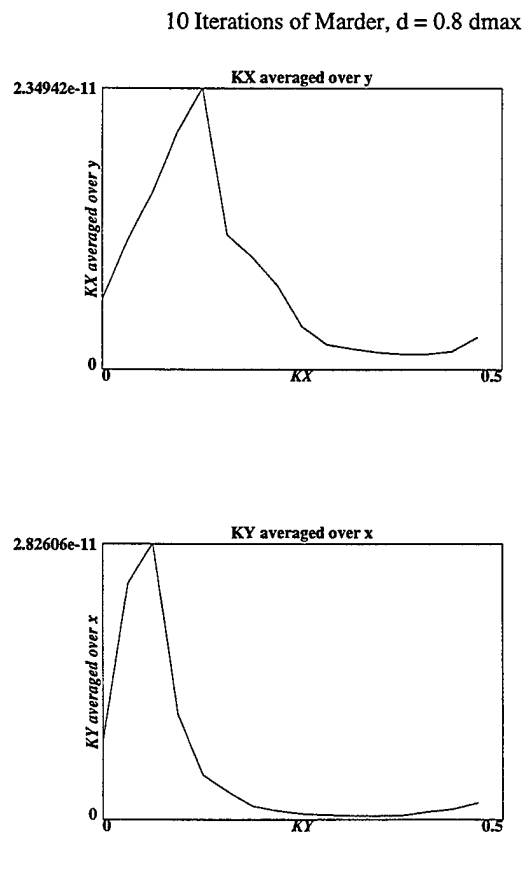
Figure 12: Error spectrum in a simulation which has had 10 iterations of aggressive Marder correction. Short wavelengths of errors are much reduced, while longer wavelengths are still present. However, the magnitude of the error is greatly reduced from the uncorrected simulation of Figure 10, and comparable to the result from Figure 11.
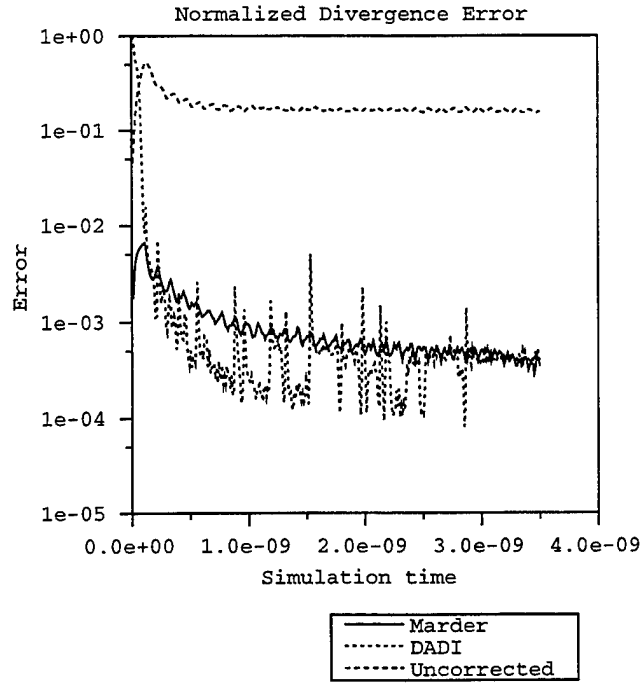
2.3.3 Comparison of Corrections on the Relativistic Beam

Figure 13: Shown here is an overall figure of merit for the divergence error in the simulation. The data was calculated by summing the magnitude of the divergence error at each mesh point, and dividing by a similar sum of the magnitude of ρ. The Marder and the DADI-based Boris correction performed comparably well. Two DADI iterations were used for the Boris correction, 10 iterations using $d = 0.8dmax$ for the Marder correction

2.4 Beam With a Large Magnetic Field Applied in Z

This case is similar to the previous case except a large magnetic field was applied in the Z direction to turn the beam, and a beam was injected from the left of the system as well as from the right. The figure shows only the rightward moving beam: the leftward moving beam curves upward instead of downward.
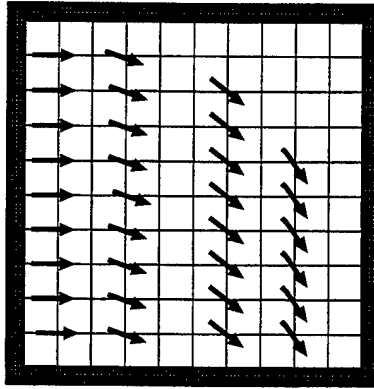

Figure 14: A beam curving in a magnetic field. Not shown is a leftward moving beam entering from the right hand side and curving upward.

The error spectra observed in this case was very similar to the spectra observed for the previous relativistic beam case, for the uncorrected simulation as well as for the Marder and Boris corrected simulations. One notable difference is that there is a much stronger DC ($k = 0$) component than in the previous case.

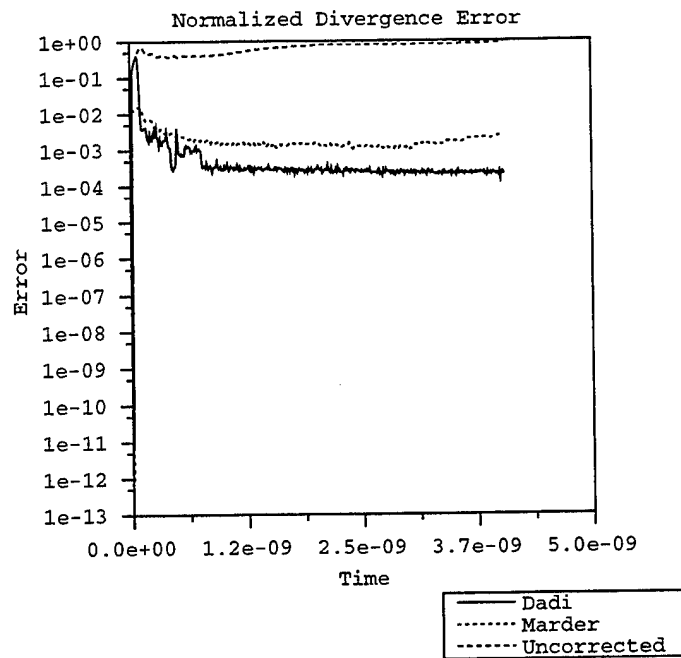### 2.4.1   Comparison of Corrections on the Curving Beam

Figure 15: Errors for the curving beam. The DADI-based Boris correction actually does better here, probably because of the long wavelength components of the error. The Marder iteration is less efficient at removing long wavelengths of error. The same parameters and number of iterations were used for the corrections here as in Figure 13.

3   Thermal Plasma

In this case a simulation of a very hot plasma is examined. This time the region is filled with a uniform plasma with very heavy (practically immobile) ions at a much cooler temperature.

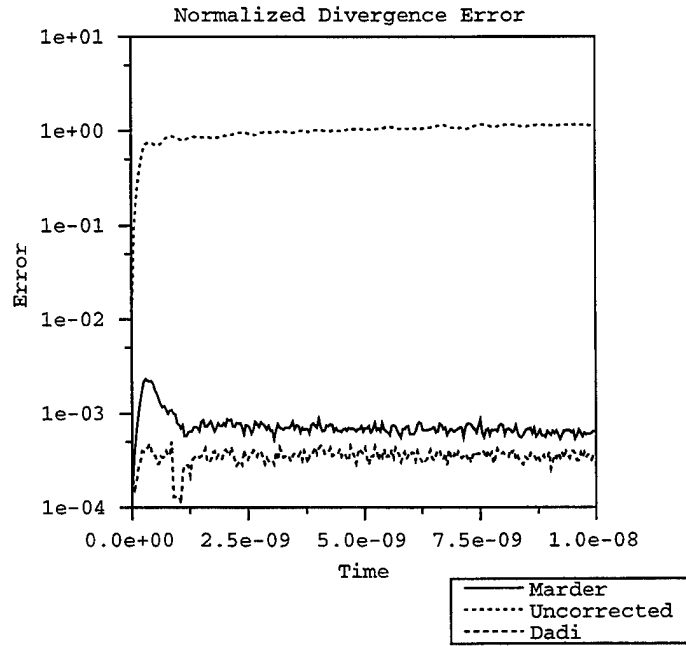Again, the error spectra is similar to that already given.

Figure 16: Errors for the thermal plasma. Again, the same parameters and number of iterations was used as before.

4   Conclusions

Tests on single-frequency errors showed that both methods of removing errors are non-dispersive, that is, an error at one wavelength won't spread to other wavelengths as the corrections are applied.

Divergence errors are not necessarily short wavelength errors for PIC simulations. Instead, errors were observed at a broad range of wavelengths. This reduces the efficacy of methods such as the Marder-Langdon method, which preferentially remove short wavelength errors.

The magnitude of the diffusion parameter d used by the Marder-type correction also had some effect on the convergence rate for different wavelengths.

The divergence error injected per timestep can be large when the particles are moving very quickly, and thus error can be introduced even more quickly than it can be removed by some corrections.

Divergence error was not observed to increase without bound, but rather reached a final value asymptotically.

The Boris correction based on the Dynamic ADI method proved to be as efficient at removing errors in the PIC simulations examined as the Marder-Langdon correction used. Ten iterations of the Marder correction is about as expensive computationally as two iterations of the DADI-based Boris correction. Unfortunately, they produce almost the same amount of correction overall, so one cannot choose the better method based on efficiency in error removal.

However, the Marder correction is much more straighforward to implement than a Poisson solver, but a Poisson solver has many other practical uses in a PIC code other than a Boris correction, and may already exist in the code for other purposes.

5 Further work

- Examine the effect of DADI's fictitious timestep on the spectral convergence with the intention of speeding up DADI.

- Similarly examine the effect of the diffusion parameter d of the Marder correction on the spectral convergence.

6 Acknowledgments

References

[1] A.B. Langdon, "On enforcing Gauss's law in electromagnetic particle-in-cell codes." Computer Physics Communications, July 1992, vol.70 (no.3): 447-50.

[2] B. Marder, "A method for incorporating Gauss's law into electromagnetic PIC codes." Journal of Computational Physics, Jan, 1987, vol.68 (no.1): 48-55.

[3] Hewett, D.W.; Larson, D.J.; Doss, S., "Solution of simultaneous partial differential equations using Dynamic ADI: solution of the streamlined Darwin field equations." Journal of Computational Physics, July 1992, vol.101, (no.1):11-24.

[4] Birdsall C. K. and A. B. Langdon, *Plasma Physics Via Computer Simulation*,Adam Hilger (1991), pp. 360.

[5] Nielsen, D.E., Drobot, A. T., "An analysis and optimization of the pseudo-current method." J. Comput. Phys. 89 (1990) 31.

[6] J.P. Verboncoeur, A.B. Langdon, and N.T. Gladd, "An object-oriented electromagnetic PIC code." Computer Physics Communications 87 (1995) 199-211.

Transverse Asymmetry in a Crossed–Field Diode

K. L. Cartwright, J. P. Verboncoeur, V. P. Gopinath and C. K.Birdsall

Electronics Research Laboratory
University of California, Berkeley, CA 94720
e-mail kc@bohm.eecs.berkeley.edu

Abstract

Recent 1d studies of cylindrical crossed-field diodes indicate that the dimension(s) transverse to the gap may play a role in delaying onset of virtual cathode oscillations for currents above the limiting current. Transverse space charge effects in smooth electrodes diodes may produce fields which warm the electrons in both the transverse and longitudinal components of velocity. Thermal emission of electrons damps virtual cathode oscillations. The effects of the transverse dimension are explored using two-dimensional planar PIC codes. The simulations confirm that adding the transverse direction does delay the onset of virtual cathode oscillations.

1 Introduction

Lau, Christenson and Chernin [1] have re-interpreted the Hull cutoff as the limiting current for a planar crossed–field diode. The cutoff is well known; a summary is given in the text by Birdsall and Bridges [3]. Recently, Verboncoeur and Birdsall [6] performed one-dimensional simulations confirming the Hull cutoff as the limiting stable current for a space-charge limited planar diode, and examined the rapid reduction of transmitted current for injection currents above the current limit at the Hull cutoff. Current injection above limiting current results in virtual cathode oscillations. In examining the limiting current in cylindrical diodes of one and two dimensions, Gopinath et al. [2] noted a transverse space charge effect in 2d which appeared to damp virtual cathode oscillations for currents in excess of the limiting current.

In this paper, the preceding works are extended to two-dimensions. The issues of numerical and physical instability are also investigated. In particular, we examine the role of the transverse dimension in delaying onset of virtual cathode oscillations. PDP1 and PDP2 were the 1d and 2d PIC (particle in cell) codes used in this study. They are available electronically via the Internet [7].

2 Theory

The critical point occurs at the Hull cutoff, $B = B_{Hull}$, with the injected current at the limiting (critical) current, $J = J_c$. For cold emission the Hull cutoff can be written:

$$B_{Hull} = \frac{m}{ed}\sqrt{\frac{2eV}{m} + u_0^2},$$

(1)

where u_0 is the electron drift velocity at the cathode, V is the gap voltage, d is the gap width, and e and m are the electron charge and mass, respectively. At the Hull cutoff, with $u_0 = 0$, the limiting current is given by $J_c/J_{CL} = 9/4\pi$, where J_{CL} is the unmagnetized Child-Langmuir limiting current:

$$J_{CL} = \frac{4\epsilon_0}{9\sqrt{\frac{m}{2e}}}\frac{V^{\frac{3}{2}}}{d^2}.$$

(2)

For more details see Birdsall[3], Christenson[5], and Verboncoeur[6].

For warm emission the Hull cutoff is defined the same as the cold case, Equation 1. Hull cutoff may depend on the injected temperature but for the case examined here $kT_e \ll eV$, so that any changes of the Hull cutoff for the warm case is a small perturbation of the cold case. The warm, unmagnetized Child-Langmuir limiting current[4] is

$$J_{CL} = \frac{4\epsilon_0}{9\sqrt{\frac{m}{2e}}}\frac{(V - V_m)^{\frac{3}{2}}}{(d - x_m)^2}\left(1 + \frac{2.66kT_e}{e(V - V_m)} + \ldots\right).$$
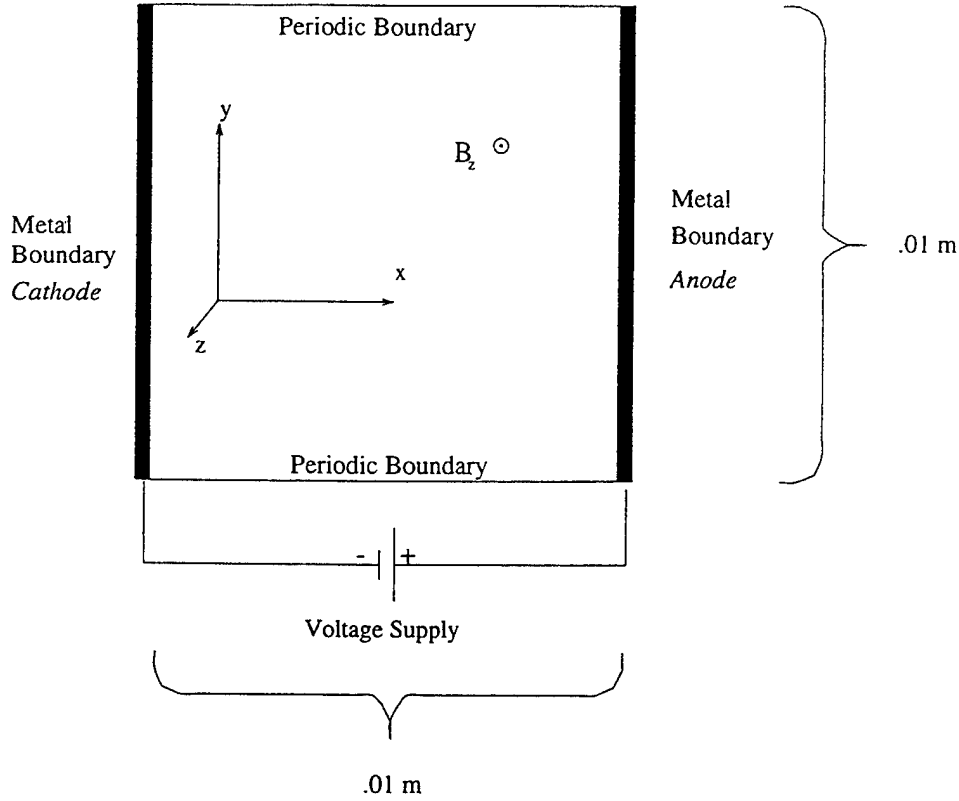
(3)

Figure 1: Sketch of 2d Simulation

Here kT_e is the electron temperature at the cathode, V_m is the minimum in potential, and x_m is the position of the minimum in potential. Tabulated values of V_m and x_m were calculated by Langmuir[4]. It should be noted here that the second term in Equation 3 increases J_c for thermal distributions. This allows the diode to be stable at higher currents.

3 Unmagnetized Child – Langmuir Diode and Numerical Noise (2d3v)

The first simulation was done with $B_z = 0$ and $J = J_{CL}/2$. When the particles were injected cold, with a small drift velocity (0.5 eV) at random positions in y, significant E_y fields were generated. This caused density fluctuations and heating in v_y. To establish this as a real phenomenon, the number of computer particles used in the simulation was increased, thus decreasing the number of real electrons each one represents. The variance or L^2 norm, $\overline{(E_y - \overline{E_y})^2}$, of E_y is plotted in Figure 2 as a function of the number of computer particles injected per grid per time step. This shows the variance (noise) of the system proportional $1/\sqrt{N_c}$, where N_c is the number of computer electrons. For a real system with

Physical Parameters	V	10 kV
	u_{0x}	4.2×10^5 m/s
	B_z	.0337 T
	J_c	- 16.9 kA/m^2
	x length	.01 m
	y length	.01 m
Numerical Parameters	Number of grids in x	400
	Number of grids in y	16
	Δt	5×10^{-13} sec

Table 1: Simulation Parameters

these parameters, 10^6 times as many electrons would be present. Extrapolating the trend shown in Figure 2 to the physical number of electrons in the system, one finds the fluctuations in field decrease to a negligible level.

In order to reduce the noise in the system, particles are injected uniformly along the cathode, in y. This is often referred to as a "quiet" injection. The number of particles injected is an integral multiple of the number of grid cells. The fluctuation level is shown in Figure 2 as a function of the number of particles injected per grid per time step. The quiet load uses the right scale and the random load uses the left scale. This brings the fluctuation down to a level that would be observed if 10^6 times as many electrons were injected randomly along the cathode. Using the quiet load, the E_y fluctuations are reduced and the resulting heating of the electrons is negligible. Thus, the observed transverse effects were numerical artifacts of the statistical nature of the simulation.

4 Critical Current Injection at Hull Field

Next, a static magnetic field is applied perpendicular to the diode gap in the z-direction as shown in Figure 1. The common parameters for these simulations are shown in Table 1. The injection current is varied from J_c to $1.06J_c$.

The 2d results obtained here are compared to the 1d results obtained by Verboncoeur and Birdsall [6]. For an injected current of J_c the results are the same. The current as a function of time (Figure 3) and phase space (Figure 7) are almost identical to the 1d results (Figures 15 and 16, respectively). The phase space plot shows that the electrons do not have a turning point, $v_x = 0$, thus the anode current is equal to the injected current. The number of particles as a function of time is steady. The L^2 norm of E_y is also small, reflecting the lack of variation in the y-direction.

When the current is raised 2 percent above the critical current, the result does not have a 1d analog. The L^2 norm of E_y for $J = 1.02J_c$, Figure 5, shows variation in the y-direction.
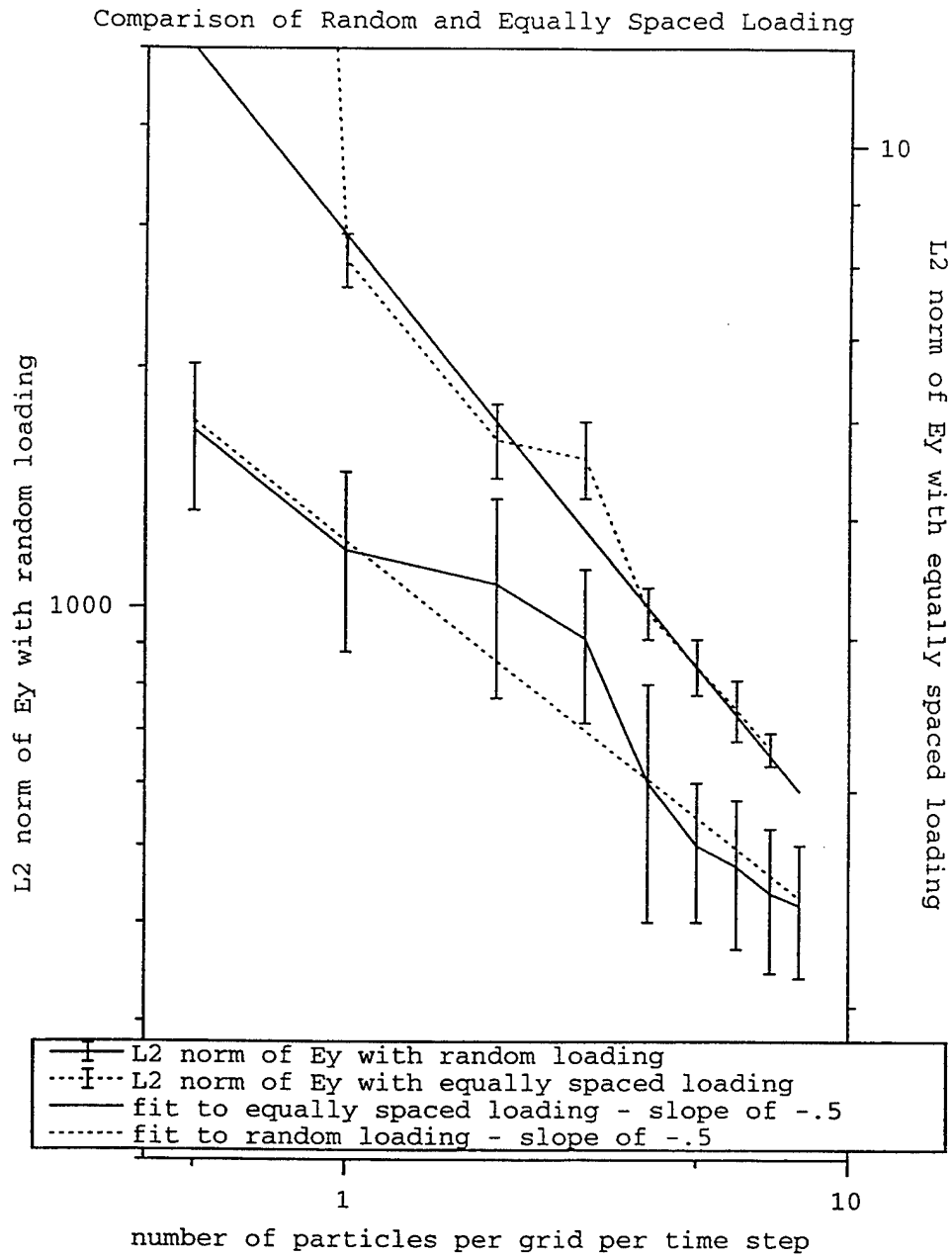
Figure 2: The variance of the E_y is plotted as a function of the number of computer particles injected per grid per time step. The uniform (quiet) load uses the right scale and the random load uses the left scale. The error bars represent the observed maximum and minimum values of the L^2 norm, $\overline{(E_y - \overline{E_y})^2}$, of E_y in time.
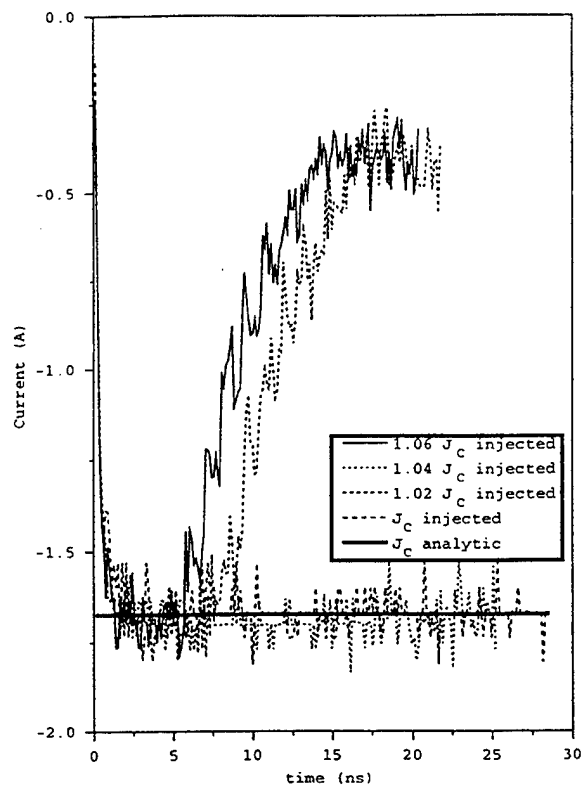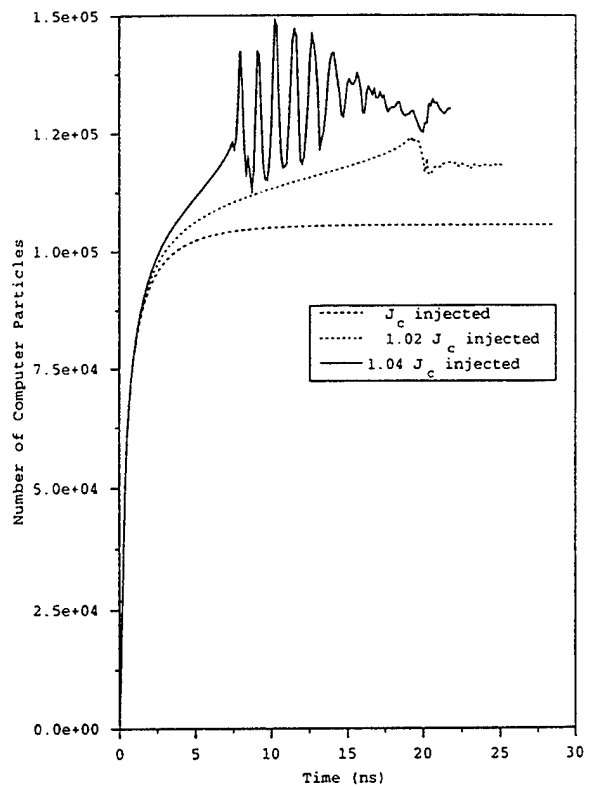
Figure 3: Cold Injection, Current through Hull Diode

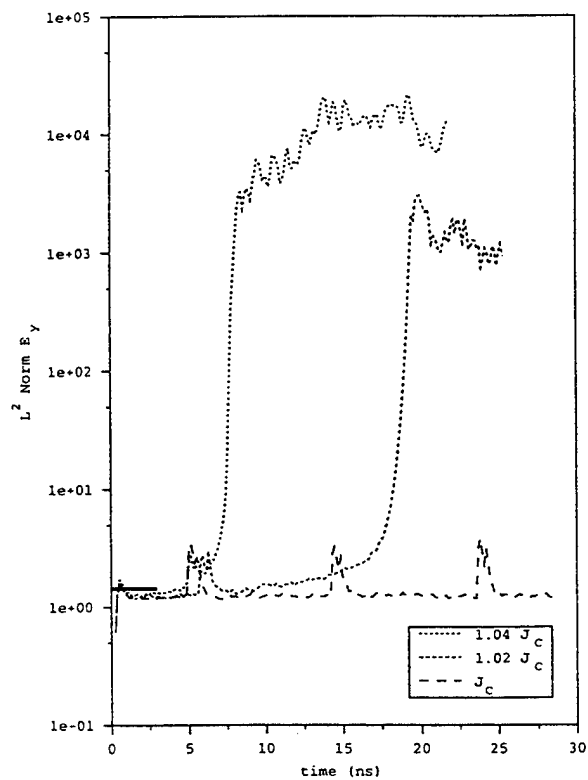Figure 4: Cold Injection, Number of Computer Particles vs. Time

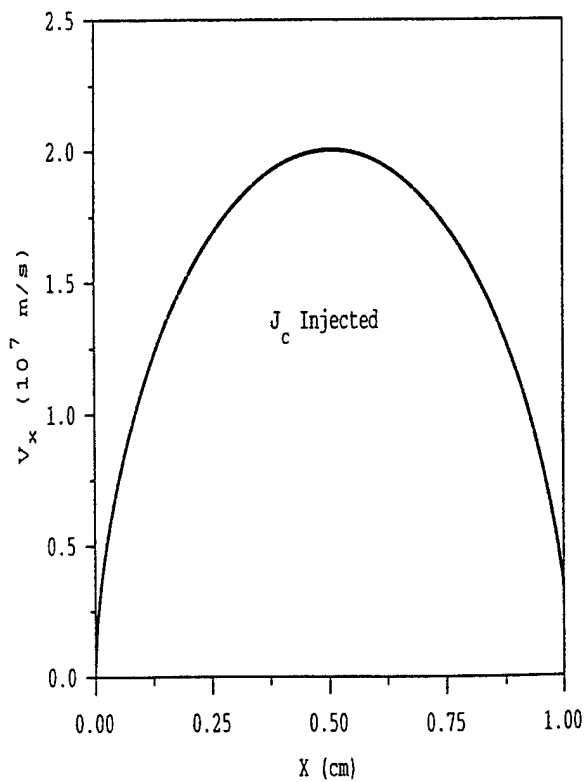Figure 5: Cold Injection, L^2 Norm of Ey vs Time

Figure 6: Cold Injection, Electron Phase Space

However the electron phase space for $J = J_c$, Figure 6, with very little variation in the y-direction, looks very much like, $J = 1.02J_c$ case. This variation in the y-direction allows the diode to have a time independent solution with low noise and no oscillations. Thus, this allows the critical (J_c) current to be transmitted. One possible explanation is when the Hull diode undergoes a transition to virtual cathode oscillations, an instability in the y-direction warms the electrons and stabilizes the diode before it becomes turbulent. The transmitted current in this case is the critical current predicted by Equation 3, which is less than the injected current. This indicates formation of a virtual cathode reflecting a portion of the electron population back to the cathode. The electrons reflected must have directed energy normal to the cathode less than the virtual cathode potential, i.e. $mu_x{}^2(x_m)/2 < eV(x_m)$.

Increasing the current by 4 percent above the critical value, J_c, the current rises to the critical value as in the first case and remains stable for about 5 ns. During this time, the space charge density in the gap is gradually increasing. The transmitted current then rapidly decays to a new mean value that is about 10 percent of the critical current. The current exhibits either a noisy or oscillatory behavior, with fluctuations of a few percent of the mean value. This is also shown in the number of computer particles, Figure 4. The L^2 norm of E_y is small until this transition occurs then it rapidly increases, as shown in Figure 5. The increase of the L^2 norm indicates that the system has some 2d structure. The electron phase space, Figure 8, recorded after the transition to turbulence has taken place shows a complex structure, with electrons traveling in both directions. The void in the center of phase space fills in completely at longer times. Even though this simulation has variation in the y-direction, the macroscopic measured current is the same as the 1d simulation that also went through a current transition.

5 Thermal Injection

Next, the injected electrons were given a small isotropic temperature, $kT_e = 0.1$ eV, in addition to a 0.5 eV drift. Since $kT_e \ll V$, the change in B_{Hull} due to the electron temperature is negligible. Equation 3 predicts the addition of a thermal spread to the emitted electrons increases the Child-Langmuir current limit for the diode, with commensurate increase of the critical current at B_{Hull}. However, the 2d diode exhibits stability for injected currents much larger than J_c. This is in contrast to the 1d results [6], which demonstrated stability with anisotropic emission temperature (v_x), but instability for isotropic emission temperature with $J > J_c$. The thermal stabilization of the unmagnetized diode was described by Birdsall and Bridges [3]. Figures 9 - 14 show the stabilized diode for injected currents of $1.02J_c$ and $1.04J_c$.

Figure 14 shows an enlarged region close to the cathode. It shows the formation of a virtual cathode reflecting a portion of the electron population back to the cathode only transmitting a current equal to critical current, J_c. Injection with thermal electrons does not show a fast transition to a low current state when the injected current is a few percent larger than the critical current.
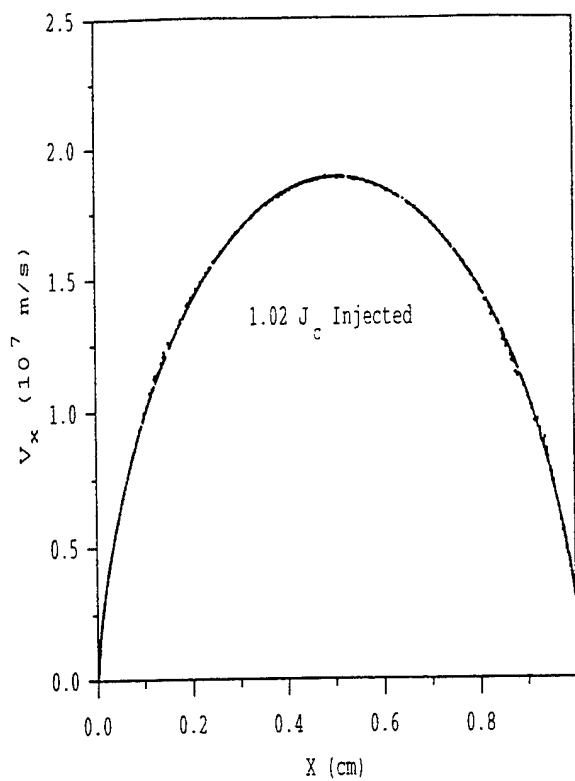
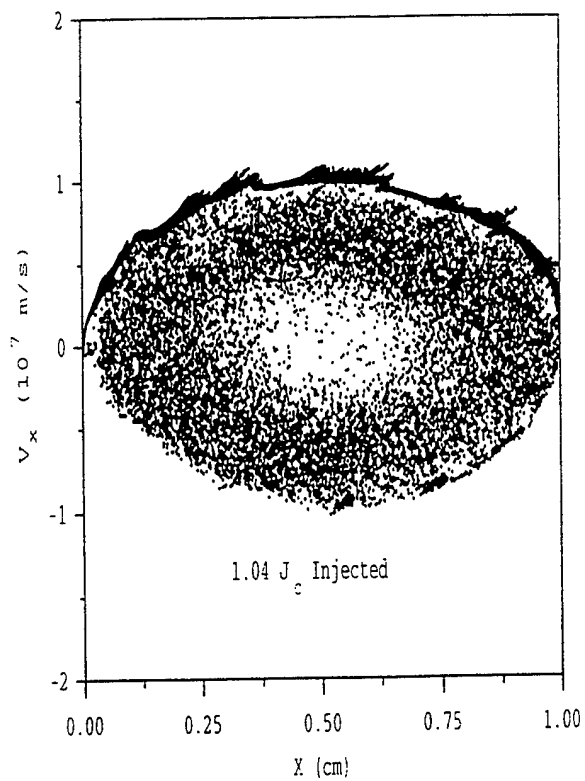Figure 7: Cold Injection, Electron Phase Space

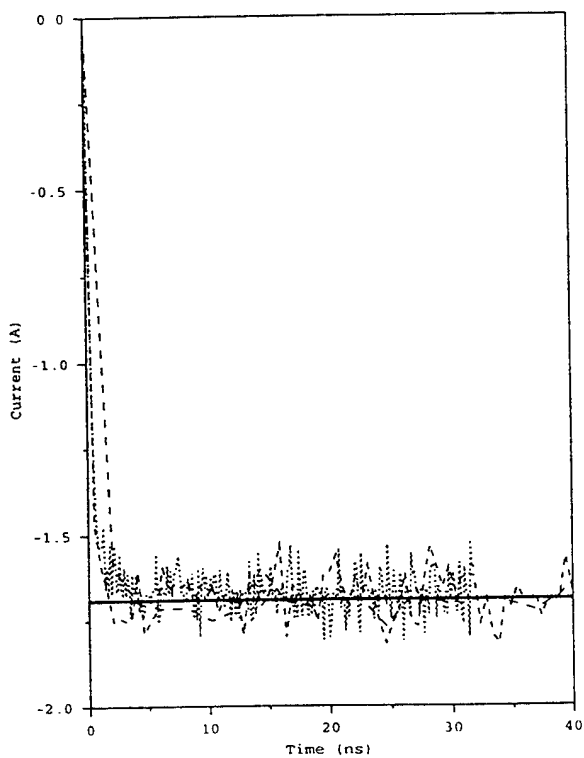Figure 8: Cold Injection, Electron Phase Space
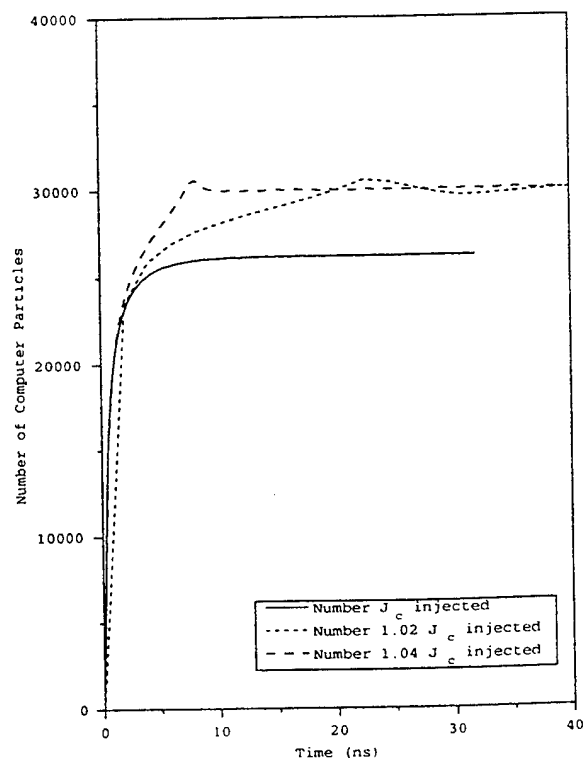

Figure 9: Warm Injection, Current through Hull Diode

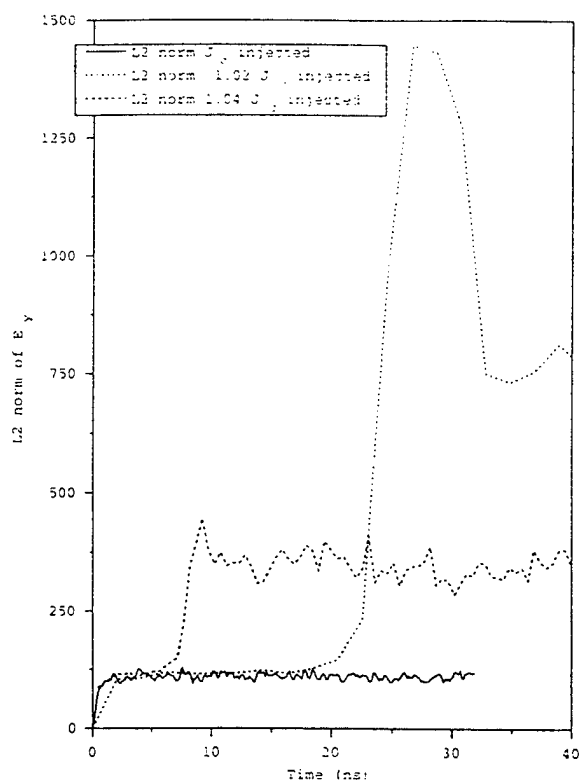Figure 10: Warm Injection, Number of Computer Particles vs. Time

78

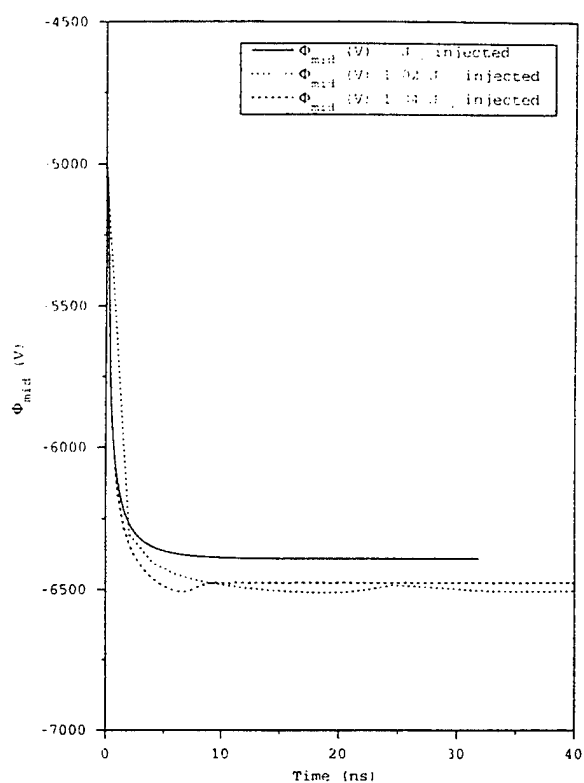Figure 11: Warm Injection, L^2 Norm of Ey vs Time

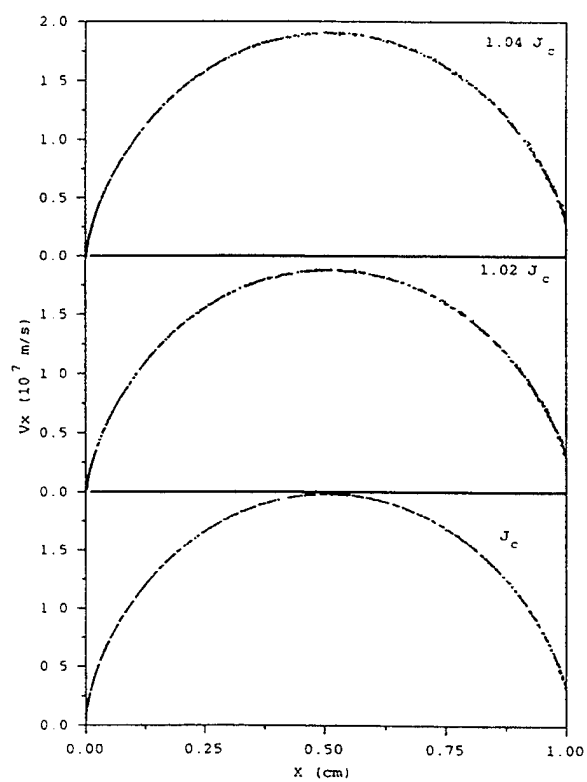Figure 12: Warm Injection, Center Potential of Diode
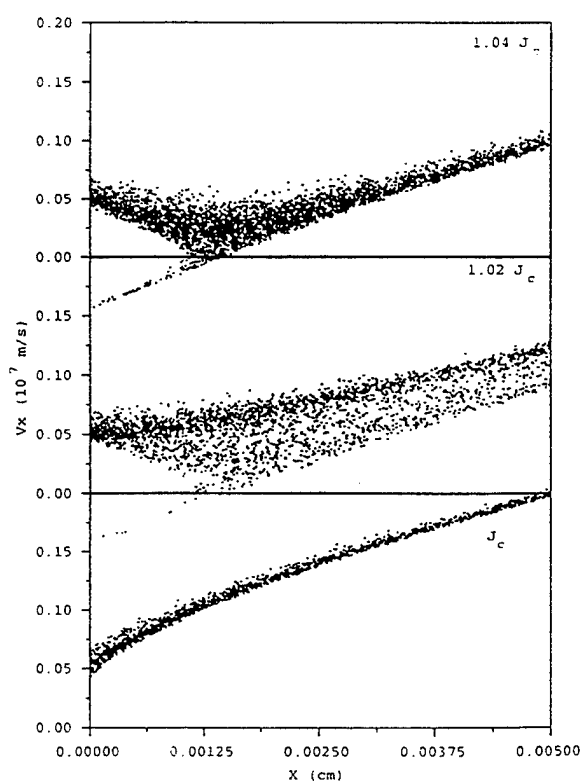

Figure 13: Warm Injection, Electron Phase Space

Figure 14: Warm Injection, Close up of
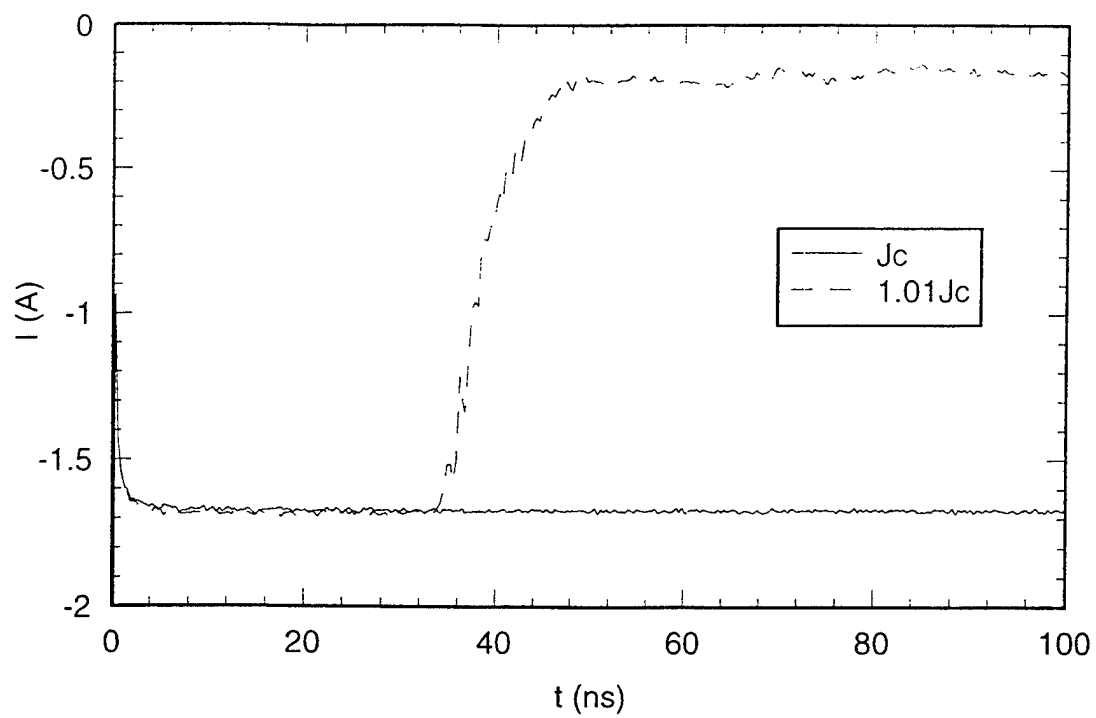Electron Phase Space next to Cathode

79

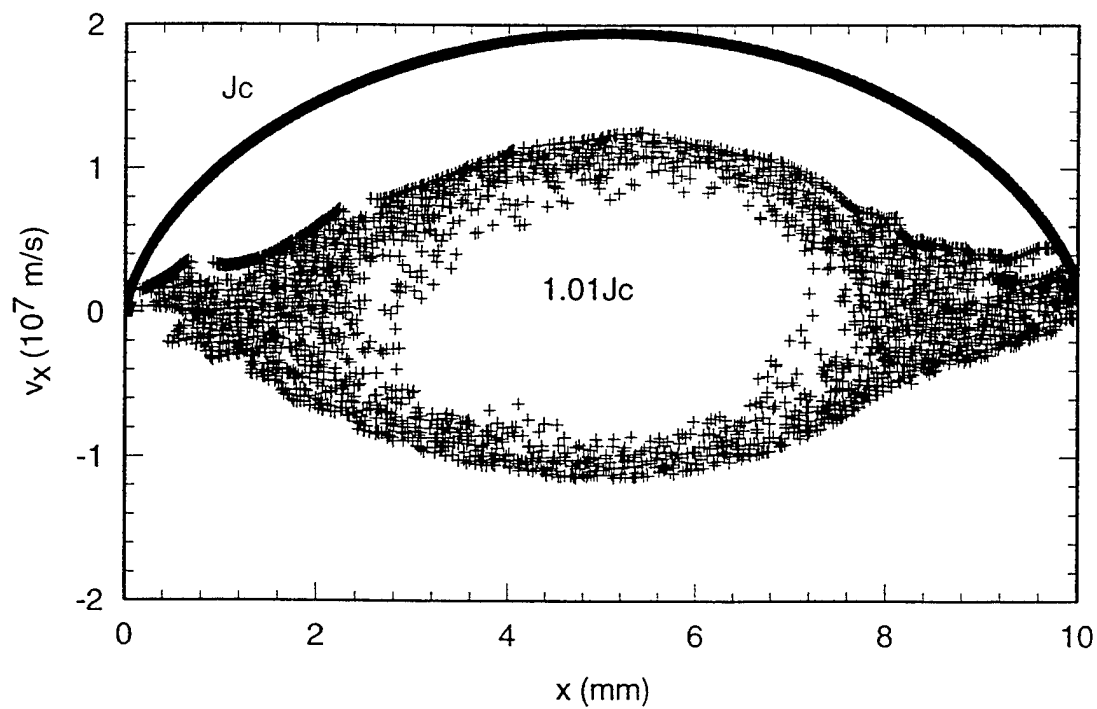Figure 15: 1d, Current through Hull Diode

Figure 16: 1d, Electron Phase Space

6 Conclusions

Numerical instabilities must be investigated in order to remove nonphysical noise from the system. In particular, the diode stability is strongly influenced by noise in the injected space charge distribution at the cathode. The numerical transverse injection effect can be reduced to the extrapolated physical level using a reduced noise scheme which injects electrons uniformly spaced along the cathode.

In the absence of the injection noise, an instability occurs above critical current which heats the electrons in the y-direction so that J_c is the current transmitted. In contrast to the one-dimensional analog at $B = B_{Hull}$ and $J = J_c$, the two-dimensional system does not undergo a rapid instability and the associated current transition for $J_c < J < 1.04J_c$; elsewhere, it behaves like the 1d case. The second dimension allows an additional degree of freedom, which allows relaxation of the space charge effects driving the instability in one dimension.

Acknowledgments

References

[1] Y. Y. Lau, P, J. Christenson and D. Chernin. "Limiting Current in a Crossed–Field Gap," *Phys. Fluids* **5**, 4486 (1993).

[2] V. P. Gopinath, J. P. Verboncoeur and C. K. Birdsall, "Simulation of Transmitted Current in a Cylindrical Cross-Field Diode", *Proc. 22nd IEEE Int. Conf. Plasma Sci.*, Madison, WI (June 1995).

[3] C. K. Birdsall and W. B. Bridges, *Electron Dynamics of Diode Regions*, Academic Press (1966).

[4] I. Langmuir, "*The Effect of Space Charge and Initial Velocities on the Potential Distribution and Thermionic Current Between Parallel Plane Electrodes*", *Phys. Review* **21**, 2 (1923).

[5] P. J. Christenson and Y. Y. Lau, "Transition to Turbulence in a Crossed-Field Gap", *Phys. Plasma* **1**, 3725 (1994).

[6] J. P. Verboncoeur and C. K. Birdsall, "Rapid Current Transition in a Crossed-Field Diode", accepted *Phys Plasma*, (1996).

[7] J. P. Verboncoeur, V. Vahedi, M. V. Alves and C. K. Birdsall, PDP1, PDC1, and PDS1: *Plasma Device One-Dimensional Bounded Electrostatic Codes*, Plasma Theory and Simulation Group, University of California, Berkeley (1990). Available via http://ptsg.eecs.berkeley.edu.

One and Two Dimensional Investigation of IAW Reflection from the Sheath

K.L. Cartwright and C.K. Birdsall

Electronics Research Laboratory

University of California, Berkeley, CA 94720

Preliminary results show that ion waves propagate from the bulk plasma into and all the way through the sheath in 1D PIC simulation. These waves are launched from one side of the system with a current source with a frequency less than the ion plasma frequency. Our one and initial 2d PIC simulations show the details of densities, potentials, particle moments and time–distance plots of the time average density minus the instantaneous density. From the time–distance plot the direction and magnitude of the ion acoustic wave is measured. From this the coefficients of reflection and transmission as a function of pulse width is calculated. Our observations are compared with laboratory experiments and theory.

Uniform Ionization - One Dimensional Case

Initial Electron Temperature	1 eV
Initial Ion Temperature	1.28e-5 eV
Center Density	1.22e14 m^{-3}
Electron Plasma Frequency	9.94e7 sec^{-1}
Ion Plasma Frequency	6.63e6 sec^{-1}
$\frac{Mass of Ion}{Mass of Electron}$	225
Debye Length	7e-4 m
Number of Debye Lengths in system	43
Acoustic Speed	2.65e4 m/s

Diagram of 1d Simulation

Metal
Boundary

Simulation Region

Refluxing
Boundary
'Infinte Plasma'

3 cm
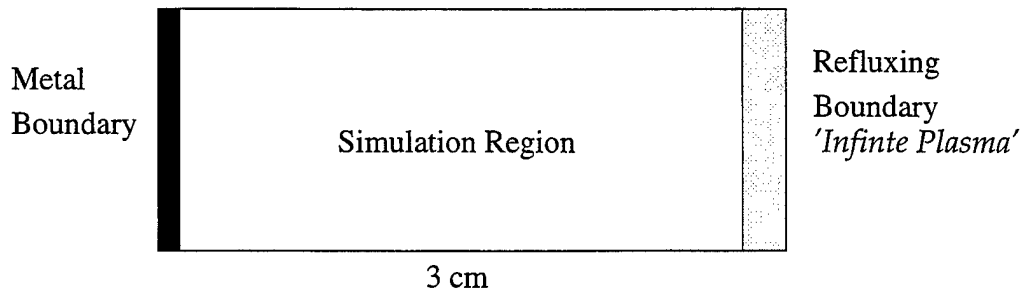
Figure 1: Diagram of 1d Simulation

Computer Model

The right boundary is refluxing; as ions and electrons reach the RHS boundary they are re-injected with a half Maxwellian of the initial temperatures. To maintain the plasma, ions - electron pairs are generated in the system at a constant rate uniformly across the system. This model would correspond to a plasma where UV light is responsible for the ionization. A diagram of the system is shown in figure 1.

To launch a wave from the refluxing wall, in addition to the particles from the refluxing boundary extra particles ion–electron pairs are added. The number of extra particles are modulated in time with a sine wave, and only one pulse is injected. The width and the height of the pulse are parameters that can be varied to get the desired wave in the simulation. This injection scheme is just a way to get a pulse into the system. A particular device was not modeled.

Why do IAW Reflect from the Sheath

An ion acoustic wave propagates, sustained by the charge neutrality of the plasma as a whole. In the sheath, however, an ion acoustic wave is no longer sustained, because the electric potential energy is higher than the electron thermal energy (pressure) which drives the acoustic wave. In the plasma, the ions and electrons oscillate in phase, with little self E. In the sheath the electric field in drives ions and electrons in opposite directions. Then, a small deviation from static charge neutrality in the sheath breaks the ion acoustic wave.

Reflection of Soliton from the Sheath

The initial condition of this computer experiment is with the simulation region filled uniformly with plasma. The simulation was run until it reached steady state. Spatial profiles of the densities, potentials, and average velocity are shown in figure 2. The potential compared to the theory by *Emmert*[1]. Also note that the position where charge separation takes place and the were the ions pass the sound speed. These positions are in agreement with the theory by *Weynants*[2].

SPATIAL PROFILES

electron velocity
ion velocity
electron density
ion density
Bohm velocity

Bohm Velocity

electron velocity
ion velocity
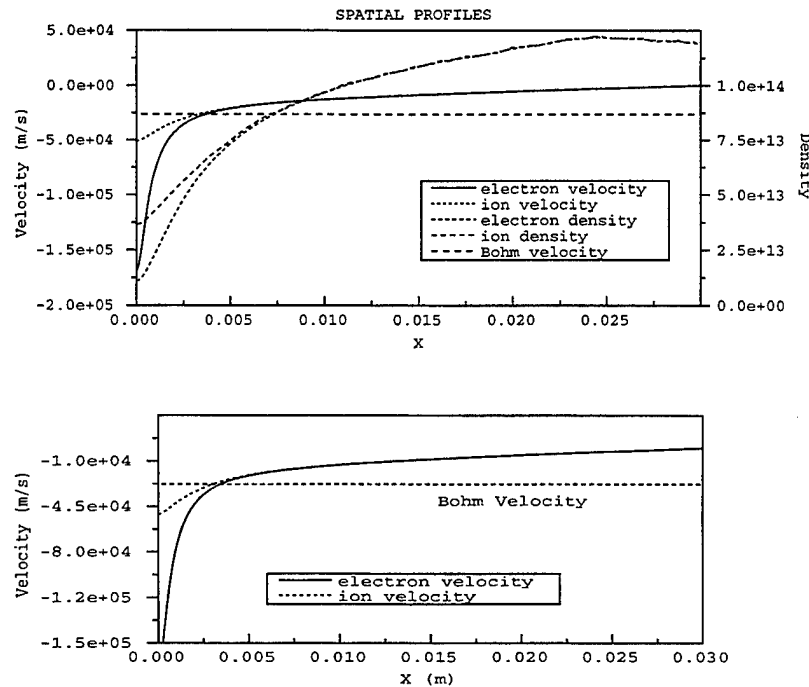
Figure 2:

Reflection of Soliton from the Sheath

The waves are then launched in this equilibrium state as stated above. Figure 3 shows the density perturbation of the pulse. The charge density of the sheath is much larger that the soliton which is a perturbation. A long time ($20\tau_i$) average of the density is taken and subtracted from the instantaneous density. A cross section (fixed time) of figure 3 is shown in figure 4. The profile of the density perturbation is taken when the wave is half way between the right edge and the beginning of the sheath. The simulated wave and a fitted soliton packet is shown.

Ion Density Perturbation

Figure 3: 1d Ion Density Perturbation

————— Best Fit to a KdV Soliton

.... Density Perturbation

This Plot shows the comparison of the density pertur-
bation and a Korteweg - deVries soliton which has the
form $sech^2(\frac{\xi}{n})$. **Figure 4**

A Constant of a Soliton Motion

One of the attributes of a soliton is the relation between its height and width, $amplitude * width^2$ is a constant, before and 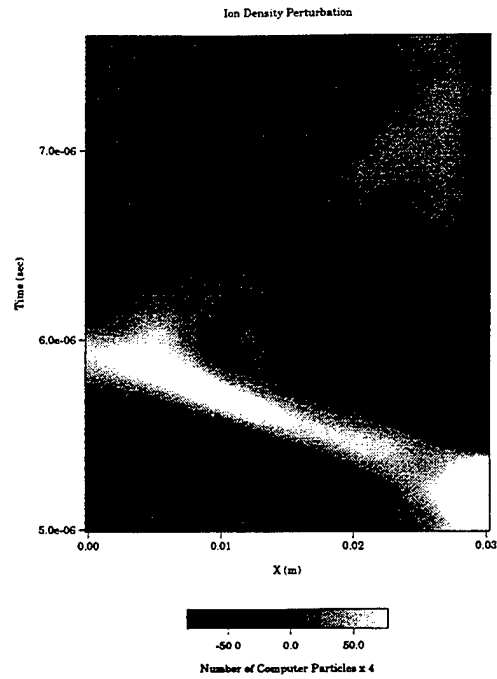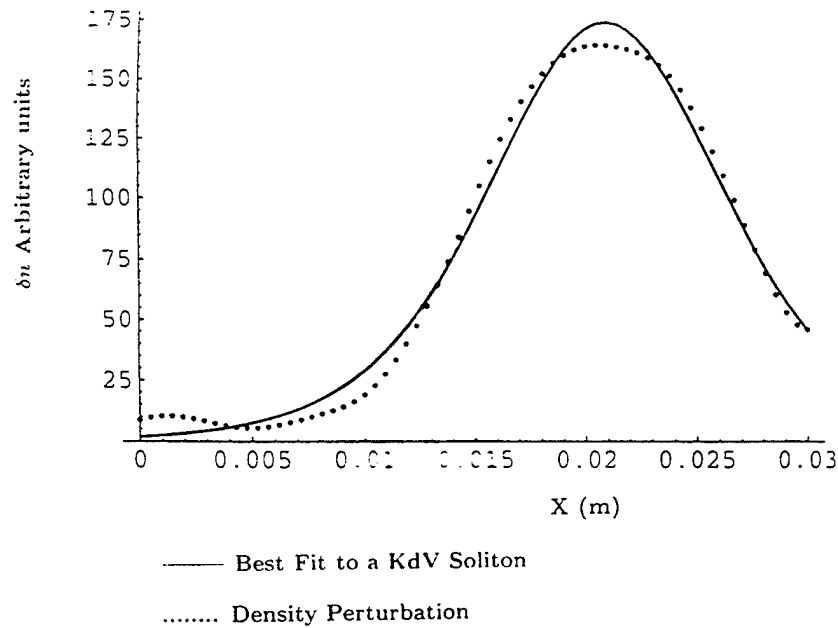after reflection. The percent deviation from this quantity is shown in figure 5. The section of data where the deviation is the largest is where the incident soliton reflects. When two solitons are present, the fitting program is still tying to fit one soliton. A closer look at this splitting process is planned for future work. For this same data, the peak position is plotted as function of x and t is shown in figure 6. From this the position where the reflection takes place can be found. It is at about .002 m. This position is closer to where Bohm velocity is reached than where charge separation occurs. Experimental data from $Cooney$[3] is also shown in this figure for comparison.
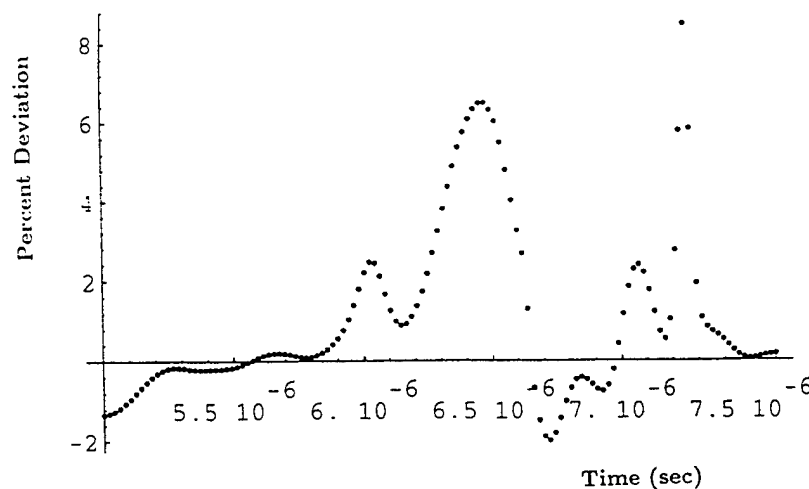
This plot shows the percent deviation of the conserved quantity Aw^2. This shows that these are Korteweg-deVries soliton and not modified KdV solitons, which have Aw as a conserved quantity.

Figure 5

Trajectories of the incident and reflected soliton near the sheath.
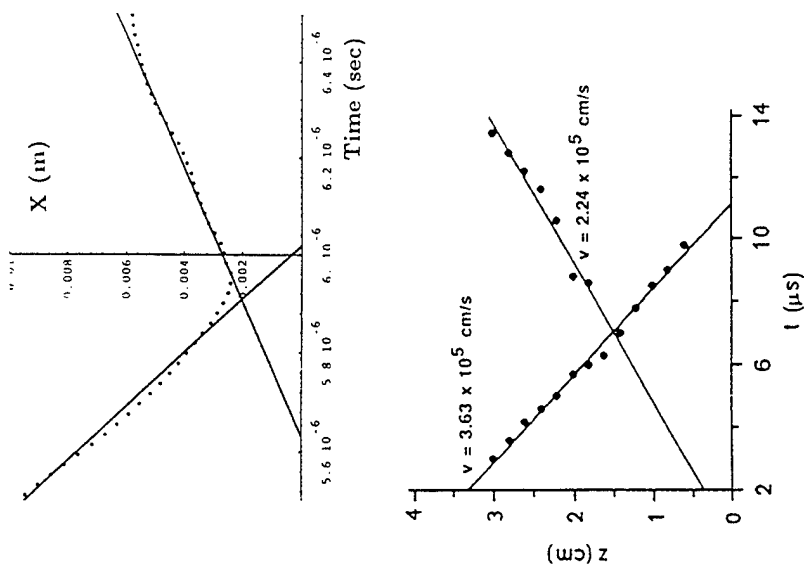
Experimentally found trajectories of the incident, reflected, and transmitted solitons near the reflector from Cooney.   Figure 6

Reflection Coefficient of Solitons from the Sheath
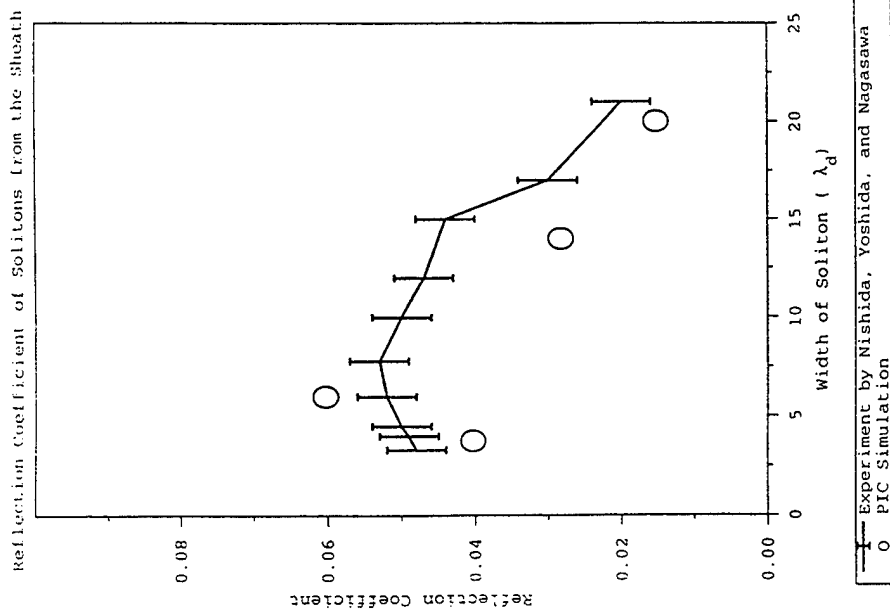
Figure 7

In Figure 7 the reflection coefficient as a function of pulse width is plotted. Also plotted in this figure is is the reflection coefficients from an experiment of $Nishida$[4]. Finding the transmission coefficients is planned for future work. When this data is obtained the relationship between R and T can be compare to the following simple theory. The conservation of energy for the incident, transmitted and reflected solitons can be written as:

$$A_i^2 w_i = A_t^2 w_t + A_r^2 w_r \tag{1}$$

Since the three waves are KdV solitons, each component satisfies the relation:

$$A_i w_i^2 = A_t w_t^2 = A_r w_r^2 = constant \tag{2}$$

From these two equation:

$$A_i^2 w_i = A_t^2 \sqrt{A_i/A_t} w_i + A_r^2 \sqrt{A_i/A_r} w_i \tag{3}$$

or

$$1 = T^{\frac{3}{2}} + R^{\frac{3}{2}} \tag{4}$$

where

$$T = A_t/A_i \ and \ R = A_r/A_i \tag{5}$$

Uniform Ionization – Two Dimensional Case

Initial Electron Temperature	1 eV
Initial Ion Temperature	1.28e-5 eV
Center Density	2.8e14 m^{-3}
Electron Plasma Frequency	1.50e8 sec^{-1}
Ion Plasma Frequency	1.00e7 sec^{-1}
$\frac{Mass of Ion}{Mass of Electron}$	225
Debye Length	4.42e-4 m
Number of Debye Lengths in system	136
Acoustic Speed	2.65e4 m/s
Y Length	.02344, .04688, or .375 m

Diagram of Two Dimensional Model

Periodic Boundary

Metal
Boundary

Refluxing
Boundary
'Infinite Plasma'

Periodic Boundary

6 cm

Figure 8:

Ion Density Perturbation

Ion Density Perturbation

-4.0e+13 -2.0e+13 0.0e+00 2.0e+13 4.0e+13
Ion Density Perturbation (1/m^3)

-4.0e+13 -2.0e+13 -4.2e+06 2.0e+13 4.0e+13
Ion Density Perturbation (1/m^3)
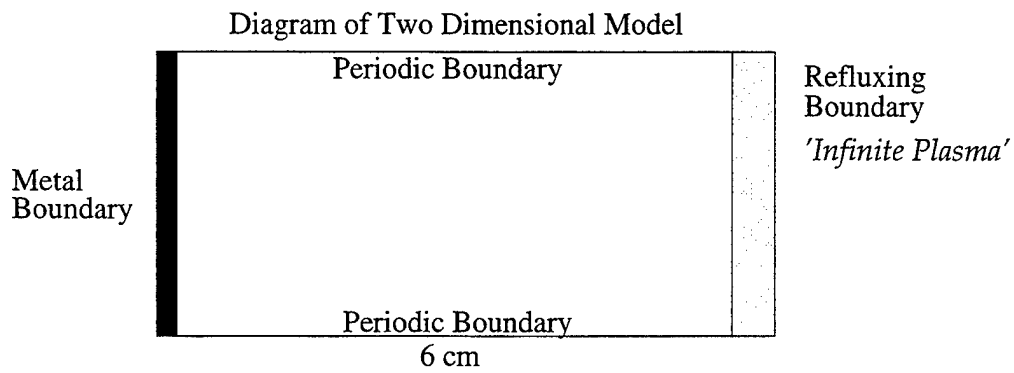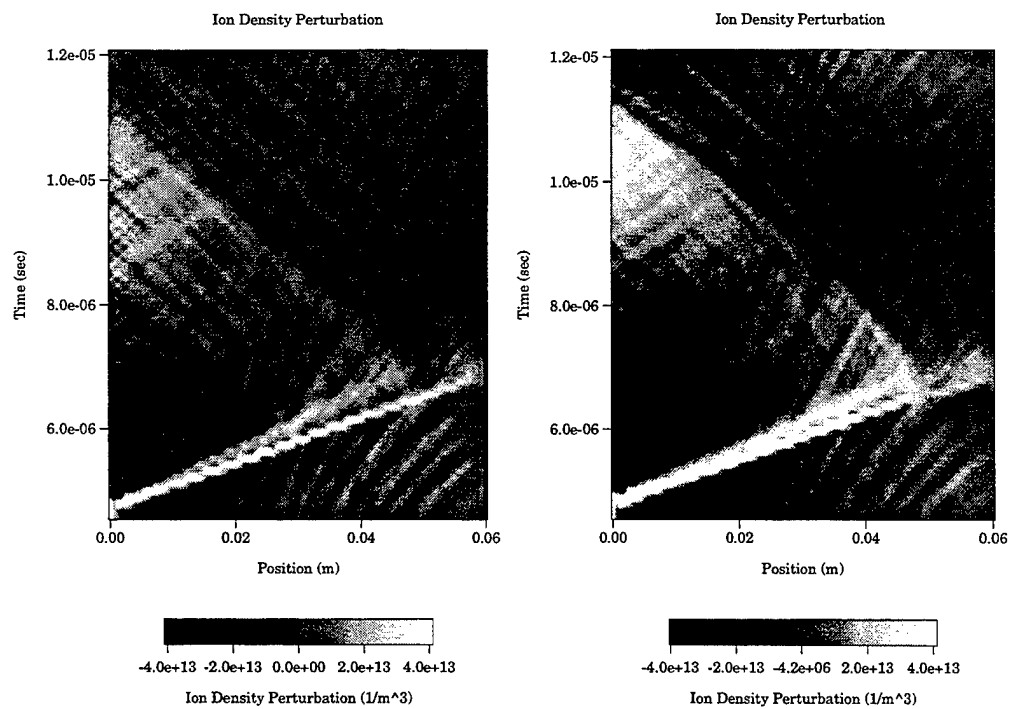
Figure 9: Waves launched with initial width of $.125\mu sec$ and $.25\mu sec$.
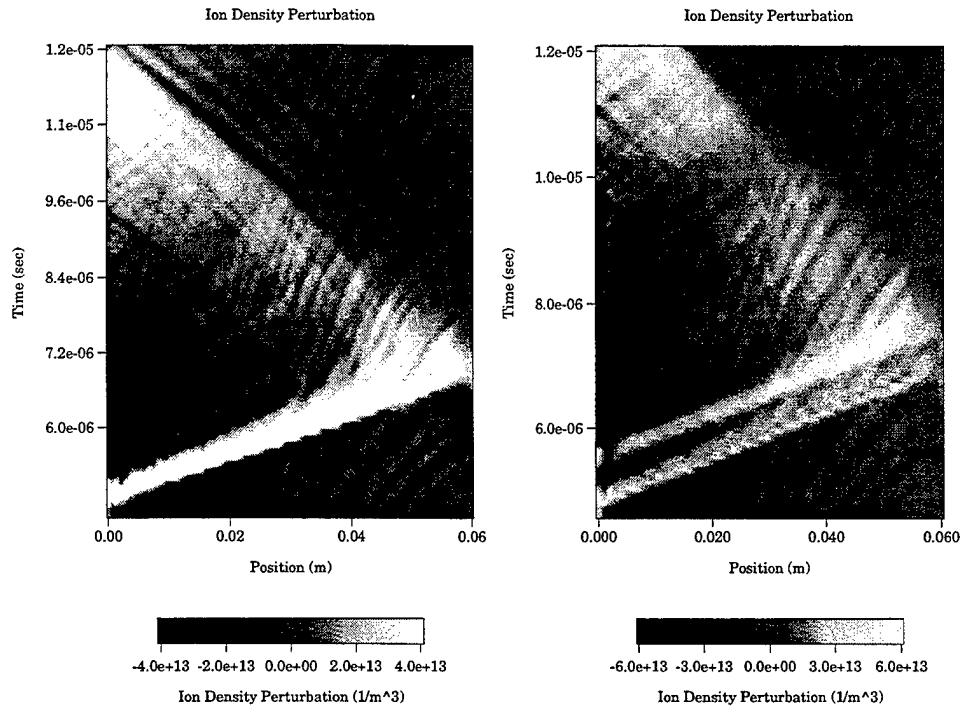
Figure 10: Waves launched with initial width of $.5\mu sec$ and $1\mu sec$.

2d Results

Time average spatial profiles are shown in figures 11 and 12. The ion perturbation for the run made with the shortest periodic direction are shown in figures 9 and 10. Snap shots of the wave in time are shown in figure 13. The velocity and and reflection points for these waves are shown in figure 14.

The 2d runs are computationally prohibitive to make; therefore, a non-linear Boltzmann electron model is being developed. A 1d implementation of this model compares well to a full PIC simulation, as shown in figure 15 . Since the model compared well with the simulation for the sheath it will be used to study ion waves in the sheath; however, this has not been done yet.
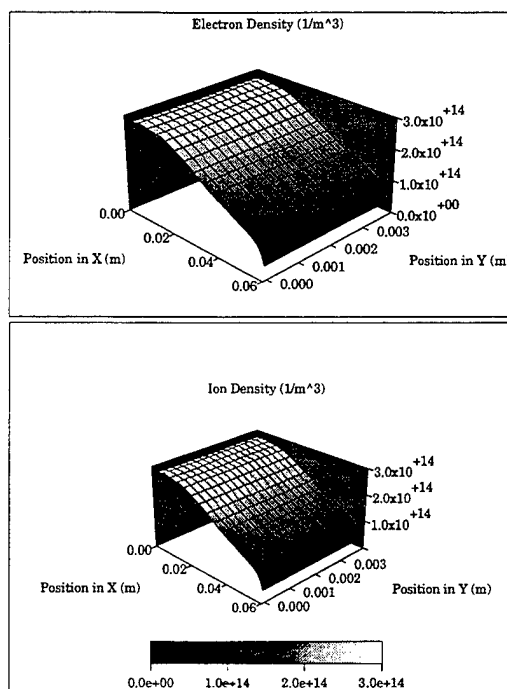
Figure 11: Spatial profiles of a 2d System
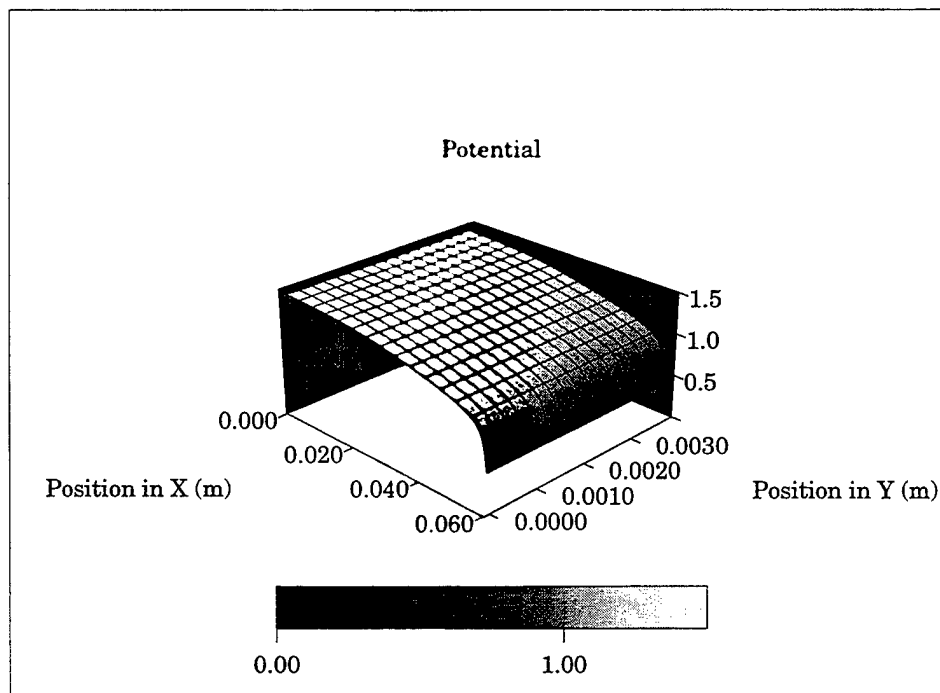
Figure 12: Spatial profiles of a 2d System
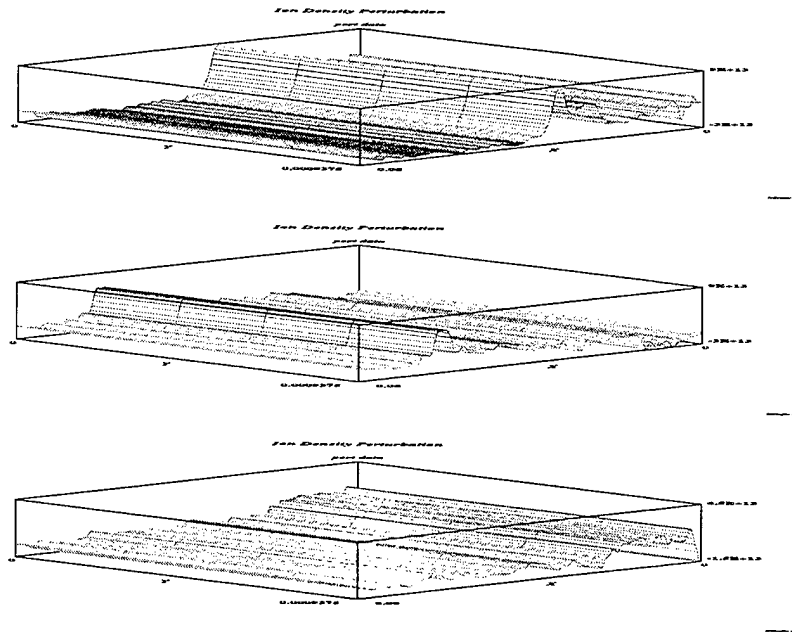
Figure 13: A 2d ion wave
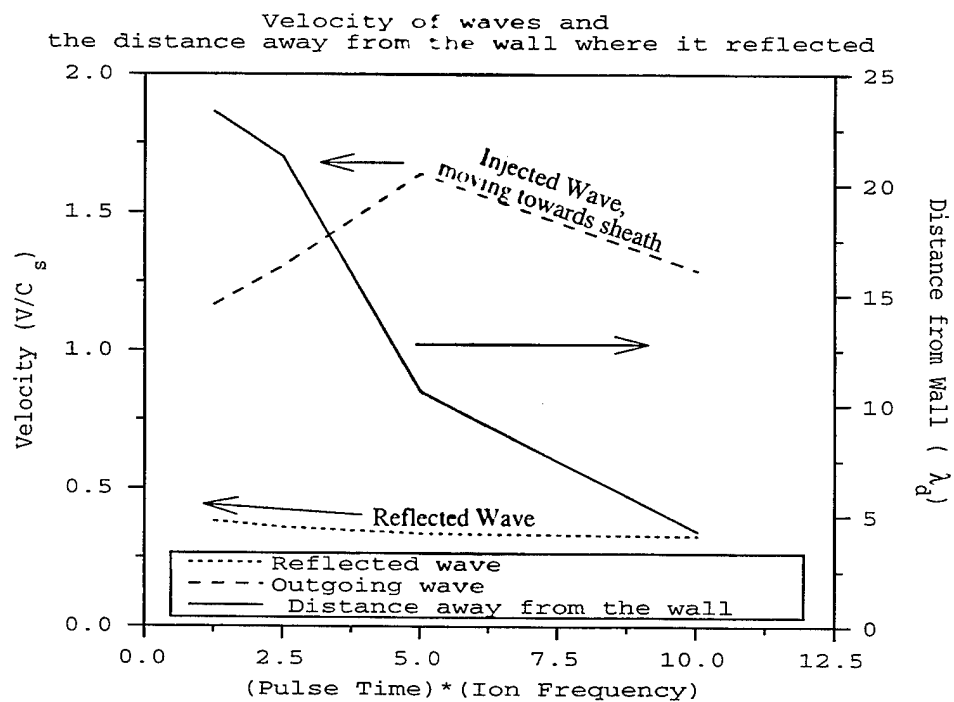
Figure 14: Velocity and Reflection points of the Wave

Boltzmann Electron Model

The method used here is based on Newton Iteration.

$$N(\phi) = 0 \tag{6}$$

For Boltzmann electrons:

$$N(\phi) = \nabla^2 \phi + (n_i(x) - n_{e0}e^{-q\phi/T}) \tag{7}$$

q is the charge of the electrons, normally -1

$n_i(x)$ is the ion density,

n_{e0} is the electron density where $\phi = 0$

T is the temperature of the electrons in eV.

Finding an Iterative Method

ϕ^n be the approximate solution to the nonlinear Possion equation at the nth iteration.

$\Delta\phi = \phi^{n+1} - \phi^n$ is the required change (assumed small) during the iteration, we may expand the equation about the present solution.

$$N(\phi^n + \Delta\phi) = N(\phi^n) + \left(\frac{\partial N}{\partial \phi^n}\right)\Delta\phi + h.o.t. \tag{8}$$

Ignoring the higher-order terms in this equation and requiring $N(\phi^{n+1}) = 0$. This equation can be rewritten as:

$$\left(\frac{\partial N}{\partial \phi^n}\right)\Delta\phi = -N(\phi^n) \tag{9}$$

or

$$\left(\frac{\partial N}{\partial \phi^n}\right)\phi^{n+1} = -N(\phi^n) + \left(\frac{\partial N}{\partial \phi^n}\right)\phi^n \tag{10}$$

Hockney and Eastwood on page 173 show that this scheme converges quadraticly if:

- There is an infinite domain.

- The initial guess is close enough to the solution.

Differentiating equation 7 with respect to ϕ:

$$\frac{\partial N}{\partial \phi} = \nabla^2 + q/T n_{e0} e^{-q\phi/T} \tag{11}$$

The iterative scheme of equation 10 then becomes:

$$(\nabla^2 + q/T n_{e0} e^{-q\phi^n/T})\phi^{n+1} = (1 - \phi^n)e^{-q\phi^n/T} - n_i(x) \tag{12}$$

Modification for Bounded System

This model is not quite yet well defined. n_{e0} is defined where $\phi = 0$; however, the value of n_{e0} is not known yet. We have chosen to keep track of the total density of the Boltzmann electrons in the system, accounting for the electrons that pass through the boundaries. This gives us one more equation for that needs to be solved.

$$N_e = \int n_{e0} \exp(\phi/T) \tag{13}$$

where the integral is over simulation area (2d) or line (1d). This can be solved for n_{e0}. At each iteration a new n_{e0} is solved for:

$$n_{e0}^{n+1} = \frac{N_e}{\int \exp(\phi^n/T)} \tag{14}$$

For particle time step N_e is updated:

$$N_e^{new} = N_e^{old} + \Gamma_{walls} + collisions. \tag{15}$$

If practice this method has converged linearly in both the 1d and 2d cases. Figure 15 show a comparison of the boltzmann electron model to PIC electrons.
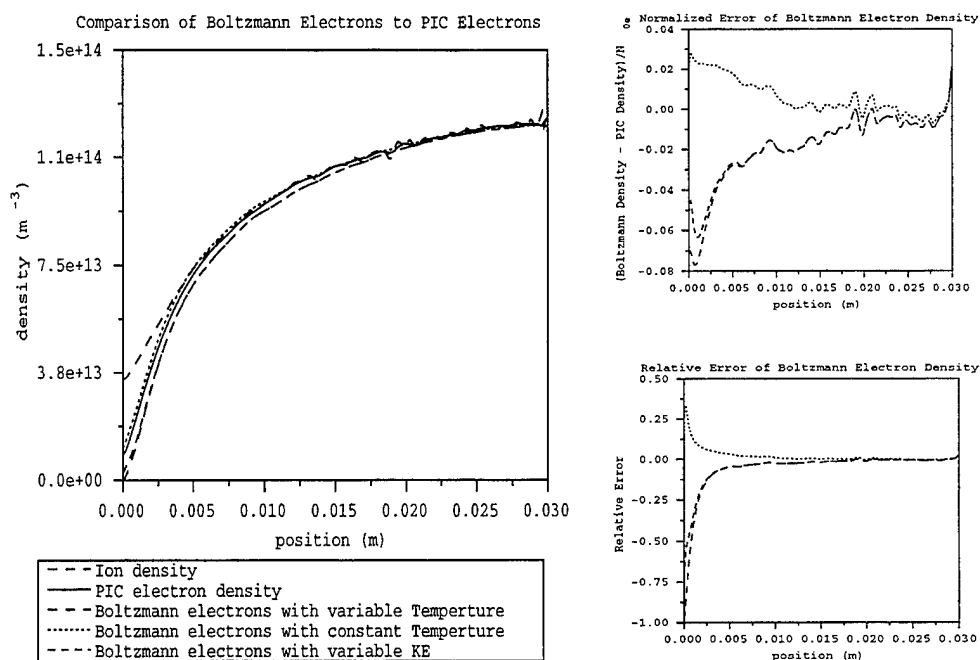
Figure 15: A Comparison of Boltzmann Electrons Model vs. PIC

References

[1] G.A. Emmert, R.M. Wieland, A.T. Mense, and J.N. Davidson, "Electric sheath and presheath in a collisionless, finite ion temperature plasma," Phys. Fluids 23(4), April 1980.

[2] R.R. Weynants, A.M. Messiaen, and P.E. Vandenplas, "Nonquasineutral theory of ion-acoustic resonances in bounded nonuniform plasma and comparison with experiments," Phys. Fluids 16(10), October 1973.

[3] J.L. Cooney, M.T. Gavin, J.E. Williams, D.W. Aossey, and K.E. Lonngren, " Soliton Propagation, collision, and reflection at a sheath in a positive ion-negative ion plasma," Phys. Fluids B 3 (12), December 1991.

[4] Y. Nishida, K. Yoshida, and T. Nagasawa, "Refraction and reflection of ion acoustic solitons by space charge sheaths," Phys. Fluids B 5(3), March 1993.

VIII. PTSG WORK CURRENTLY IN PROGRESS

Two-Dimensional Investigation of Ion Acoustic Waves Reflection from the Sheath

Keith L. Cartwright

(Professor C. K. Birdsall)

The goal of this work is to find the mechanism in the presheath, sheath, and wall region that reflect, transmit, and absorb ion acoustic waves. Ion waves are observed to propagate from the bulk plasma into and completely through the sheath to the wall. These waves have a frequency less than the ion plasma frequency. Ion waves have been purposely launched as well as spontaneously generated by an ion acoustic instability. This instability is due to relative drifts of warm electrons and cool ions in the presheath. Our one and two dimensional PIC simulations show the details of densities, potentials, fields, velocity moments, and time-distance plots of the average density minus the instantaneous density. The density perturbation shows the waves partially reflected before they reach the sheath edge. From the time-distance plot the direction and magnitude of the ion acoustic wave is measured. From this the coefficients of reflection and transmission as a function of width of the wave (1d and 2d) and the incident angle (2d) is calculated. The goal of this work is to find the mechanism that reflect ion acoustic waves.

Transverse Asymmetry in a Crossed-Field Diode

Keith L. Cartwright, John P. Verboncoeur, and Venkatesh P. Gopinath

(Professor C. K. Birdsall)

Recent studies of cylindrical crossed-field diodes indicate the transverse dimension may play a role in delaying onset of virtual cathode oscillations for currents above the limiting current. Transverse space charge effects in smooth diodes can result in fields which warm the electrons. Thermal emission of electrons damps virtual cathode oscillations, as shown by C. K. Birdsall. The effects of the transverse dimension are explored using two-dimensional planar PIC codes. This investigation indicates the transverse dimension is important in delaying the onset of virtual cathode oscillations for currents above the limiting current. The work so far has been limited to the behavior of the diode at $B = B_{Hull}$; this will be extended to regions of larger magnetic fields.

PIC-MCC with Variable Particle Weights

David Cooperberg and Dr. Vahid Vahedi

(Professor C. K. Birdsall)

In order to use particle-in-cell (PIC) simulation codes for modeling collisional plasmas such as self-sustained discharges, it is necessary to add interactions between charged and neutral particles. In conventional Monte Carlo schemes, the time or distance between collisions for each particle is calculated using random numbers. This procedure allows for efficient algorithms, but is not compatible with PIC simulations where the charged particle trajectories are all integrated simultaneously in time. A Monte Carlo collision (MCC) package including the null collision method has been developed, as an addition to the usual PIC

charged particle scheme, by V. Vahedi and M. Surendra. The new scheme being studied involves allowing for varying particle weights in order to reduce the number of computer particles needed to represent selected species. This variable-weight scheme allows for a significant reduction in simulation size at run-time, as in the case of highly electro-negative discharges where the ion densities may be far greater than the electron density. Also, by choosing the number of computer particles to be used through the duration of the run, a consistent level of numerical fluctuation may be maintained. However, there are some energy exchange questions to be resolved (as between electrons of different weights), as raised by W. S. Lawson and P. C. Gray.

Particle Simulation of Surface Waves

David Cooperberg

(Professor C. K. Birdsall)

We are investigating surface waves via electrostatic particle simulation of a warm, unmagnetized, bounded 2d3v plasma. Our study focuses on a slab configuration in which the plasma is periodic in the y direction and is bound in the x direction by grounded, absorbing, conducting walls. Our prior simulation has produced dispersion relations and eigenfunctions for surface waves analogous to a symmetric Gould-Trivelpiece waves in cylindrical systems. The Ky = 0 cut-off of the asymmetric mode defines the series resonance. Secondary branches (O'Brien) were also observed whose cut-offs represent Tonks-Dattner resonances. We are now studying two species, low-voltage, collisional systems sustained by resonant interaction with surface waves. These systems are driven with applied voltages of order T_e. This investigation is important for both basic sheath understanding and for applications such as large area plasma processing, new light sources, lasers, and ion sources. We are also initiating electromagnetic simulations to verify our electrostatic results.

Comparison of Stability Characteristics of Planar and Cylindrical Crossed-Field Diodes

Venkatesh P. Gopinath* and John P. Verboncoeur*

(Professor C. K. Birdsall)

Simulations of cylindrical crossed-field diodes for anode/cathode radius ratios of 2 and 5 indicate that the limiting current curve in the region $B < B_H$ in cylindrical diodes follows the planar theory and simulations very closely. Cylindrical diodes also follow planar theory predicting transition to turbulence in the region $B > B_H$. Larger radius ratio (10, 20) diodes show somewhat larger limits. We are examining a possible explanation for this behavior.

*Post-Doctoral Researcher

Ion Energy Distributions in Capacitively-Coupled RF Plasma Reactors

Emi Kawamura

(Professor C. K. Birdsall)

Lawrence Livermore National Laboratory

Drawing on a review of previous works on ion energy distributions (IED) arriving at the target in the collisionless regime, we determined what factors influence the shape of the IEDs. This regime is of great interest to experimentalists and modelers studying the new generation of high-density sources in which the sheath is much thinner than in the conventional RIE systems. Then, we conducted some particle-in-cell simulation results of a current driven rf plasma sheath. The results show that for tion/trf << 1, the sheath is resistive and the IEDs are broad and bimodal with a dominant low energy peak. Here, tion is the ion transit-time across the sheath, and trf is the rf period. As tion/trf increases, the sheath becomes capacitive, the IED narrows, and the two peaks become more equal in height.

Performance Evaluation of Dynamic ADI and the Conjugate Gradient Method Used to Compute Two-Dimensional Electrostatic Fields in Wholly Bounded Systems

John Morgan Oslake

(Professor C. K. Birdsall)

A 2D electrostatic field solver for wholly bounded systems has been developed using preconditioned conjugate gradient methods. One intended purpose was to compare the performance between this field solver and a field solver based on Dynamic ADI. Dynamic ADI is currently being used within an Object-Oriented Particle-in-Cell (OOPIC) code for simulating plasmas. An important consideration in the development of all PIC codes is improving simulation speed. Under certain conditions, the conjugate gradient methods have been demonstrated to offer substantial improvements over Dynamic ADI in terms of computational speed and robustness. Conjugate gradient methods, on the other hand, place some serious restrictions on the numerical structure of the problem, such as limiting Neumann boundary conditions to first-order accuracy.

Numerical Solution of Waveguide Eigenproblem for Microwave Device Simulation

John Morgan Oslake

(Professor C. K. Birdsall)

The calculation of eigenfrequencies and their corresponding field modes for wave guides is important for electronic device simulation. An application of particular interest is slow-wave structures for microwave amplification. The development of competitive numerical methods to solve this problem are currently in progress. We are investigating a Krylov subspace method based on Arnoldi's method, as well as various acceleration techniques such as domain decomposition.

Noise and Stability of Crossed-Field Devices

John P. Verboncoeur* and Venkatesh P. Gopinath*

(Professor C. K. Birdsall)

The issues of stability and noise in crossed-field devices have persisted for seventy years, dating back to A. W. Hull (*Physical Review 18,* Vol. 31, 1921). We study stability is studied using our 1D PIC code, PDP1, for various electron emission conditions and applied magnetic fields. We find that small perturbations of the electron energy distribution function (EEDF) can change the nature of the diode, including transition from laminar to turbulent behavior, onset/quenching of virtual cathode oscillations, and bistability. The stability in turn impacts the noise properties, with turbulent states exhibiting time-dependent fields. This basic research is applicable to the crossed-field amplifier class of microwave tubes, where signal-to-noise ratio is an important performance criterion.

*Post-Doctoral Researcher

Microwave-Beam Device Modeling

John P. Verboncoeur,* Peter Mardahl and Keith Cartwright

(Professor C. K. Birdsall)

The Multi-University Research Initiative (MURI) is a tri-service program to advance the state of the art in high power microwave devices. The objectives of the research include high power, low noise, and broad bandwidth. Collaborative efforts are underway to model a number of these devices, including high-power multi-cavity klystrons, Cerenkov masers, and helical and grating traveling wave tubes. Novel devices will also be considered. The modeling is performed using our 2D code, OOPIC (see *http://ptsg.eecs.berkeley.edu/* for more information).

One of the devices currently being examined is the Cerenkov maser, which is a microwave device using an electron beam in a dielectric-loaded waveguide, as in the Figure 1. The purpose of the work on the Cerenkov maser is to compare simulated results using XOOPIC with theory and experiment.

Tests of dispersion have shown good agreement with theory for the TM01 mode, however, the power and gain of the device have not been accurately simulated yet: obtaining these measurements will be the aim of continuing work.

*Post-Doctoral Researcher

OOPIC: An Object-Oriented Electromagnetic Particle-in-Cell (PIC) Code

John P. Verboncoeur,* Peter Mardahl, and Keith Cartwright

(Professor C. K. Birdsall)

The object-oriented paradigm provides an opportunity for advanced PIC modeling, increased flexibility, and extensibility. Particle-in-cell codes for simulating plasmas are traditionally written in structured FOR-TRAN or C. This has resulted in large legacy codes that are difficult to maintain and extend with new models. In this ongoing research, we apply the object-oriented design technique to address these issues. The resulting code architecture, OOPIC (Object-Oriented Particle-in-Cell), is a two-dimensional (x-y, r-z) relativistic electromagnetic/electrostatic PIC-MCC (particle-in-cell, Monte Carlo collisions) plasma simulation. OOPIC includes a growing number of boundary conditions, and can model complicated configurations, including internal structures, without recompilation. It is applicable to models from DC and RF discharges to high power microwave tubes. See *http://ptsg.eecs.berkeley.edu/* for more information.

*Post-Doctoral Researcher

IX. U.C. BERKELEY PARTICIPATION IN MURI

I. INTRODUCTION: Statement of Work

We have begun applying our electron beam-interactive circuit simulation-visualization codes, OOPIC and XOOPIC, to

(a)   e-beam driven microwave sources;
(b)   novel beam configurations;
(c)   vacuum microelectronics.

The code is particle-in-cell (PIC), electromagnetic, relativistic, object-oriented (in C++ language), presently two dimensional (x, y and r, z) running on PC's and workstations. OOPIC development is now almost through a 3 year AFOSR grant, already initially presented, with excellent reception. The development is multi-institutional, with 4 participants (2 universities, 2 firms).

Under (a), a Monte Carlo collision module is being added in order to simulate plasma-filled interaction circuits, from first principles (as self-consistent as possible). One objective is to investigate plasma focusing of an e-beam, either uniform or with periodic lenses. Another is to find the reasons for the enhanced plasma-filled guide behavior observed experimentally. In addition, OOPIC will be made three dimensional (x, y, z, and/or r, θ, z), capable of simulating almost all known and proposed devices.

Under (b), OOPIC will be applied to a set of e-beam interactive circuit devices, where the interactive circuits include disk-loaded waveguide, sheath helix, resistive-wall, as well as very general impedance or Kirchhoff wall circuits, allowing great flexibility for TWT's, klystrons, transit-time devices and crossed field devices. A novel step is to revive multiple beam-multiple interaction circuit devices (high circuit impedance, large (net) perveance).

Under (c), OOPIC will be applied to single and multiple field emitters (cones), first with verification of field emission to space-charge limited beam flow, then with application to the multiple beam-multiple interaction circuit devices above in (b), complementing work being done at NRL.

Under (a, b, c) there will be interaction with national labs and industry in applying OOPIC for their problems, with the possibility our students residing on-site for extended periods. Object-oriented (modular) OOPIC is very user friendly, flexible and extensible.

Microwave-beam device modeling

Dr. John P. Verboncoeur, Peter Mardahl and Keith Cartwright

(Professor C. K. Birdsall)

The Multi-University Research Initiative (MURI) is a tri-service
program to advance the state of the art in high power microwave
devices. The objectives of the research include high power, low
noise, and broad bandwidth. Collaborative efforts are underway to
model a number of these devices, including high power multi-cavity
klystrons, Cerenkov masers, and helical and grating traveling wave
tubes. Novel devices will also be considered. The modeling is
performed using our 2D code, OOPIC (see http://ptsg.eecs.berkeley.edu/
for more information).

  One of the devices currently being examined is the Cerenkov maser,
which is a microwave device using an electron beam in a dielectric-loaded
waveguide, as in the figure. The purpose of the work on the Cerenkov maser
is to compare simulated results using XOOPIC with theory and experiment.

  Tests of dispersion have shown good agreement with theory for
the TM01 mode, however, the power and gain of the device have
not been accurately simulated yet: obtaining these measurements
will be the aim of continuing work.

Here are our project AFOSR-MURI titles, not ordered:

All of these carry the generic title:

MICROWAVE HIGH POWER ELECTRON BEAM DEVICE SIMULATIONS, MOSTLY USING OUR AFOSR CODE, OOPIC.

(1) High voltage dielectric loaded slow-wave guides (Cerenkov maser).

(2) Electron beam optics.
   Full space charge, magnetized, relativistic, ion focusing due to background gas (deliberate or not), more.

(3) Disk-loaded slow waveguide.
   Many aspects: for example, numerical model dispersion and impedance, field emission due to high RF power, including secondaries (even without a beam, so-called "dark current"), more.

(4) R-theta extension of OOPIC.(for, e.g., magnetrons).
   Now r-z and x-y, fully EM, relativisitic, with electrostatic versions.

(5) Crossed field stability, turbulence and noise characterizations.
   Both planar and cylindrical (coaxial); attention to velocity distributions at the cathode, and secondary electrons.

(6) Relativistic, high perveance klystrons
   High perveance, hollow beam, multi-cavity, self-consistent cavities and Kirchhoff Law cavities; impedance/admittance wall gain control and output cavity couplings.

(7) Traveling wave tubes with many beams and circuits in parallel,
   For higher impedance, higher (effective) perveance. larger power-bandwidth product, higher efficiency, at "large C".

OOPIC NEXT STEPS (not priority ordered)

(1) R-θ EM version

(2) GUI completion (or, re-do) OOPIC [PC]

(3) Set of **Input Files** on **typical tubes**

     klystron
     dielectric loaded guide
     disk loaded guide
     sheath helix
     electron gun (curved boundaries)
     depressed collector (curved boundaries)
     transit time devices
     magnetron (cylindrical, planar, ES, EM)
     general impedance wall amplifiers

(4) Third dimension Z-R $\rightarrow$ Z-R-θ, R-θ $\rightarrow$ R-θ-Z

     x,y $\rightarrow$ x,y,z
     Perhaps small m# in θ

(5) Complete secondary particle emitter, total physics, full dependence on incidence, full f(v,θ) for emitted particles, $\gamma_{sec} > 1$

(6) Geometry editor (mouse driven boundaries, volume, etc.) [UNIX]

(7) Curved boundaries

(8) Internal f(v) in some **volume** (specified) or at some area (specified)

(9) **Volumes** with σ & ε [maybe $\sigma(X)$, $\varepsilon(X)$]

(10) **Surfaces** with $\sigma_{parallel}$, σ_{perp} [σ conductivity]

(11) Driven electrodes, external, internal, complete external circuit

(12) R,L,C external circuits (terminal connections)

(13) On the fly changes in parameters and graphics

(14) Multiple Spatial Regions

(15) Subcycle Fields

(16) Subcycle Particles

(17) Collision package: multiple gases, tabled cross sections, Coulomb collisions

(18) Magnetic field: static B (e.g. from Poisson), slowly varying B(t)

(19) Periodic boundaries

(20) Magnetostatic field solve (non propagating waves)

(21) Nonorthogonal mesh

(22) Piecewise curvilinear boundaries

(23) Parallel processing (distributed and massively parallel)

13 September 1995

PERFORMANCE EVALUATION OF DYNAMIC ADI AND THE CONJUGATE GRADIENT METHOD USED TO COMPUTE 2D ELECTROSTATIC FIELDS IN WHOLLY BOUNDED SYSTEMS.

By John Morgan Oslake

The main objective was to compare the CPU speeds between a field solver implemented in OOPIC using Dynamic ADI (DADI) and a field solver using the conjugate gradient method.

A 2D electrostatic field solver (Poisson equation) has been developed using the conjugate gradient method (CG). Implementations have been carried out in Cartesian and cylindrical coordinates. The cylindrical implementation is in primitive stages. The Cartesian implementation supports internal structures, periodic boundary conditions in both coordinate axes directions, and Dirichlet and Neumann boundary conditions. The Neumann boundary conditions are limited to first order accuracy. However, there is no restriction on the value of the Neumann boundary conditions as there is in DADI. If Neumann boundary conditions are not used, then the CG field solver is demonstrated to be second order accurate. Computational verification of the order of accuracy for DADI is not possible due to the erratic behavior of the errors.

Preconditioning by symmetric successive over relaxation (SSOR) and an approximate Cholesky factorization has been implemented CG in Cartesian geometry. As the number of cells increases, the performance of the field solver is significantly enhanced by preconditioning in problems without Neumann boundary conditions For problems with Neumann boundary conditions an effective preconditioner for CG has yet to be developed.

Comparisons have been made between the OOPIC version of DADI and the conjugate gradient method using SSOR as preconditioner. Test cases were performed in Cartesian geometry with Dirichlet boundary conditions. Under these assumptions CG offers performance improvements in terms of computational speed and guaranteed accuracy. (See table below for comparative timing data.)

Further work into implementing a more generalized conjugate gradient like method might be beneficial. Iterative methods, such as GMRES, which do not require symmetry or positive definiteness of the operator would be capable of handing second order accurate Neumann boundary conditions.

TIMING RESULTS

Timing results were obtained for solution of Poisson's equation in (x,y) coordinates with Dirichlet boundary conditions on the unit square. The timing data is gathered using the gprof UNIX utility. Precision is of type float. Compilation was performed on a DEC Alpha with g++ using flag -O3 for optimization.

The tolerance for both schemes is chosen so that the L2 error of the CG method is primarily due to the truncation error inherent in the finite difference scheme and not the error due to the iterative method. Decreasing the tolerance further would certainly decrease the magnitude of the residuals (to within machine precision), but would have no added effect on reducing the error. Typically, the tolerance is 1e-6.

Let rho be the charge distribution and phi be the potential as in Poisson's equation for electrostatic fields. Let $|r|$ denote the magnitude of the residual as defined by $|rho-Laplacian(phi)|$. Then for the case where rho is NOT equal to 0, both DADI and CG are iterated until $|r| < |rho|*EPS$ where EPS is the tolerance. In the case where rho = 0, iteration using DADI is terminated when $|r| < EPS$ and CG terminates when the L2 norm of the change in updates to the solution is < EPS.

For rho = 0, the terminating condition used for CG requires fewer iterations than the terminating condition imposed on DADI. This exploits the property of monotonic residual decay in CG which DADI does not possess.

Method	Number Cells	Number Time Steps	CPU Time (seconds)	Time per Time Step	DADI Time/ CG Time
Analytic Phi = 1					
CG w/ SSOR	8	6000	10.68	0.00178	6.936
DADI	8	6000	74.08	0.01235	
CG w/ SSOR	32	200	13.13	0.06565	2.935
DADI	32	200	38.54	0.19270	
CG w/ SSOR	128	5	14.27	2.85400	2.915
DADI	128	5	41.60	8.32000	
Analytic Phi = x+y					
CG w/ SSOR	8	6000	11.51	0.00192	6.501
DADI	8	6000	74.83	0.01247	
CG w/ SSOR	32	200	13.12	0.06560	2.929
DADI	32	200	38.44	0.19220	
CG w/ SSOR	128	5	13.77	2.75400	2.414
DADI	128	5	33.24	6.64800	
Analytic Phi = sin(PI*x)*cos(PI*y)					
CG w/ SSOR	8	6000	10.11	0.00169	7.780
DADI	8	6000	78.68	0.01311	
CG w/ SSOR	32	200	12.87	0.06435	3.200
DADI	32	200	41.18	0.20590	
CG w/ SSOR	128	5	16.54	3.30800	2.452
DADI	128	5	40.55	8.81100	

REFERENCES

[1] Birdsall C.K., Langdon A. B., Plasma Physics Via Computer Simulation, Adam Hilger (1991).

[2] Doss, S., Miller K., "Dynamic ADI Methods for Elliptic Equations." SIAM Journal of Numerical Analysis, Volume 16, Number 6, October 1979.

[3] Hewett, D.W., Larson, D.J., Doss, S., "Solution of Simultaneous Partial Differential Equations Using Dynamic ADI: Solution of the Streamlined Darwin Field Equations." Journal of Computational Physics, July 1992, Volume 101, (No. 1):11-24

[4] Shewchuk, J., "An Introduction to the Conjugate Gradient Method Without the Agonizing Pain." Article, Department of Computer Science, Carnegie Mellon University, August 4, 1992, Edition 1 1/4.

[5] Strikwerda, J., Finite Difference Equations and Partial Differential Equations, Wadsworth and Brooks (1989).

Numerical calculation of dispersion relation for slow-wave structures.

J.M. Oslake, C.K. Birdsall
Electronics Research Laboratory
University of California
Berkeley, CA 94720

Slow-wave structures support microwave amplification via electromagnetic coupling with an injected electron beam. Critical in the design of such devices is the relationship between the dispersion relation of the wave and the geometry of the guiding structure. From the dispersion relation key quantities such as phase velocity can be determined.

To this end, a computer model is developed which first numerically solves a wave equation in finite difference form subject to boundary conditions periodic in z and conducting elsewhere. Here the direction of wave propagation is along the z-axis. The solution produces a sequence of eigenfrequencies and eigenfields beginning with cut-off. Fourier decomposition of each eigenfield along selected mesh lines coincident with the electron beam is then performed to establish a correspondence between eigenfrequency and wave number. From this data the dispersion relation for the slow-wave structure can then be formed. Arbitrarily many points in the dispersion relation can be determined at the cost of increased computation time. An example showing the first two TM passbands for a ridged waveguide in xz coordinates is demonstrated.

Future work hopes to incorporate plasma loading with frequency dependent dielectric constant.

1

18 Dec. 1995

Re: Volunteering to help on MURI simulations

Dear MURI members,

Our Plasma Theory and Simulation Group (PTSG) at UC Berkeley (led by Ned Birdsall) has created a number of plasma simulation tools over the years, which you may view on our WWW home page:
    http://ptsg@eecs.berkeley.edu

Our codes are PIC-MCC, based on first principles, self-consistent, electrostatic and electromagnetic, and are free. The codes follow electron and ion motion, in various (user-set) boundaries (metal, dielectric, emitting, absorbing). They also include charged particle collisions with neutrals (scattering, excitation, ionization, charge exchange). The codes are easy to run, with many models possible simply by modifying the input files. They are also tranparent (easy to modify).

Our microwave beam device code (OOPIC) is applicable to many MURI high power microwave device problems. OOPIC is a 2d3v relativistic electromagnetic object-oriented PIC-MCC code in xy and rz, with a Monte Carlo Collision (MCC) model, for collisions between charged particles and neutrals. Examples presented at the OOPIC Release Workshop are attached below.

The MCC feature may be very attractive to some of you working in high power microwaves (HPM). Some examples are:

   the erosion of cathodes due to ion bombardment (due to residual or
   intentional presence of gas);

   plasma (ion) focusing of electron beams;

   plasma-filled slow and fast wave structures.

There are many others as well.

We wish to gauge the need and uses for this feature in the context of high power microwaves. That is, are you interested in ions, collisional processes, and plasma focusing?

We are pleased to offer cooperative help, on all MURI problems, not just the collisional ones, much as provided at the two Workshops which we presented earlier this year. Please give us your device dimensions, voltages, currents and other pertinent parameters (which might be type of gas and pressure). Include your objectives and questions to be resolved, as well as references (reports, experimental results, etc.). We will then try to set up your problem on OOPIC and to help you to obtain first runs, on your workstations. After that, you will do the running (chasing through parameter changes etc.). If needed, we will visit you briefly to assist in making headway in the simulations and comparisons with theory and experiments.

We cannot promise to attack all problems in this area, but we will give all suggested problems consideration.

Please reply to us (johnv@eecs.berkeley.edu with cc to birdsall@eecs.berkeley.edu) or this mailing list (muriall@gregor.llnl.gov)

John Verboncoeur, Research Engineer, UC-Berkeley C. K. (Ned) Birdsall, Professor in the Graduate School, UC-Berkeley

ATTACHMENT: OOPIC Examples, including some demonstrations presented at the OOPIC Release Workshop (Sept.1995):

MICROWAVE HIGH POWER ELECTRON BEAM DEVICE SIMULATIONS

(1) High voltage dielectric loaded slow-wave guides (Cerenkov maser).

(2) Electron beam optics. Full space charge, magnetized, relativistic, ion focusing/de-focusing due to background gas (deliberate or not), more.

(3) Disk-loaded slow waveguide. Many aspects: for example, numerical model dispersion and impedance, field emission due to high RF power, including secondaries (even without a beam, so-called "dark current"), more.

(4) R-theta extension of OOPIC (for, e.g., magnetrons). Now r-z and x-y, fully EM, relativisitic, with electrostatic versions.

(5) Crossed field stability, turbulence and noise characterizations. Both planar and cylindrical (coaxial); attention to velocity distributions at the cathode, and secondary electrons. (Excellent ties to Y.Y. Lau, Michigan; this collaboration has produced 10-15 journal articles and conference papers for our two groups collectively in the last 2 years).

(6) Relativistic, high perveance klystrons. High perveance, hollow beam, multi-cavity, self-consistent cavities and or Kirchhoff Law cavities; impedance or admittance wall gain control and distributed output cavity couplings.

(7) Traveling wave tubes with many beams and circuits in parallel. For higher impedance, higher (effective) perveance, larger power-bandwidth product, higher efficiency, at "large C", C>0.1. Similar paralleling for klystrons. Requires 3d3v code development.

Currently we are giving highest priorities (ordered) to:

> (6) Relativistic, high perveance klystrons.
> We are now planning visits, soon, to the Phillips Lab by members of
> my group, in order to tie our initial computer experimental results
> to their lab experimental results.
> (5) Crossed-field stability, turbulence and noise characterizations.
> We have found high interest (in the Tri-Services) in such for
> magnetrons (such as CFA's) and have now several publications, This
> is an old field but we have uncovered some neat new results,
> primed by Y.Y. Lau's analytical work at Michigan.
> (3) Disk-loaded slow waveguides.
> We have some initial beam-circuit results, to be enlarged upon.
> We have a (computer) solution to eigenfrequencies
> and eigenfunctions for the numerical model (as obtained from
> Langdon's OOPIC theory); this complements lab cold testing on
> such circuits (e.g., effects of disk thickness, length and
> diameter of added ferrules, etc.), a great time saver for an
> experimentalist.

Item (7) deserves some expansion. First of all, this is longer range, most probably requiring several 3d3v versions of OOPIC, being started. (7) involves using many electron beams in parallel (in order to achieve

effectively higher perveance, or, lower beam impedance: higher currents at lower voltages), along with many interaction circuits in parallel (could be slow or fast waveguides, or klystron-like circuits), achieving effectively higher circuit impedance.

Also to be done is some analytic modeling to go with statements on use of "large C" TWT's, with high circuit impedance and low beam impedance (i.e., high perveance), for larger power-bandwidth product, higher efficiency, something Birdsall did at Hughes, with the first 50 kW TWT amplifier, made with Birdsall's ring-bar circuit, before 1955.

X. DISTRIBUTION LIST

Air Force Office of Scientific Research
Barker

Department of Navy
Roberson

Bell Telephone Laboratories
Gottscho

Berkeley Research Assoc.
Brecht, Gladd

Cal. Inst. of Technology
Bridges, Gould

Cornell University
Otani

Dartmouth
Hudson

FM Technologies
Mako

George Mason Univ.
Rine, Acquah, Guillory, Peter

Goddard Space Center
Storey

Hughes Research Lab., Malibu
Hyman, Harvey

Hughes Aircraft Co.
Adler, Longo

IBM
Theilhaber

JPL
Liewer

Lam Research
Barnes, Benjamin, Morey, Rafinejad

Lawrence Berkeley Laboratory
Fawley, Kaufman, Lee

Lawrence Livermore National Lab.
Byers, Chen, B.Cohen, R. Cohen, Drake, DiPeso,
Friedman, Hewett, Langdon, Procassini,
Rognlien, Schwager, Smith, Vahedi

Litton Electron Devices
Siambis, Vaughan

Los Alamos Scientific Lab.
Brackbill, Mason, Peratt, Wood, Winske, Thomas

Mass. Inst. of Technology
Bers, Danly

NASA - Lewis Research Center
Freeman

Naval Research Laboratory
Armstrong, Freund, Haber, Jackson, Joyce,
Kodis, Parker, Zaidman

NIST
Roberts, Whetstone

Northeastern University
Chan

Oak Ridge National Laboratory
Leboeuf

Osram-Sylvania
Godyak, Piejak, Li, Rogoff

Phillips Lab
Arman, Hendricks, Schumlak, Hussey

Princeton Plasma Physics Lab
Okuda, Parker

SatCon
Gerver

SAIC
Drobot, Mankofsky

SLAC
Phillips

University of California, Berkeley
Arons, Birdsall, Graves, Lichtenberg, Lieberman,
Roth, Verboncoeur, Cooperberg, Mardahl,
Cartwright, Kawamura, Gopinath, Kaufman

University of California, Davis
DeGroot, Luhmann

University of California, Irvine
Rynn, Chen

University of California, Los Angeles
Dawson, Decyk, Chen

University of Illinois
Kushner

University of Iowa
Knorr, Goree

University of Maryland
Frey

University of Michigan
Lau, Getty

University of Tennessee
Rader

University of Wisconsin
Emmert, Hershkovitz, Shohet, Wendt

Varian Associates
Anderson, Grant, Helmer

Vista Research Inc.
Crystal

Washington University
Shrauner

Australian National University
Boswell

Dublin City University
Turner

Queens University, Belfast
Graham

Universität Innsbruck, Austria
Kuhn, Schrittwieser

I.N.P.E., Brazil
Alves, Bittencourt, Montes

University of Toronto, Canada
Stangeby

Riso National Laboratories, Denmark
Lynov, Rassmussen

Culham Laboratory, England
Eastwood, Hockney

Imperial College, England
Burger

Oxford University, England
Allen

University of Montreal
Moison

IPP-KFA, Germany
Reiter

Max Planck Institute für Plasmaphysik,
Germany
Chodura, Lackner

University Bayreuth, Germany
Schamel

Kyoto University, Japan
Matsumoto

Nagoya University, Japan
Kamimura, Tanaka,

Osaka University, Japan
Mima

Pohang Institute of Science and Technology,
Korea
Lee, Oh

Ruhr-Universitat, Bochum, Germany
Riemann

Shizuoka University, Japan
Saeki

Tohoku University, Japan
Ishiguro, Sato

University of Tromso, Norway
Armstrong

Centro de Electrodinamica, Lisbon, Portugal
Brinca

Ecole Polytechnique, Lausanne, Switzerland
Hollenstein, Howling

Oslo University, Norway
Pesceli, Trulsen

Technical University Wien, Austria
Winter

University of Kiel
Piel, Klinger

University P. Sabatier
Boeuf

Ecole Polytechnique
Adam

JAIST (Kanazawa)
Honda

Hitachi Res. Lab.
Matsui

Mitsubishi Heavy Industry
Mochizuki

University of Sidney
Falconer

MURI DIRECTORY

Air Force Office of Scientifice Research
Barker, Nachman

Army Research Laboratory
Abe, Corrigan, Kehs, Libelo

Cornell University
Kerslick, Nation

Hughes Aircraft Company
Butler, Goebel

Litton
Hargreaves, Scheitrum, Symons, Wong

Lockheed Martin Corporation
Furuno

Naval Research Laboratory
Parker, Zaidman

Naval Surface Warfare Center
Kreager, Vanzant

Northrop Grumman
Armstrong

Phillips Laboratory
Agee, Arman, Hackett, Hendricks, Spencer

Physics International
Benford, Levine

Stanford Linear Accelerator Center
Caryotakis, Paterson, Phillips, Siambis

Teledyne
Goren, Zavadil

Texas Tech University
Hatfield, Ishihara, Kristiansen, Krompholz,
Zeiher

University of California, Berkeley
Birdsall, Gopinath, Verboncoeur

University of California, Davis
Hartemann, Heritage, Lombardo, Luhmann,
McDermott

University of California, Los Angeles
Lin

University of Maryland
Antonsen, Calame, Carmel, Destler, Granatstein,
Guo, Lavush, Lloyd, Reiser, Rodgers,
Shkvarunets

University of Michigan
Gilgenbach, Lau

University of New Mexico
Abdallah, Fleddermann, Gahl, Schamiloglu

University of Wisconsin
Basten

Varian Associates
Huffman, Lob, Schaefer

Westinghouse
Kupiszewski